

FINAL REPORT

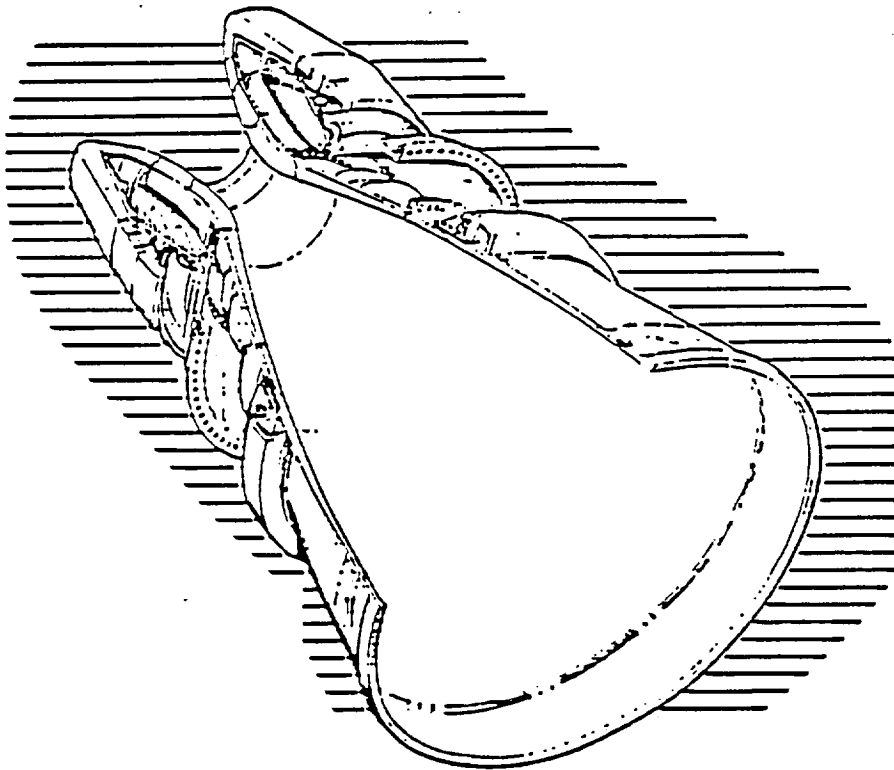
Standardization of the Carbon-Phenolic

Materials and Processes

Volume I

Experimental Studies

August 31, 1988



Nasa Grant NAG8-545

Marshall Space Flight Center

Final Report

Volume I, Experimental Studies

(for period 1 September 1985 to 31 August 1988)

for

Standardization of the Carbon-Phenolic

Materials and Processes

NASA Grant No. NAG8-545

Prepared for

National Aeronautics and Space Administration

Ronald L. Nichols, NASA Technical Officer

George C. Marshall Space Flight Center, Alabama 35812

Prepared by

William B. Hall

Professor of Chemical Engineering

Mississippi State University

Mississippi State, Mississippi 39762

The following personnel assisted in the work performed under this grant: professors -- E. G. Baker, C. George, and G. R. Lightsey; graduate assistants -- Melinda J. Woods, Adhaz K. Datta, and K. K. Porvez; student assistants -- Patti George, John Hairston, Lori Barksdale, and Amy Steele; administrative assistants -- Billy Williams and Polly Hodges.

TABLE OF CONTENTS

I.	INTRODUCTION	1
	Fig. 1 - I - Shuttle	2
	Fig. 2 - I - Top View Shuttle System	3
	Fig. 3 - I - Solid Rocket Booster	5
	Fig. 4 - I - SRM Nozzle	6
	Fig. 5 - I - Materials of Construction in Nozzle	7
	Fig. 6 - I - Construction of Nozzle	8
	Fig. 7 - I - Material Supplier Flow Sheet.....	9
II.	NOZZLE MANUFACTURE	11
	Fig. 1 - II - Impregnation of Cloth	12
	Fig. 2 - II - Generic Autoclave Curing Cycle for Carbon-Phenolic Composites.....	13
	Fig. 3 - II - Generic Hydroclave Curing Cycle for Carbon-Phenolic Composites.....	14
III.	PHENOLIC RESIN	16
	Fig. 1 - III - Hardening of Phenol Alcohols	37
IV.	DIFFERENTIAL SCANNING CALORIMETRY (DSC)	42
	Fig. 1 - IV - DSC Cell and Cross Section.....	44
	Fig. 2 - IV - Typical Peak Integration of 8625-01 System.....	50
	Fig. 3 - IV - Typical Peak Integration of 8626-01 System	51
V.	CARBON CLOTH	53
	Fig. 1 - V - Typical Non-Circular Synthetic Fiber and Corresponding Spinnerette Hole Shapes.....	55
	Fig. 2 - V - Stress-Strain Diagram.....	59
	Fig. 3 - V - Polacrylonitrile Process.....	67

Fig. 4 - V - Isotropic Pitch Process for Carbon Fibers	69
Fig. 5 - V - Mesophase Pitch Process for Carbon Fibers	71
Fig. 6 - V - SEM Photograph of Surface of CCA-3 Rayon Precursor Fiber (x1200)	74
Fig. 7 - V - SEM Photograph of Surface of CCA-3 Rayon Precursor Fiber (x1527)	74
Fig. 8 - V - SEM Photograph of Surface of CCA-3 Rayon Precursor Fiber (x5100)	75
Fig. 9 - V - SEM Photograph of Surface of SWB-8 PAN Precursor Fiber (x5100)	76
Fig. 10 -V - SEM Photograph of Surface of SWB-8 PAN Precursor Fiber (x5100)	76
Fig. 11 -V - SEM Photograph of Cross Section of CCA-3 Rayon Precursor Fiber (x5100)	77
Fig. 12 -V - SEM Photograph of Cross Section of SWB-8 PAN Precursor Fiber (x5100)	77
VI. BREAKING LOAD AND DEFLECTION TESTING EQUIPMENT.....	79
Fig. 1 - VI - Apparatus for Breaking Carbon Fibers	80
Fig. 2 - VI - Circular Grips for Holding Fibers	81
Fig. 3 - VI - Digital Recorder for Breaking Apparatus	81
VII. DETERMINATION OF BREAKING LOAD OF TEXTILE FABRICS USING THE RAVELED STRIP AND CUT STRIP METHODS.....	84

VIII. CARBON FABRIC STUDIES	85
Fig. 1 - VIII - Breaking Load vs Location for CCA-3 and SWB-8 (0.5" Gauge)	87
Fig. 2 - VIII - Breaking Load vs Location for CCA-3 and SWB-8 (1.0" Gauge)	89
Fig. 3 - VIII - Breaking Load vs Location for CCA-3 and SWB-8 (1.5" Gauge)	91
Fig. 4 - VIII - Breaking Load vs Location for CCA-3 and SWB-8 (2.0" Gauge)	93
Fig. 5 - VIII - Deflection vs Location for CCA-3 and SWB-8 (0.5" Gauge)	95
Fig. 6 - VIII - Deflection vs Location for CCA-3 and SWB-8 (1.0" Gauge)	98
Fig. 7 - VIII - Deflection vs Location for CCA-3 and SWB-8 (1.5" Gauge)	99
Fig. 8 - VIII - Deflection vs Location for CCA-3 and SWB-8 (2.0" Gauge)	102
Fig. 9 - VIII - Breaking Load vs Gauge Actual and Linear for CCA-3 (Fill)	103
Fig. 10 - VIII - Breaking Load vs Gauge Actual and Linear for CCA-3 (Warp)	104
Fig. 11 - VIII - Breaking Load vs Gauge Actual and Linear for SWB-8 (Fill)	107
Fig. 12 - VIII - Breaking Load vs Gauge Actual and Linear for SWB-8 (Warp)	108
Fig. 13 - VIII - Deflection vs Gauge Length Actual and Linear for CCA-3 (Fill)	110

Fig. 14 - VIII - Deflection vs Gauge Length Actual and Linear for CCA-3 (Warp)	111
Fig. 15 - VIII - Deflection vs Gauge Length Actual and Linear for SWB-8 (Fill)	114
Fig. 16 - VIII - Deflection vs Gauge Length Actual and Linear for SWB-8 (Warp).....	115
Fig. 17 - VIII - Breaking Load vs Gauge Actual Values for CCA-3 and SWB-8.....	116
Fig. 18 - VIII - Deflection vs Gauge Length (Raw Data) Actual and Linear for CCA-3 and SW-8	118
Fig. 19 - VIII - Breaking Load vs Location (Raw Data) Ravel and Cut Tests for CCA-3 and SWB-8.....	121
Fig. 20 - VIII - Breaking Load and Deflection (Raw Data) CCA-3 and SWB-8, 1.5" Gauge	125
Fig. 21 - VIII - Breaking Load and Deflection (Raw Data) CCA-3 and SWB-8, 2" Gauge	126
IX. CARBON BLACK REINFORCING FILLER	127
Fig. 1 - IX - Past Filler, Vendor B	135
Fig. 2 - IX - Present Filler, Vendor A	136
Fig. 3 - IX - Present Filler, Vendor B	136
X. REFERENCES FOR PHENOLIC RESINS, CARBON CLOTH AND CARBON BLACKS	139
XI. EXPERIMENTAL STUDIES	142
A. Percent Residual Volatiles.....	142
Fig. 1 - XI - Residual Vols Preparation Time	143
Fig. 2 - XI - MSFC Round Robin Test for Residual Volatiles	145

B.	Original Residual Volatiles Test Procedure	146
C.	Proposed Residual Volatiles Test Procedure	147
D.	Volatile Content	148
E.	Proposed Volatile Content Test.....	149
	Fig. 3 - XI - Percent Volatiles Uncured Prepreg, for 1 Hour at 325 ⁰ F	150
F.	Humidity Exposure Studies	151
	Fig. 4 - XI - Effect of Humidity on Uncured Prepreg	152
	Fig. 5 - XI - Days of Exposure to 100% Relative Humidity	153
G.	Effect of Permeability on Residual Volatiles	154
	Fig. 6 - XI - Weight Loss After Exposure to Dessication	155
	Fig. 7 - XI - Days of Exposure in 100% Humidity	156
	Fig. 8 - XI - Days of Exposure to 100% Relative Humidity Followed by 72 Hours of Desiccation.....	157
	Fig. 9 - XI - Hours Cured at 325 ⁰ F	159
	Fig.10 - XI - Percent Residual Volatiles versus Hours Cured at 325 ⁰ F	160
	Fig.11 - XI - Desorption Time Dependency Study In Air Circulating Oven at 325 ⁰ F	161
	Fig.12 - XI - Desorption Time Dependency Study In Vacuum at 220 ⁰ F	162
H.	Percent Resin Flow Test Procedure	163
I.	Prepreg Storage Conditions/Life	164
XII.	TRAVEL	168
XIII.	CONCLUSIONS.....	169
XIV.	RECOMMENDATIONS	171

I. INTRODUCTION

The interest in carbon-phenolic composite materials by NASA is due to its use as the ablative material in the solid rocket motor nozzle of the shuttle system. The shuttle system is a three component system composed of the Orbiter, External Tank (ET), and Solid Rocket Boosters (SRB), as shown in Figures 1 and 2. The Orbiter is the size of a large commercial airliner and weighs 178,000 pounds as constructed, and is capable of carrying 50,000 pounds of cargo, giving a total mass of approximately 228,000 pounds at lift-off. The Orbiter contains the crew quarters, the flight control systems (Guidance, Propulsion, Navigation, and Electronic), the cargo bay, and the main engines. There are three main engines which utilize liquid oxygen and liquid hydrogen as propellant. These engines furnish about 20% of the thrust during lift-off.

The External Tank contains the propellant used in the Orbiter's main engines: 143,000 gallons of liquid oxygen and 383,000 gallons of liquid hydrogen, approximately 1,585,000 total pounds of fuel. The tank is 154 feet long and is 27.5 feet in diameter and has a total mass of 1,660,000 pounds at lift-off. The external tank is the load bearing portion of the shuttle system as the Solid Rocket Boosters and Orbiter are both structurally attached. Since both the Orbiter and Solid Rocket Boosters generate thrust, the mechanical loading on the external tank is complex during the first two minutes of flight.

The two Solid-propellant Rocket Boosters are 149 feet long and 12.2 feet in diameter. Each Solid Rocket Booster has a total mass of 1,250,000 pounds at lift-off, which includes 1,110,000 pounds of solid propellant. A cut-away view of the Solid Rocket Booster is shown in Figure 3 along with the components mass distribution. The Solid Rocket Boosters furnish about 80% of the thrust at lift-off.

The complete shuttle system has a mass of approximately 4,500,000 pounds at lift-off which includes 3,805,000 pounds of propellant. The consumption of the fuel results is

Space Shuttle

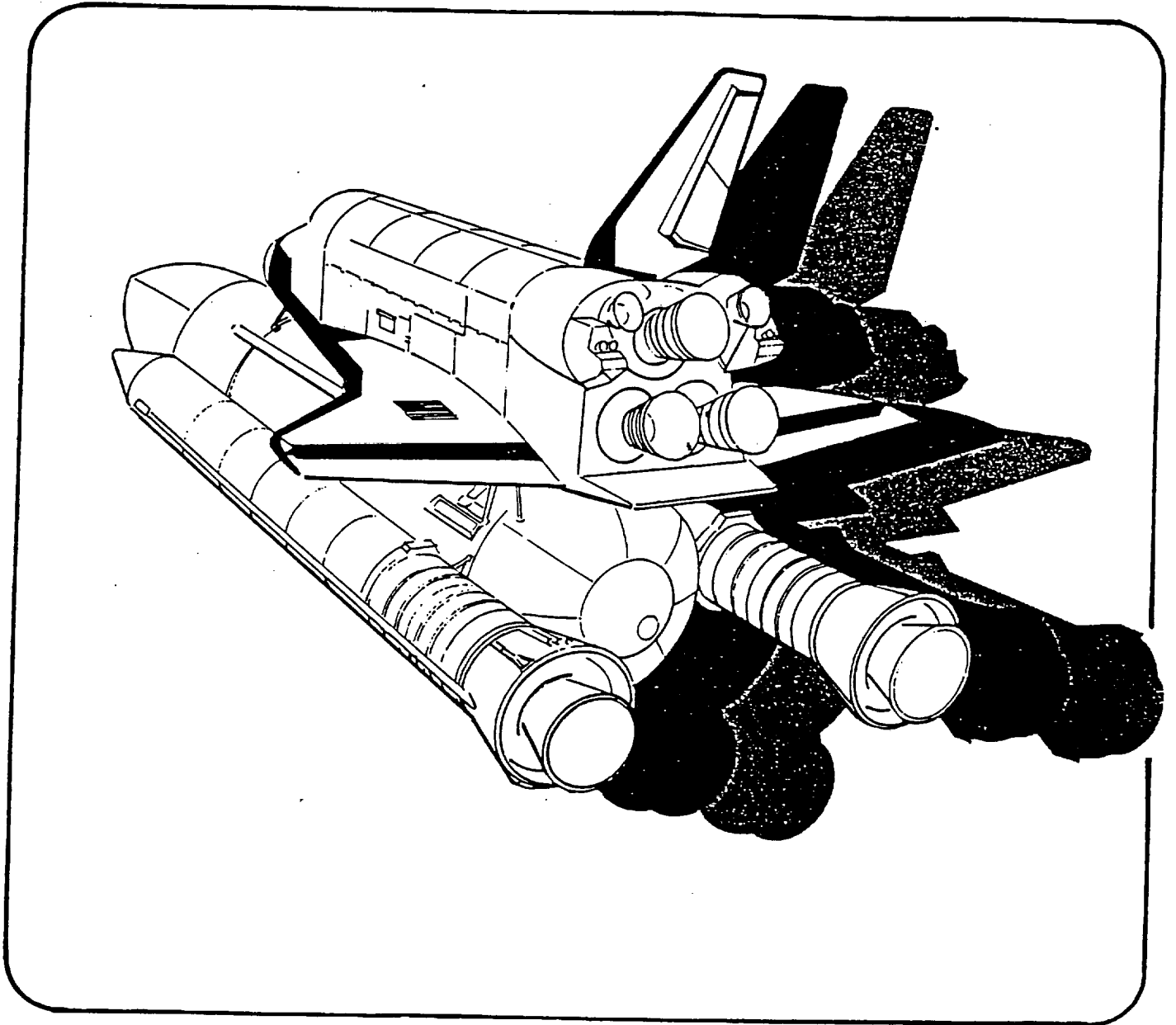


Fig. 1 - 1 - Shuttle

EXTERNAL TANK
MARSHALL SPACE FLIGHT CENTER

SOLID ROCKET BOOSTERS
MARSHALL SPACE FLIGHT CENTER

ORBITER
JOHNSON SPACE CENTER

SPACE SHUTTLE MAIN ENGINES
MARSHALL SPACE FLIGHT CENTER

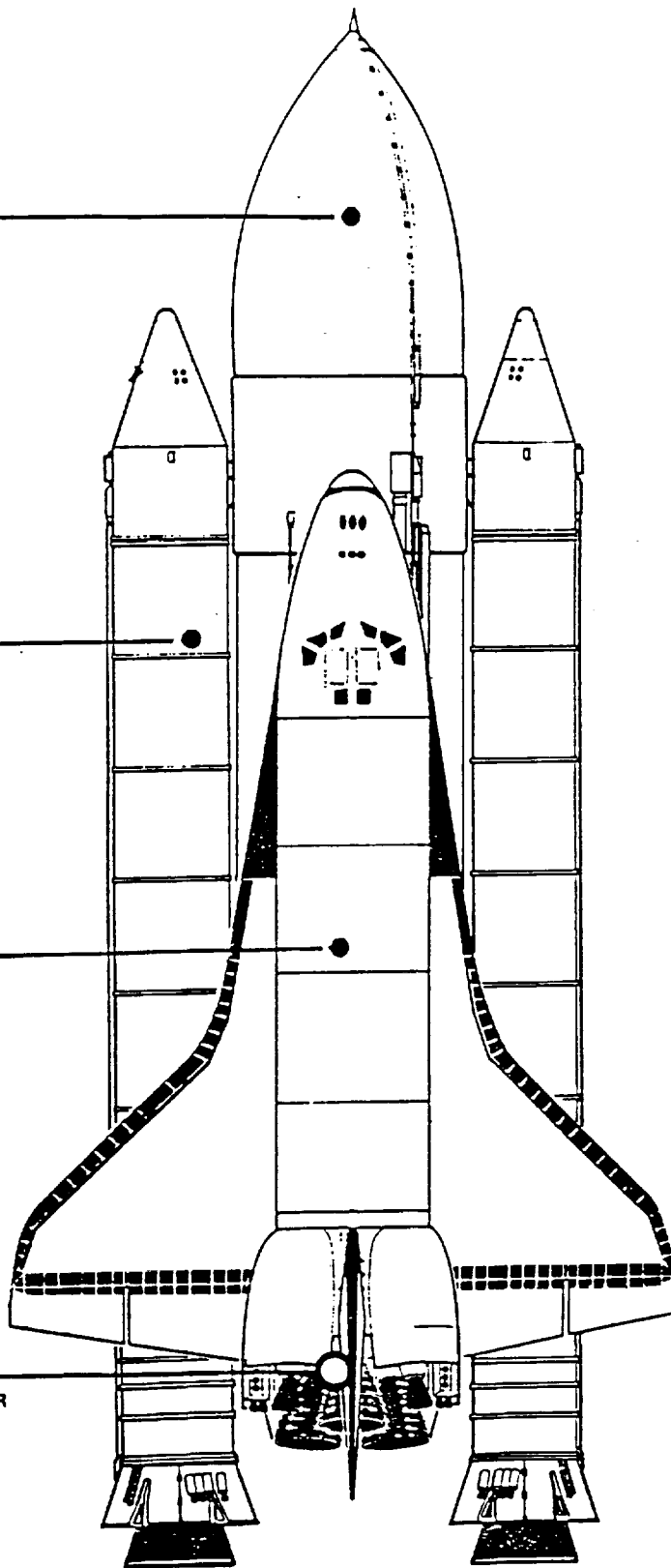


Fig. 2 - 1 - Top View Shuttle System

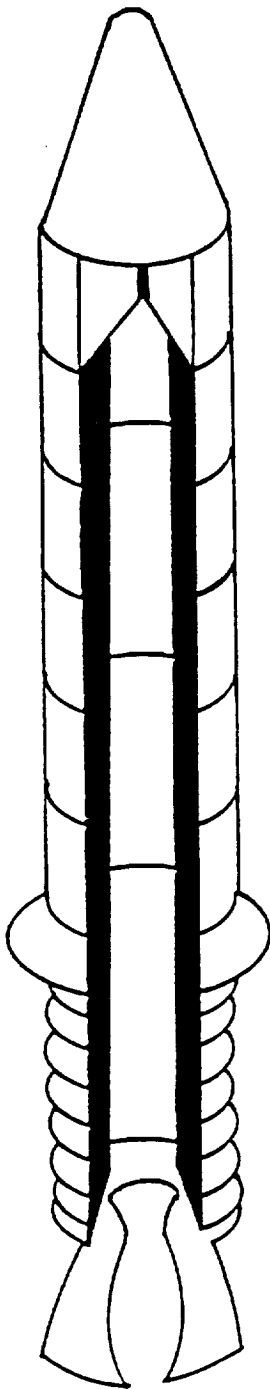
about 18,000 pounds/second reduction in the mass of the shuttle system during the first two minutes after lift-off.

SOLID ROCKET MOTOR (SRM) NOZZLE

A cut-away isometric view of the solid rocket motor nozzle is shown in Figure 4. Note that the exhaust gas flow will be from upper left down through the throat to the lower right when viewing the nozzle as shown. It can also be seen in Figure 3. The materials of construction of the nozzle are shown in Figure 5, with the outer layer always being carbon cloth-phenolic resin composites. The material of interest in this project. The nozzles are all made from 360° ring components and assembled into the completed nozzle as shown in Figure 6. The nomenclature of each ring section is also given in Figure 6 along with nominal effects of the completely consumed solid propellant on the carbon-phenolic material. The ring construction can be visualized if Figure 5 is used in conjunction with Figure 4, placing Figure 5 on the left side of Figure 4 and rotating counter clockwise 360°.

NOTE 1: The extreme heat and erosion of the burning propellant is controlled by the carbon-phenolic composite by ablation. Ablation is a complex process, but basically is a heat and mass transfer process where a large amount of heat is utilized to sacrificially remove material from the surface. Phenolic materials ablate with the initial formation of a char. The depth of the char is a function of the heat conduction coefficient of the composite. The char layer is a very poor heat conductor so it protects the underlying phenolic composite from the high heat of the burning propellant.

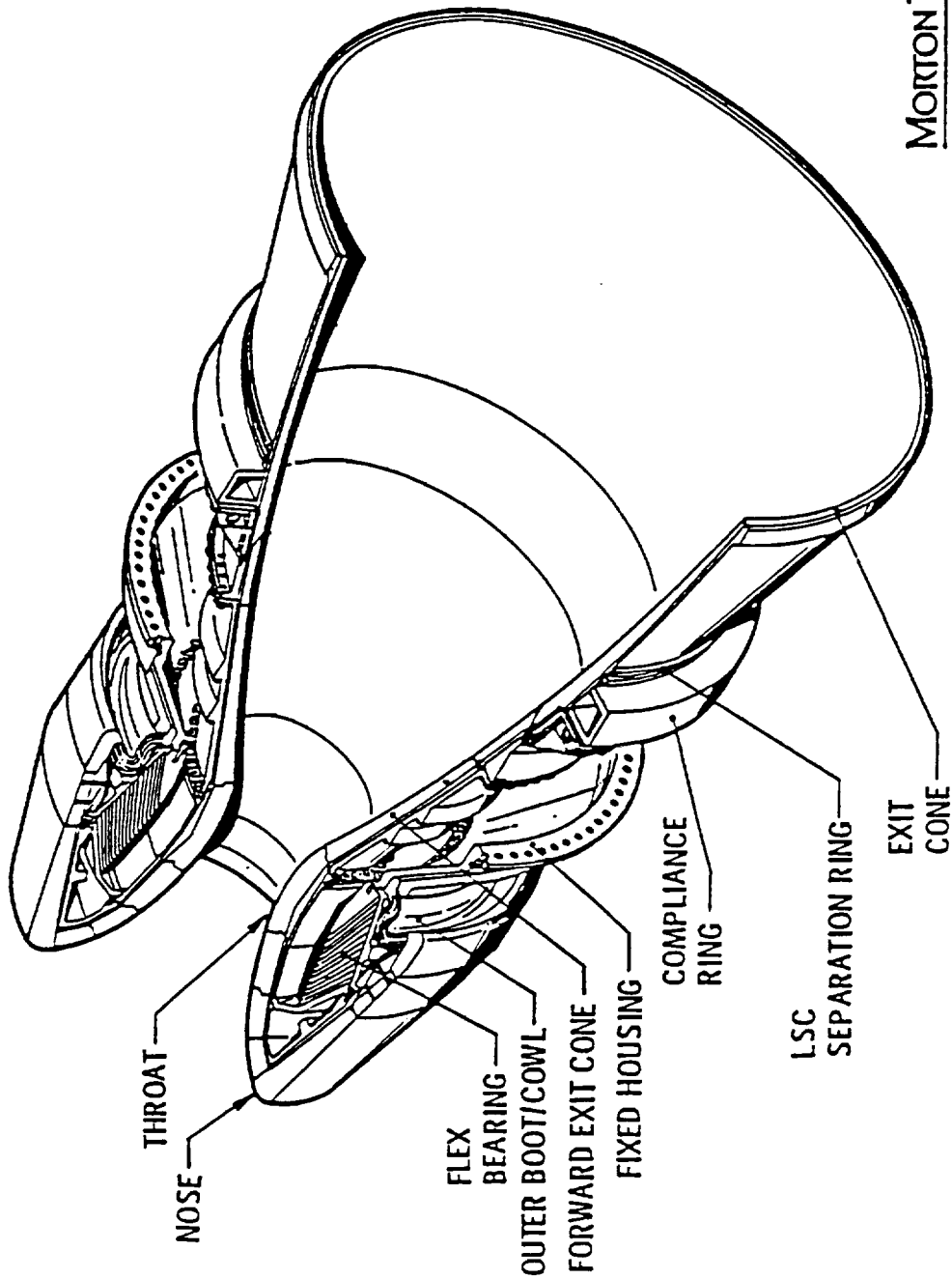
The solid rocket motors are manufactured by Morton Thiokol, Incorporated at Wasatch Division, Brigham City, Utah. The nozzle component ablative liners (carbon cloth-phenolic resin composites) are tape wrapped, hydroclave and/or autoclave cured, machined, and assembled. The tape that is utilized is from a prepreg broadcloth furnished by either of two qualified suppliers. The materials flow sheet for the nozzle ablative liners are



Item	Weight (lb)
Case	98,196
Insulation	18,670
Liner	1,345
Inhibitor	1,895
Nozzle Assembly	23,317
Igniter Assembly	479
System Tunnel	546
Instrumentation	12
Assembly Attach Provisions	286
External Insulation	501
Controlled Inerts	145,247
Uncontrolled Inerts	231
Total Inerts	145,478
Motor Propellant	1,110,136
Igniter Propellant	137
SRM Assembly	1,255,751

Fig. 3 - 1 - Solid Rocket Booster

SRM NOZZLE



MORTON THIOKOL, INC.
Wasatch Operations

Fig. 4 - 1 - SRM Nozzle

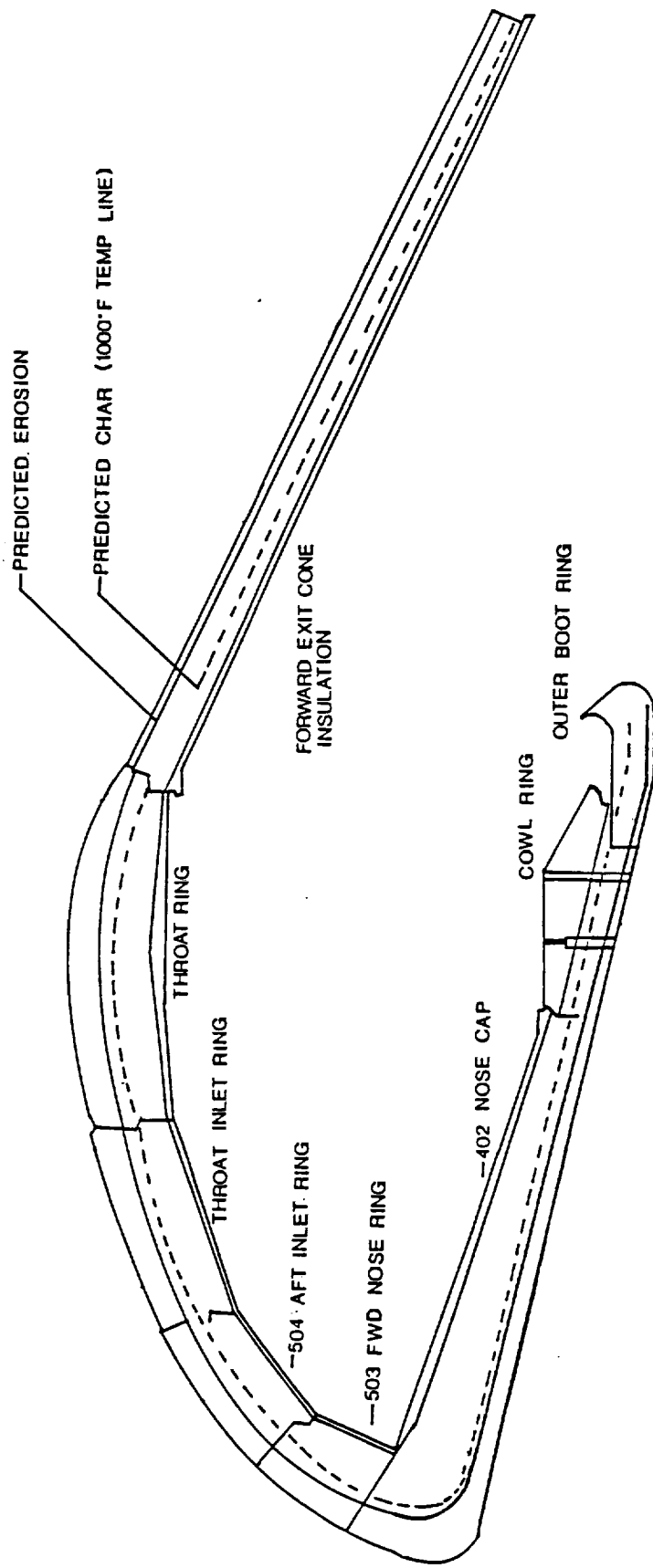


Fig. 6 - 1 - Construction of Nozzle

Materials Supplier Flow Sheet for Carbon Phenolic Nozzle Components

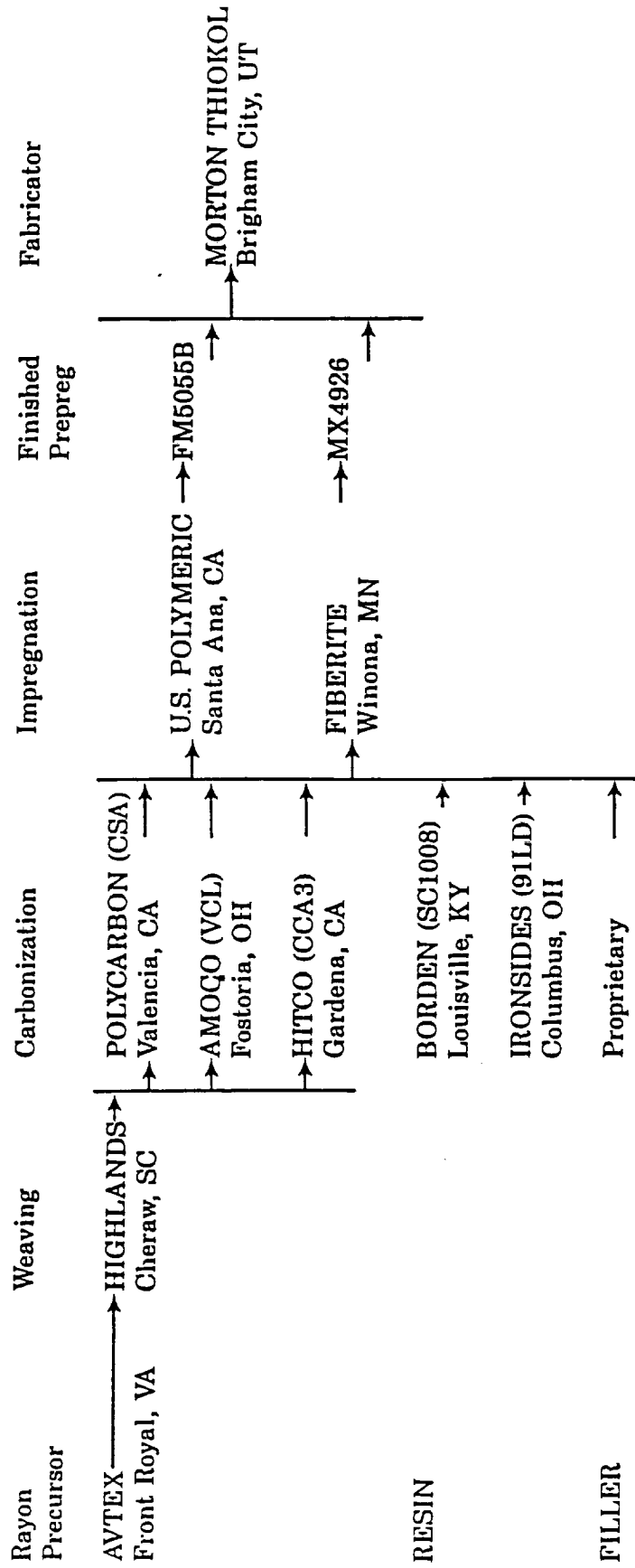


Fig. 7 - 1 - Material Supplier Flow Sheet

shown in Figure 7. The prepreg is a three component system: phenolic resin, carbon cloth, and carbon filler.

II. NOZZLE MANUFACTURE

The resin filler and cloth are combined to form prepreg at the sites of the two prepreg suppliers. The resin and filler are mixed in a large heated container and the cloth is drawn through this solution. Impregnation is accomplished by gravity or rolling the cloth through dual rollers as shown in Figure 1.

The prepreg is shipped to MTI as rolls of broadgoods, approximately 50" wide. The broadgoods are bias cut and the resulting parallelograms are sewn together at the ends to form a new roll. These rolls are slit into proper widths for tape wrapping, 5 to 8 inches, and then rolled onto cardboard cores to size of 15 to 18 inches in diameter. The bias cut is necessary for the prepreg to conform to desired configuration. The tape is wrapped on a rotating mandrel which has been machined to generate the desired inside shape. The wrapped part is debulked periodically by applying heat and pressure to the tape, forcing it against the mandrel. Debulking decreases changes in shape, volume, and tape movement during curing. The debulked part is cooled by a blast of cold CO₂ to stop staging of the resin immediately after the roller passes.

After wrapping is completed, the billet and mandrel are bagged for further processing. The bagging material consist of layers of perforated film, bleeder cloth, and vacuum bag (inside layer to outside layer). A vacuum is pulled on the system, which is then placed in an autoclave. A vacuum is continuously pulled inside the vacuum bag as the autoclave is pressurized to 250 psig and temperature raised to 310°F. A generalized autoclave cure cycle is shown in Figure 2. The vacuum is used to help pull off the volatiles as the phenolic resin is cured.

Upon completion of the autoclave cure, the outside surface of the billet is machined to required dimensions using proper grinding equipment.

The billet and mandrel are then prepared for the hydroclave cure by bagging with layers of perforated film, bleeder cloth and water tight rubber bags (inside layer to outside layer). A vacuum is then pulled on the system, which is then placed into the

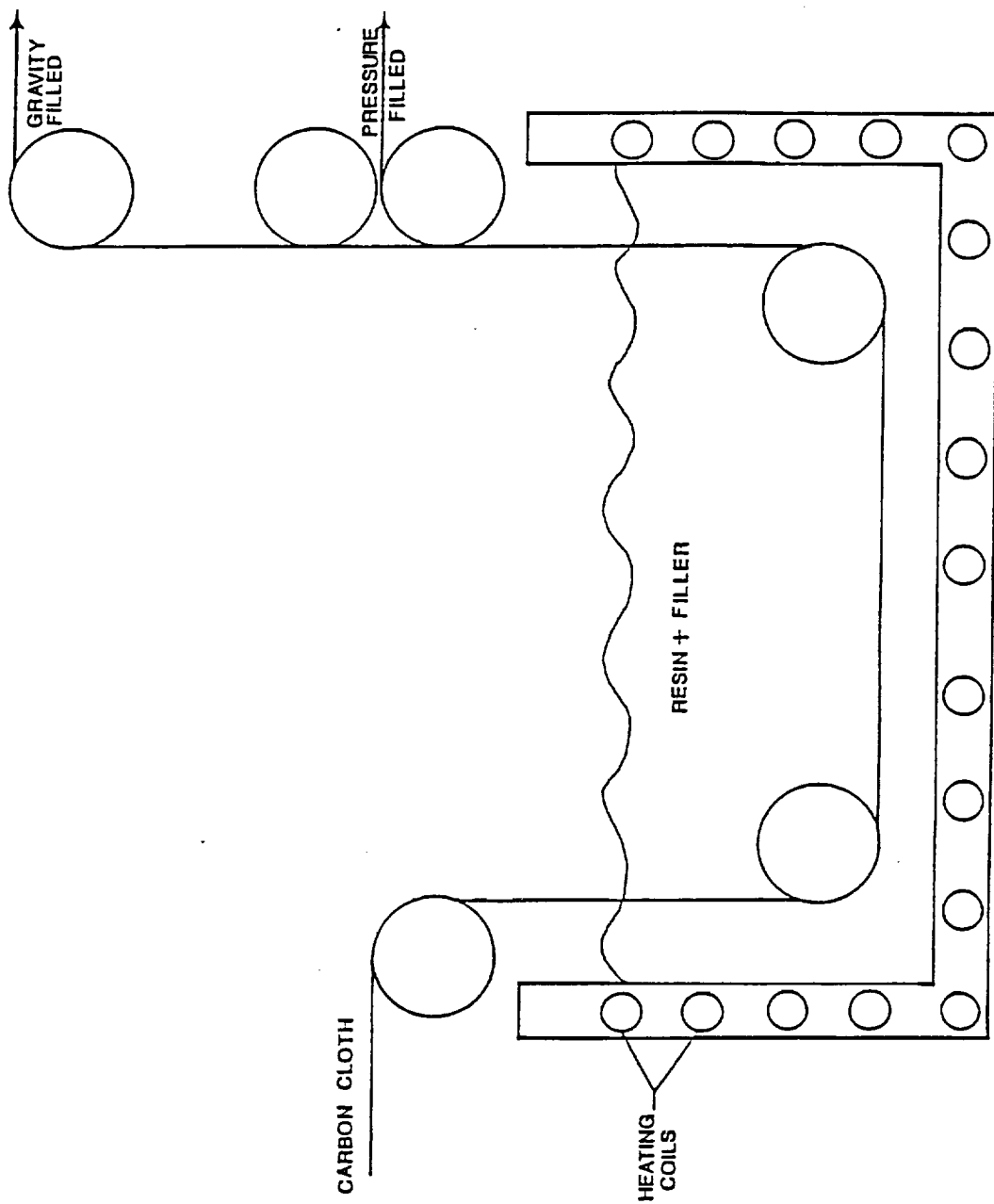


Fig. 1 - II - Impregnation of Cloth

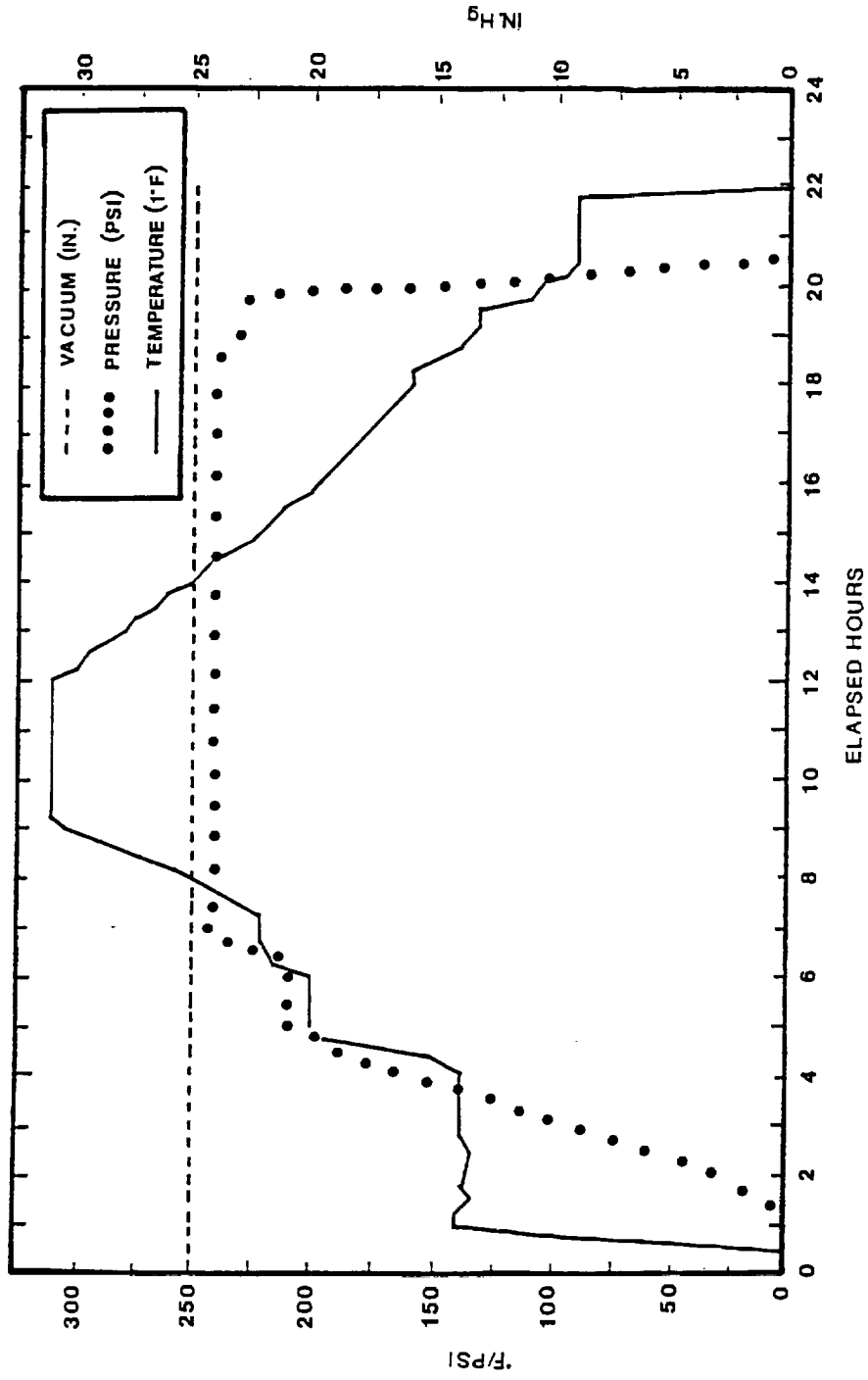


Fig. 2 - II - Generic Autoclave Curing Cycle for Carbon-Phenolic Composites

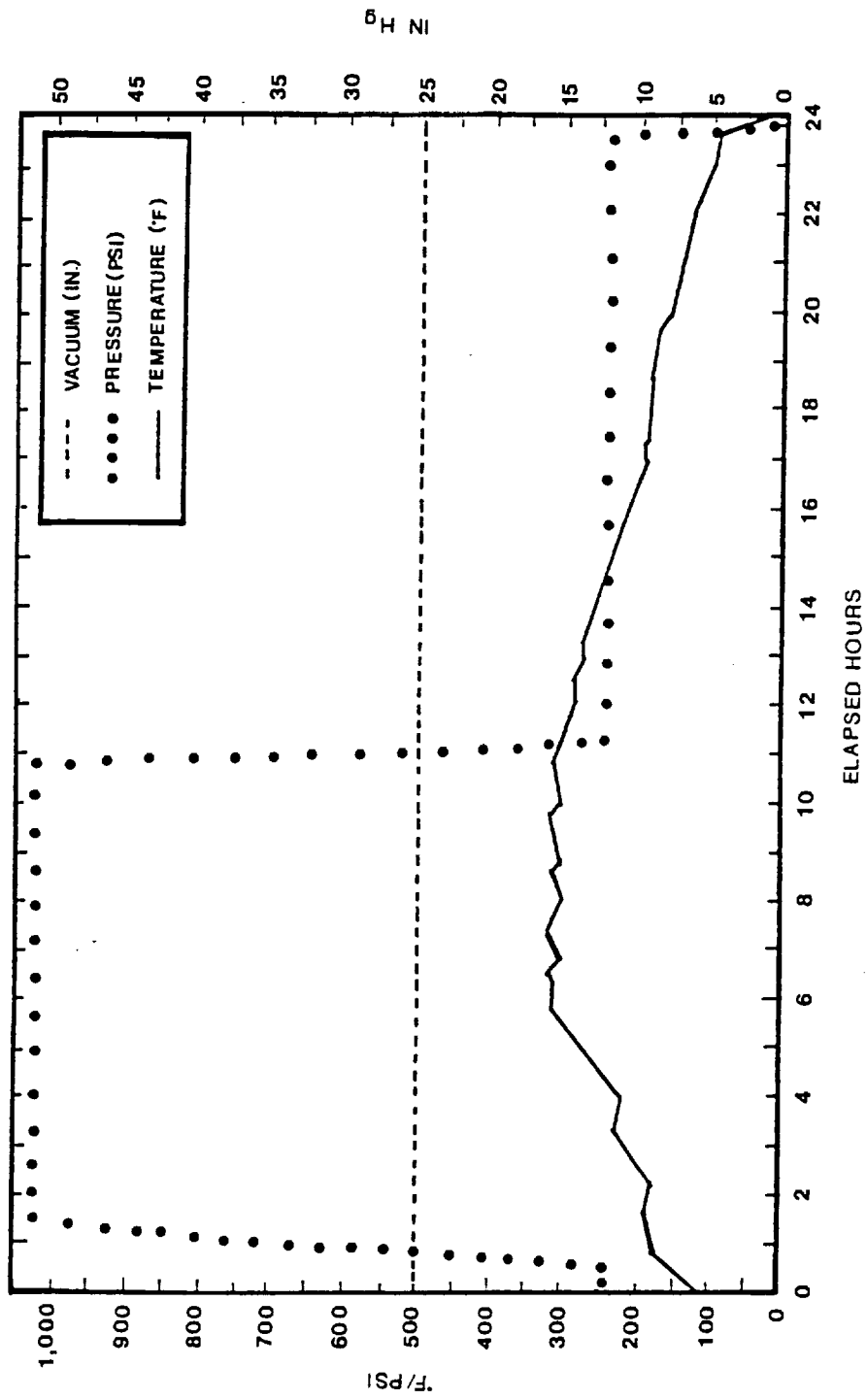


Fig. 3 - II- Generic Hydroclave Curing Cycle for Carbon-Phenolic Composites

hydroclave. The hydroclave is pressurized to 1000 psig and temperature raised to 310°F and these conditions maintained for approximately 5 hours. The autoclave/hydroclave cure may be reversed or left off depending upon the particular part being processed. After the final cure is completed, the part is machined to specifications, examined by nondestructive evaluation (NDE) for defects, and then placed in storage.

III. PHENOLIC RESIN

Generically, phenolic resin are produced from the reactions of phenols and formaldehyde.

The polymers derived from the interaction of formaldehyde and phenols differ in one important respect from other polycondensation products, in that polyfunctional phenols can commonly form a variety of isomers of varying chain length, with the additional possibility of cross linkages. The products derived from polycondensation of amines with acids (polyamides) and of alcohols with acids (polyesters), are certainly mixtures of various chain length molecules, but for a molecule of a certain chain length, only one type structure is possible, because the monomers are monofunctional. As a result, kinetic and related studies are feasible, on the assumption that the growth of a chain proceeds from one polymer length to the next in a smooth and regular manner. But in the case of the aldehyde-phenol polymers because of the polyfunctional nature of the monomers there are numerous and varied crosslinks. Each step of the reaction producing a chemical configuration which may or may not be similar to the preceding one, its physical properties may have been altered; for instance, its melting point changes. The only consistent and regular change for these polyfunctional growth reactions is that you have continuous increases in molecular weight.

Polyfunctional phenols may react with formaldehyde in positions both ortho and para to the hydroxyl group which means that the condensation products will exist as numerous positional isomers for any chain length. This peculiarity not only makes kinetic studies extremely difficult, but also makes the organic chemistry of the reaction very complex and tedious to unravel. There is a further problem, in practice the most useful form of the aldehyde-phenol resins are the hardened, cross-linked type, which are not amenable to most of the common methods of chemical or physical examinations. At least as early as 1872, it was known that resinous material could readily be formed by the interaction of aldehydes and phenols from the work of von Baeyer et al. The initial experiments resulted

In soluble amorphous products whose properties elicited little interest. In the late 1880's insoluble, cross-linked products were reported, but attempts to repeat these experiments were generally not very successful, in that no two reaction products of the same process had exactly the same properties. O-hydroxybenzylalcohol was formed by a low temperature, alkaline catalyzed reaction of formaldehyde-phenol in 1894. The first patent for an aldehyde-phenolic resin product intended for use as a substitute for hard rubber was approved in 1889. Ortho- and Para-Methylolphenol patents were issued in 1894 and 1895 respectively. In the early 1900's, the first commercial product was produced as a substitute shellac for the Louis Blumer Company, using a ratio of one mole of aldehyde per mole of phenol. In 1907, Dr. Leo Baekeland (Charter Member AICHE) produced a product of commercial importance from the reaction of formaldehyde and phenol under laboratory conditions, which became known as bakelite, and sometimes called the first of the plastics, it was a hard and crystalline material. In 1909, two patents, which were the basis for infra-structure of aldehyde-phenolic resin industrial development, were issued to Baekeland describing the difference between acid and alkali catalyzed reactions. In 1909 Baekeland presented a paper in which he described a resin made with acid catalysis using a formaldehyde to phenol ratio of less than one which came to be known as a "novolac". The aldehyde-phenolic resins of chemistry began to grow quite rapidly after this and their development can be divided into four periods of time as follows:

1. From the earliest investigations up to about 1907, was the period when general information was being accumulated on the types of polymer products obtained by the condensation of aldehydes and phenols under various conditions, such as time, temperature, pressure, catalyst, and ratios of the monomers.

2. During the period from 1907 to approximately 1920 was the time during which speculations on the structure of the resin, as they were commercially developed were being discussed. During this period the Bakelite Corporation dominated the industry. There was little or no new experimental work done during this period. Through the years

there continued to be speculation and studies on the structures of these polymers but little was accomplished in establishing the molecular configuration of the compounds, during the time frame of 1907-1920. The polymers during this time did become divided into two classes; one based on the pH of the catalyst and the second based on the ratio of raw materials, whether the F/P ratio was greater or less than one.

3. Little or no new or different experimental production investigations, either chemical or physical, were performed during the years between 1920 and outbreak of World War II in 1939. During this period, the probable structure of the main features of novolaks was established. Novolak (present day spelling) is the name applied by Baekeland to the aldehyde phenol resins formed with acid catalyst and a slight molar excess of phenols (ratio of less than one F/P). These have stable compositions and do not react, or polymerize with other novolaks without heat and hardening agents. Data was accumulated and hypothesis advanced on the more complex structures of resoles, but little of definite characterization was accomplished as to their chemical structure. Resoles are base catalyzed formaldehyde phenol resins made with excess aldehydes, these polymers were also being investigated concurrently with the novolaks and produced long chain and cross-linked compounds in some respects quite similar to novolaks.

4. Systematic examination of the behavior of aldehyde phenol complexes, confirmation of the structure of novolaks and resoles as ascertained in the third period, and a considerable amount of investigative work on the synthesis of complex aldehyde-phenols and related compounds has been performed between the end of World War II and the present day. As a result of these later investigations, a much clearer picture has evolved in regard to resole and novolak structures, although it would be an exaggeration to suggest that all the details have, even now, been resolved. Modern day instrumental technology along with the "need to know" in these later years has led to the accumulation of considerable knowledge relating chemical structure to physical and mechanical properties.

Most studies have been directed at controlling the molecular structure by varying the ratio of aldehydes to phenols, heat, pressure, time and catalysis, in order to obtain desired properties of final polymers. Research performed by varying aldehyde-phenol ratios developed two classes of polymeric materials called Bakelite resins. Base catalyzed resins, called resoles prepared with higher than a 1:1 mole ratio of formaldehyde-phenol ratio, can be used to form crosslinked, insoluble, and infusible compositions in a controlled fashion, whereas, the lower than 1:1 mole ratio of formaldehyde-phenol, the products remain soluble in many organic solvents. Acid catalysis yield permanently stable compositions, called novolaks; whereas base-catalyzed materials can be advanced in molecular weight, becoming more viscous; simply by increasing temperature.

The pH of a F/P mixture of 1:1 in solution form made with the 37-40% formaldehyde solution and pure phenol is about 3.0, this may be taken as a reference or "neutral point" in the study of these polymers. An acid catalyst is added to lower the pH, produces a change in the rate of reaction that is proportional to the change in the rate of H ion concentration. A basic catalyst may either be a mineral or organic base. The pH of 4-7, an intermediate range, and 7-11 a more basic one, are the two basic ranges which result in somewhat different types of reactions.

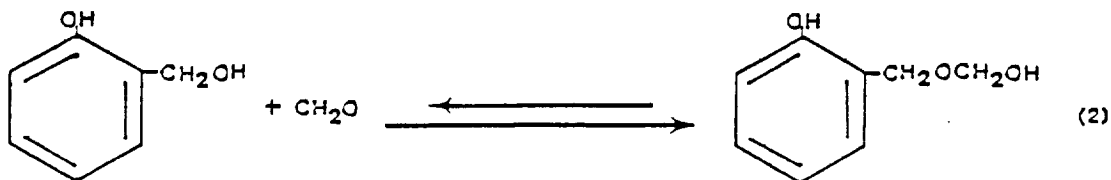
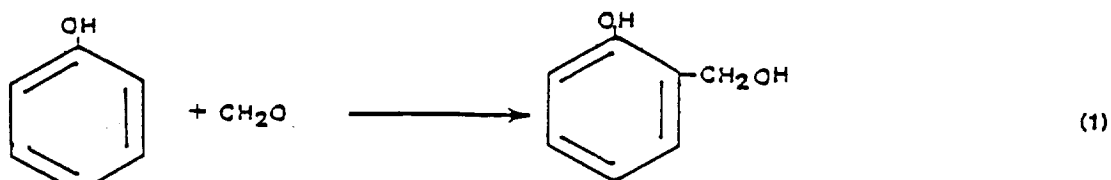
The resins of interest in this project, are base-catalyzed resoles. The molecular structure and physical properties of the resins depend on the specific catalyst and molecular ratio of the reactants used, as well as the time, temperature, and pressure of the polymerization process. As phenol is multi-functional, resole phenolic resins are produced by a formaldehyde-phenol molar ratio range of 3.0 to 1.0 under basic conditions, and result in long chain and much cross linking of polymers.

Phenols combine with aldehydes or ketones to form a variety of products. The nature of the product depends on the choice of the phenol and the aldehyde or ketone and on the conditions of reaction, as well as the ratio of the monomers. Most of these reactions take place in solutions of "inert" organic solvents. Inert in the sense that they

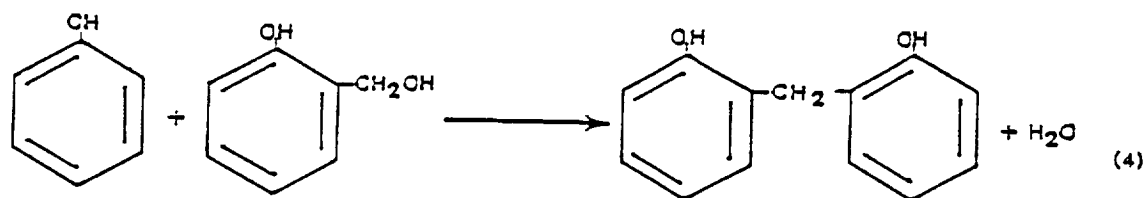
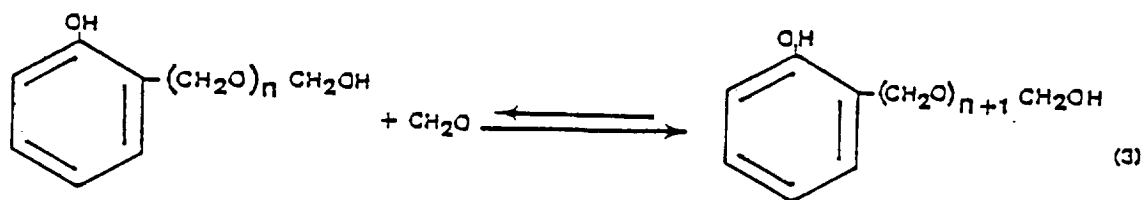
are simply carriers for the polymerization process of the aldehyde and phenol compounds. The two most common polymer reactions are the addition of methylol groups to the phenol and the subsequent formation of a methylene derivative of a biphenol. The dimers possessing methylol groups (Eq. 1) are commonly referred to as phenol alcohols; the short-chain two ring methylene derivatives (Eq. 5) are known as dihydroxydiphenylmethanes. The long-chain resins, whose commercial importance overshadows all other aldehyde-phenol products, are polynuclear products derived from the simple methylol and methylene derivatives mentioned above.

The phenol alcohols occupy a position of major importance among the numerous products derived from phenols and aldehydes or ketones. Besides being intermediates in the manufacture of most, if not all, resinous phenolic products, they represent in themselves an interesting class of highly reactive organic chemicals. It is possible to prepare phenol alcohols from nearly all phenols having at least one free, (Free in the sense that the position has only a reactive hydrogen) position, ortho or para on a ring carbon atom. Because of their commercial importance and high reactivity, the phenol alcohols based on formaldehyde will be considered in greatest detail.

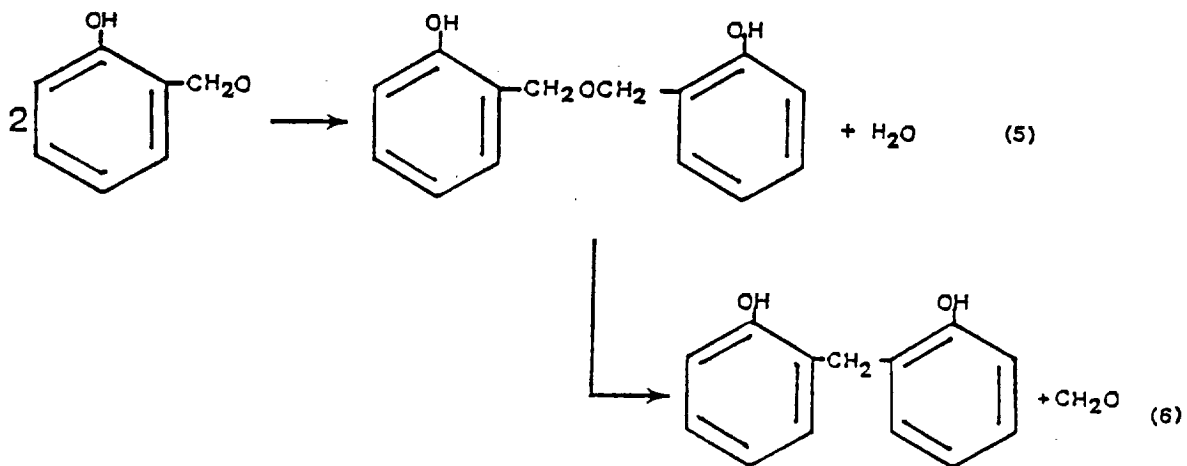
In the synthesis of formaldehyde-phenol resin numerous different types of reaction have been established. Among these are hydroxymethylations of phenol and variously substituted phenolic rings (Eq. 2-3). This reaction is called methylolation or hydroxymethylation, and exist in complex equilibria with other products and the raw materials.



In the formation of aldehyde-phenols there are condensation reactions illustrated in the equation below (4). Equation 4 represents the formation of a methylene bridge structure with the splitting out of a water molecule. This methylene bridge formation is usually referred to as cure. The term cure simply refers to the condensation polymerization step with the splitting out of a molecule of water, and is applied to the reactions forming methylene bridges as a resin increases in molecular weight.

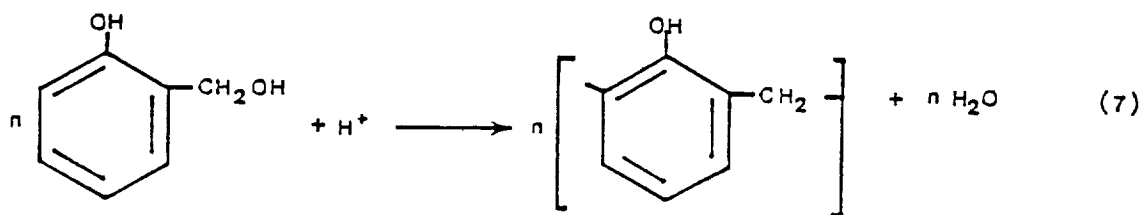


In Equation 5 below a reaction between two molecules of aldehyde-phenols is shown, a condensation polymerization reaction resulting in an ether linkage. The methiol group on a phenol alcohol is very reactive, and may enter into a variety of other chemical combinations that can affect the resin properties. For example, this ether linkage may undergo further condensation reaction to produce a methylene linkage and liberate an aldehyde as shown in Eq. 6. This ether type linkage is unstable which causes the additional step in the reaction.



The mechanisms and specific rates of many of these reactions are known to be different and markedly dependent on factors such as pH, catalyst, temperature, and pressure, and ratio of aldehyde to phenol. Methylation frequently takes place rapidly upon the mixing of reactants, and the reaction is reversible. The reaction is catalyzed by either acids or bases. The formation of the high molecular weight polymer chains and networks is irreversible under the conditions of use. This curing reaction, the splitting out of molecules of water and/or aldehydes, may be carried out using either acid or basic catalysts. The splitting out of the aldehyde simply amounts to providing an additional aldehyde for further polymerization.

Under acid conditions, the methylolphenol quickly condenses to form a low molecular weight polymer (hydroxyphenylene methylene) as follows, Eq. 7:

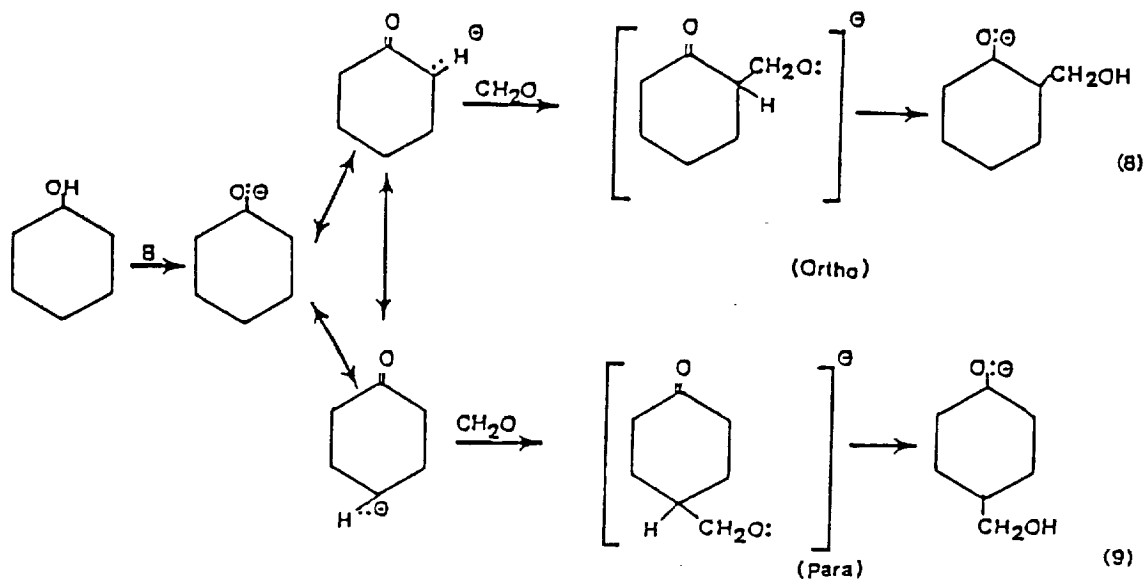


Under basic conditions the monomeric acid and dimeric methylool derivatives are stable.

This aldehyde-phenolic resin formed under acidic conditions (novalac) are generally infusible but soluble in some polar organic solvents. Under basic catalytic conditions the resulting polymers are called resoles. Since the aldehyde-phenolic resin, used as the matrix in the manufacture of 2D carbon/phenolic composites, is formed under basic conditions, the remainder of this discussion will emphasize the chemistry of the resole aldehyde-phenolic resins.

Prepolymers of Resole Resins

The phenol-formaldehyde reaction under base-catalyzed conditions is similar to the Aldol condensation reaction and forms ortho- or para-methyloolphenol, (Eq. 8 and 9) as shown below.



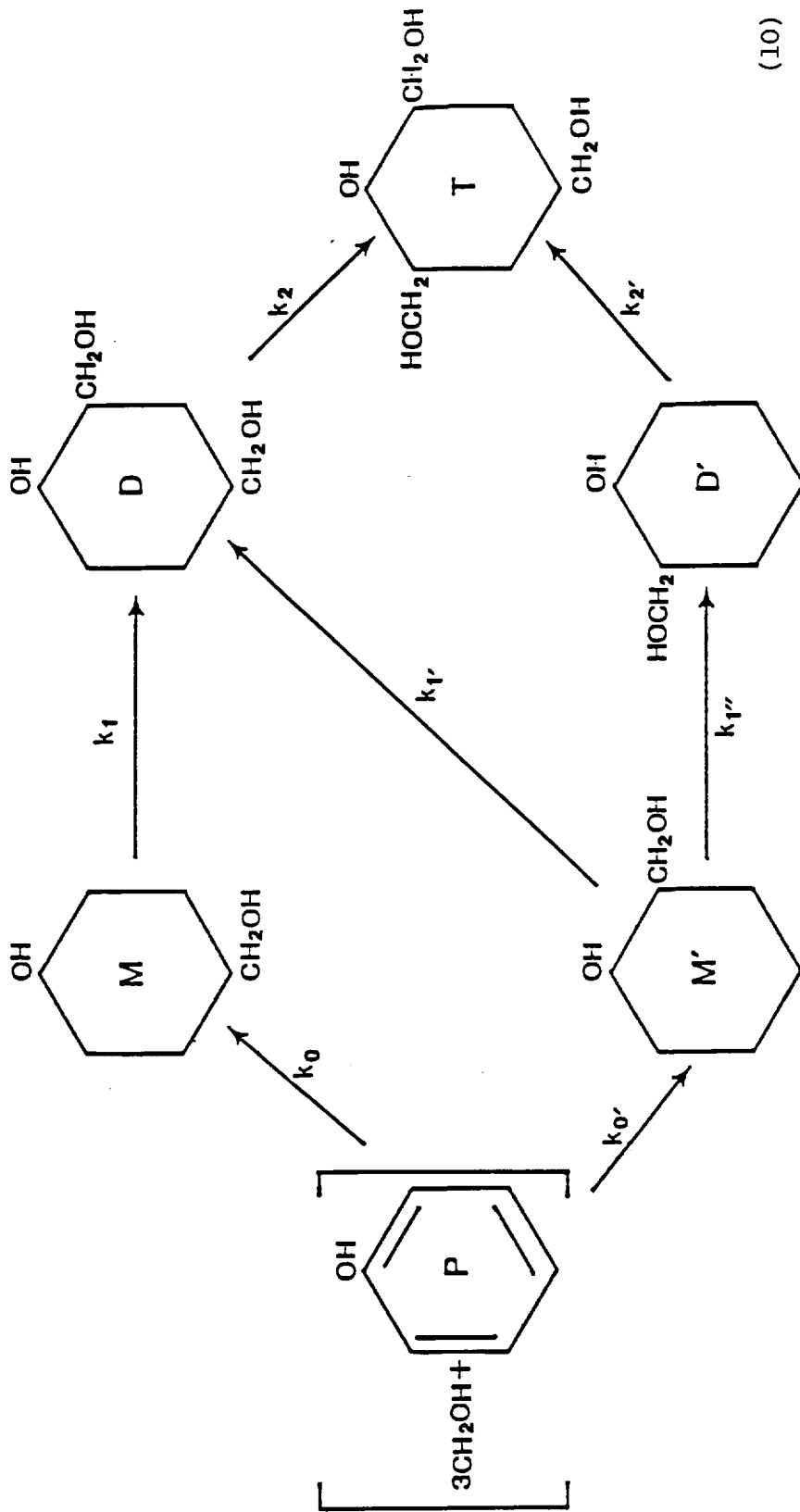
The above reaction, Eq. 8, represents the ortho reaction, a para position reaction, Eq. 9, is similar with an equilibrium between the two but shifted toward the ortho side. Organic amines, inorganic hydroxides and quarternary ammonium compounds are frequently used as catalysts in these reactions. The above reaction (9) was studied by Martin. In his research on this subject, all reactions were carried out at 30°C, and the amount of formaldehyde used was equivalent to the total number of (three) available reactive phenolic nuclear positions, the two orthos and the para. This provided for complete conversion to trimethylolphenol (Eq. 10), and in order to preclude possible differences in ionization constants for the several reactions, one equivalent of NaOH catalyst was used, in all cases.

In the presence of an excess amount of formaldehyde the monomethylol phenol will react further to form the three possible ortho-para dimethylol derivatives and will eventually be converted to 2,4,6,- Tri(hydroxymethyl) phenol, or Trimethylolphenol as shown in Eq. 11.

The numerical values of each of the reaction rate constants are given in Table 1 at 3:1 F/P ratio as determined by Freeman and Lewis using a quantitative paper chromatographic technique. Freeman and Lewis further showed that essentially no substitution occurs at either of the two meta positions. Presumably because of lack of necessary spacial arrangement.

Table 2 gives the relative reactivities of the nuclear positions for the reaction of various phenol alcohols with p-Methylolphenol serving as the reference phenol.

From the data on the relative reactivities of the various methylolphenols Freeman and Lewis also have made predictions as to the course of the reactions where less than 3 moles of formaldehyde per mole of phenol is used. It was thought that o-methylolphenol would be the first product formed in appreciable quantity. The o-methylolphenol concentration in the reaction mixture, after an early increase, would then remain



(10)

TABLE 1

REACTION RATE CONSTANTS FOR PHENOLS AND METHYLOL PHENOLS WITH FORMALDEHYDE

<u>Rate Constant</u>	Second Order Rate Constant (l/gmole/sec.)
k_0	6.2×10^{-6}
k_0'	10.5×10^{-6}
k_1	7.5×10^{-6}
k_1'	7.3×10^{-6}
k_1''	8.7×10^{-6}
k_2	9.1×10^{-6}
k_2'	41.7×10^{-6}

TABLE 2

REACTIVITY OF INDIVIDUAL NUCLEAR POSITIONS IN METHYLOLPHENOLS

<u>Compound</u>	Position Relative <u>to Phenolic Hydroxyl</u>	Relative Reactivity (p-HBA 1.0)
p-Methylolphenol	ortho	1.0
Phenol	ortho	1.4
Phenol	para	1.7
(Methylolphenol)	para	2.0
(Methylolphenol)	ortho	2.3
2.4-Dimethylolphenol	ortho	2.4
2.6-Dimethylolphenol	para	11.1

essentially constant for sometime since its rate of reverse reaction would be about as great as its rate of formation. It would be the first phenol alcohol to disappear as the process continued. The p-methylolphenol would appear later than the ortho isomer, but it would increase in concentration as the reaction proceeded. 2,4,-dimethylolphenol would appear still later and would, owing to its low reactivity, become in time a major constituent of the reaction mixture. On the other hand, 2,6-dimethylolphenol, because of its very high reactivity, would never be found in large quantity. These predictions are in general agreement with the results obtained by Sprengling and Freeman by analysis of a reaction mixture obtained with a 4:1 mole ratio of formaldehyde to phenol.

DeJong et al made a detailed study of the hydroxymethylation of phenols in the pH range 1-11 and between 70° and 130°C in dilute aqueous solution. The rate constants were found by taking the tangent of the conversion plot at zero time. The rate equation is:

$$(dF/dt)_{t=0} = k[P]_0^n [F]_0^n$$

Where $[P]_0$ and $[F]_0$ are the initial concentrations of phenol and formaldehyde. It was concluded that the reaction was bimolecular since the initial rates were nearly proportional to the concentration of both reactants. The rate of reaction was found to be directly proportional to the hydroxyl ion concentration above a pH of 5 and up to approximately 1 mole of caustic per mole of phenol. A minimum in the rate was found at a pH around 4; below this, the reaction shifted to one catalyzed by acids. The pH of 4 here agrees reasonably well with the earlier suggestion that an equally molar ratio of formaldehyde/phenol which has a pH of about 3 could be considered a reference or "neutral" point, for reactions of this type.

Orientation of methylol groups was studied by Sprengling and Freeman in 1950. Assuming that both an ortho and a para position relative to the phenolic hydroxyl group were available for reaction, the question arose as to where the methylol group would enter the benzene ring. A study of the reaction at a ratio of 1 to 1.4 F/P, using sodium hydroxide as catalyst, was made. When the reaction was complete, the phenolic hydroxyl groups of the phenol alcohols were etherified by treatment with oxygen to carboxylic acid groups according to a scheme by Meyer. The acids were used to estimate the quantity of each phenol alcohol present in the original mixture. An inspection of the data shows that the p-methylolphenol and the 2,4-methylolphenol were the major products (Table 3).

Martin made a similar study using 2.1:1 mole ratio of formaldehyde to phenol. At this ratio, the p-methylolphenol and the 2,4-methylolphenol were also found in greatest quantity. At the higher formaldehyde to phenol ratio, a small quantity of the 2,6-dimethylolphenol also was detected. A study of the data in Tables 1, 2, and 3 show reasonable agreement.

These factors have been studied in detail by Freeman and Lewis, and a graph depicting the formation and disappearance of each phenol alcohol capable of formation and disappearance from phenol by the addition of one, two, or three methylol groups to sodium phenate has been plotted. This graph is shown here as Fig. 1 on next page. The effect of methylol substitution on the overall rate of formaldehyde consumption also has been analyzed. As methylol substitution proceeds, the apparent reactivity of the system, formaldehyde-phenol, clearly increases. This increased reactivity of the system is caused by the formation of methylolphenol and 2,6-dimethylolphenol, both of which are more reactive with formaldehyde than is phenol, refer to Table 2. The rate of reaction eventually levels off and approaches that of 2,4-dimethylolphenol, the last remaining component of the system that is reactive with formaldehyde.

Era et al have studied the effect of the mole ratio of formaldehyde to phenol on the reaction kinetics using DSC and DTA. They found the activation energy of the addition polymerization to be about 99 KJ/mol and for the condensation reaction the activation energy was about 81 KJ/mol. The addition reaction was shown to be second order, where as the condensation reaction was first order. It was also found that the higher the F/P ratio, the lower the heat of reaction. F/P of 1.0 gave a heat of reaction of 370 J/g, where as a F/P of 1.2 gave a heat of reaction of 150 J/g.

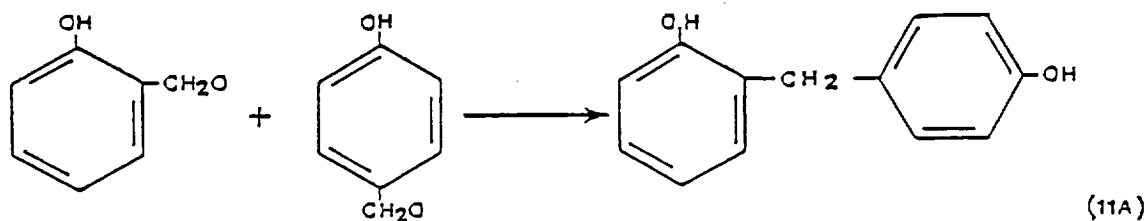
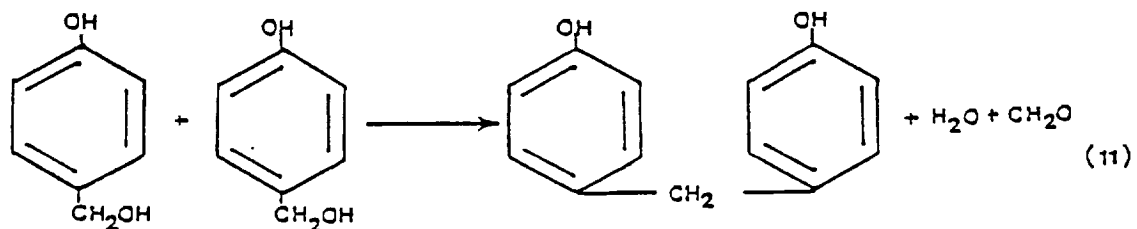
TABLE 3
REACTION PRODUCTS OF THE
FORMALDEHYDE-PHENOL REACTION

<u>Components of Reaction Products</u>	<u>Mole % present</u>
Phenol	5-10
o-Methylolphenol	10-15
p-Methylolphenol	35-40
2,4-Dimethylolphenol	30-35
2,6-Dimethylolphenol	none
2,4,6-Trimethylolphenol	4-8

Dihydroxydiphenolalkanes can be obtained by the direct reaction of aldehydes with phenols under basic conditions. Although the products may be identical with those formed with acidic catalysts, the mechanism of reaction is much different. Phenol alcohols are the first products formed in the reaction when basic catalysts are employed. If the phenol alcohol is relatively stable under alkaline conditions the reaction may tend to stop at this stage. However, most phenol alcohols do not exhibit such stability and may be converted to dihydroxydiphenylalkanes by continued heating with aqueous caustic. In general, phenol

alcohols with para methylol groups show a greater tendency toward conversion to a methylene derivative than those with an ortho methylol groups. As might be expected, phenols which are capable of reacting readily with formaldehyde to form a methylol derivative are usually equally capable of forming a methyl derivative. 2,6-Dimethylphenol, 2,4,5-trimethylphenol, 2,4,6-trimethylphenol, and B-naphthnol are particularly susceptible to rapid conversion to a methyl derivative under alkaline conditions.

Dihydroxydiphenylalkanes (methylene bridge) presumably could be formed by either of two mechanisms under alkaline conditions. The formation of an intermediate phenol alcohol could react with free phenol in the system to give a methyl derivative as shown in Eq. 5, splitting out a molecule of water or the reaction could occur between the two phenol alcohols with the splitting out of a molecule of formaldehyde and a molecule of water, Eq. 11, in which case the molecule of formaldehyde is available for further polymerization. The methylene bridge being the more stable of the two, would dominate in an equilibrium situation. Also, the same equations do occur in the ortho position, or even one molecule having an ortho methylol and the second one having a para methylol group, as shown in (11A) above.



The condensation of phenol alcohols with each other under alkaline conditions is more likely to give a dihydroxydiphenylalkanes free of by-products than other reactions, but the reaction conditions must be carefully controlled. The formation of dibenzyl ether does not occur to any significant extent under the strongly alkaline conditions of resole formation, (Eq. 13) except as a possible intermediate step.

The average number of methylol groups on a phenol nuclei in a particular resole mixture will depend upon the formaldehyde-phenol ratio, time, temperature, catalyst, and concentration, which will affect the subsequent crosslinking (curing) reaction, and thus the polymer network properties. It is necessary to distinguish between the F/P ratio and concentration since there must be a solvent present, which does not take part in the reactions.

Typical molecular structures in any given resole are dependent to a great extent on the F/P ratio used. However, triethylamine when used as a catalyst tends to favor the formation of ether bridges, whereas sodium hydroxide favors methylene bridges, as indicated earlier the type reactions differ between low and high basicity, the ranges of 4-7 and 7-11.

Reaction temperature plays an important role in the formation of methylene bridges and dibenzyl ether linkages. King's studies indicated methylene bridge formation occurs at lower temperature than the ether bridge formation, whereas Hanus data show that the reverse is true. This is perhaps due to the difference in purity of reactants, catalyst used and the materials of the reaction vessels as well as conditions of time, solvents, and temperature used during their polymerization periods.

Brown studied the heat of reaction for various molar ratios of F/P. In his work resins from 1:1 to 1.5:1.0 ratios were polymerized and then evaluated by pressure DSC. The results are tabulated in Table 4 below:

The peak area is proportional to heat of reaction. The data here implies that the largest amount of heat, and therefore the largest number of reactions occur at a ratio of 1.3:1.0. This appears to be at variance to some degree with the data of Era et al shown in Table 3, however, other factors than the F/P ratio may have influenced the location of the peak. A molar ratio of 1.5:1.0 F/P would theoretically, give a maximum cross-link density in the cured polymer, and hence produce the largest amount of heat.

Cure of Aldehyde Phenolic Resins

One of the most valuable features of the aldehyde phenolic resins is the ease and rapidity with which they may be converted to well-knit, highly cross-linked products. The crosslinking or curing reaction of resole aldehyde phenolic resins is carried out by heating the mixture of mono and polynuclear methylolphenols.

TABLE 4
DSC STUDY OF PEAK AREA/MG SAMPLE SEVERAL
MOLAR RATIO OF FORMALDEHYDE/PHENOL (F/P)

<u>F/P Ratio</u>	<u>Peak area/mg Sample</u>
1.1 : 1.0	5.19
1.1 : 1.0	5.97
1.2 : 1.0	6.96
1.3 : 1.0	7.53
1.4 : 1.0	6.84
1.5 : 1.0	6.11

Unlike many polymeric systems where cure results by repetition of a single process, the cure of a phenolic resin is extremely complex, involving a number of competing reactions each of which may be profoundly influenced by reaction conditions and the structure of the phenol used to prepare the resins. A further complicating factor is introduced by the possibility of reaction at either or both the ortho and para positions of the phenol. This leads not only to the formation of a large number of isomeric products but also to products of varying reactivity depending on the location of the functional group, and the steric spacing in which the molecules can intertwine.

In the purely thermal hardening of phenol alcohol or one-stage resins, the formation of dibenzylethers (Eq. 13) is a very important reaction with the substituted phenols if the hardening temperature is held below about 160°C. The reaction also occurs above 160°C but assumes somewhat less importance if the resins are derived from trifunctional phenols. If the system is alkaline, methylene derivatives appear to be formed exclusively.

The dibenzyl ethers are unstable at high temperatures, above about 140°C, and may undergo further reactions. The methylene bridge, on the other hand, is a very stable linkage and normally it is not destroyed below the point of complex decompositions of the resins. Since conditions are seldom neutral the methylene bridge is probably the most common linkage found in a cured one-stage resin derived from a trifunctional phenol.

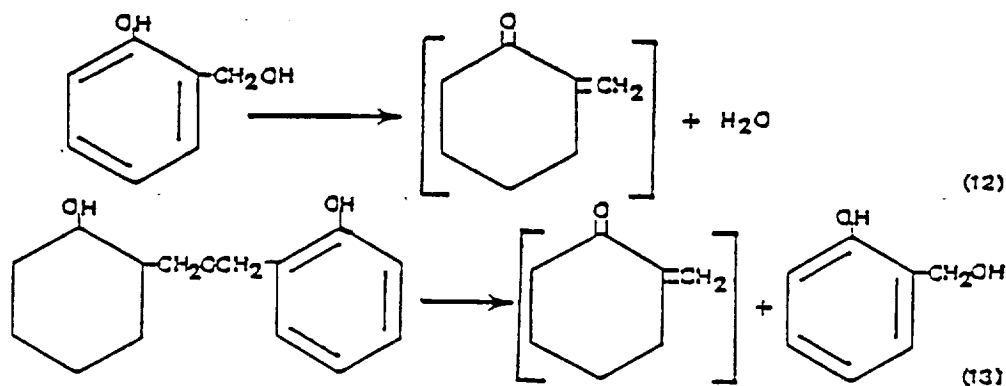
At temperatures between approximately 160°C and 250°C, a second phase of condensation, may occur in a F/P resin, the molecular weight first increases due to cross-linking and then declines. During this period the number of dibenzyl ether linkages decreases rapidly while the number of methylene bridges usually increases resulting in decrease in molecular weight due to splitting out of CH₂O. Small quantities of raw materials may be eliminated as volatile products. Simultaneously reactions involving the formation of quinone methides and their polymerization and oxidation-reaction products occur. These reactions lead to extremely complex products (Equations 8 and 9).

Figure 1 outlines a number of thermal reactions that have been discovered as a result of studies with phenol alcohols. An effort has been made to arrange the reactions in the chart so that a separation into those occurring below about 160–170°C, the first phase, and those occurring at higher temperatures, the second phase, may be visualized. This separation has been made on a more or less arbitrary basis, and some overlapping obviously occurs. Such a diagram only serves to emphasize why a clearcut description of the thermal curing processes, applicable to all types of resins cannot be given. The numbers on the arrows refer to numbered compounds on the same page.

In pyrolysis of formaldehyde/phenol resins, the behavior and the properties of the final products seldom are affected by the initial composition. Up to about 300°C additional crosslinkage may occur, along with decomposition of ether linkages. Between 300°C and 450°C decomposition begins in which the methylene bridges on the ends of chains are destroyed, with a significant weight loss, but little loss of length of chains. At this point, there is little if any breaking of the chain. With temperatures 500° and higher the main section of the polymer chain begins to break, destroying methylene bridges and any remaining ether bonds, this causes significant decreases in polymer lengths, which causes shrinkage of the final product. As the temperature rises further and approaches 800°C, severe carbonization occurs and the structure fuses. The carbonization process is the removal of further amounts of hydrogen and oxygen reducing the amount of polymer present and raising the percent of elemental carbon in the remaining matrix. As temperature continues in this high mode virtually all the polymer is reduced to elemental carbon in effect destroying the resin or the composite as the case may be. Properties such as density, pore structure, and other physical and mechanical properties of these polymers are seldom affected by relatively small differences in the original composition, but as carbonization occurs, physical and mechanical properties are drastically changed.

but as carbonization occurs, physical and mechanical properties are drastically changed.

The most important of these 2nd phase reactions appears to be the dehydration of methylol phenols or the ether breakdown to give an alcohol and quinone methides as shown in the following reactions, Eqs. 12 and 13.



The unsubstituted benzoquinone methides are unstable and rearrange to form the ethylene, acetylene and ether structures as shown in the following reactions, Eqs. 14-16

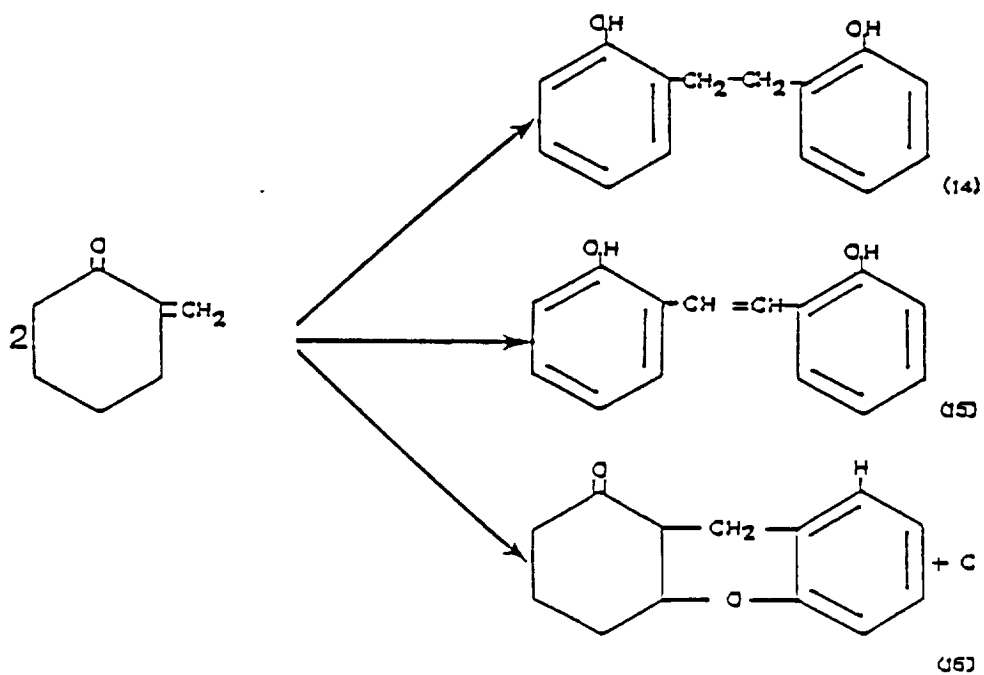
The curing of resol phenolic resins occurs when heated for a period of time, the result is the cross linking of the polymer chains. Two primary reactions take place; one is the formation of methylene bridges with the resulting splitting out of a molecule of formaldehyde and a molecule of water and the second the splitting out of a molecule of water. The measurement of the amounts of water and formaldehyde serve as a measure of the amount of crosslinking which takes place (Eq. 5 and 6.). The reactions take place at temperatures in the range of 150°C or higher.

Table 5
MOLE RATIO OF REACTANTS

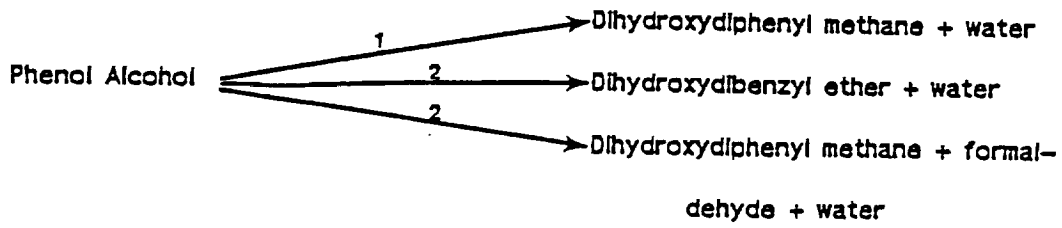
Reflux No.	F/P	Reflux Temp. °C	Time hrs.	TEA Catalyst	NaOH
1	1.7/1	75	2	0.0186	-----
2	1.7/1	75	2	-----	0.0186
3	1.3/1	98	0.66	0.0262	-----
4	1.3/1	98	0.50	-----	0.0262

At temperatures above 150°C some side reactions take place, among these in the largest quantities are the quinone methides shown in Eqs. 12 and 13.

The unstable quinone methides rearrange into the three compounds shown in the above Eqs. 14-16. The existence of the above compounds are thought to be present in the resol polymers which have been exposed to heats above 150°C.



First Phase



1: + Phenol;

2: + Phenol alcohol

3: - Formaldehyde;

4: - Water

5: Oxidation;

6: Reduction

Second Phase

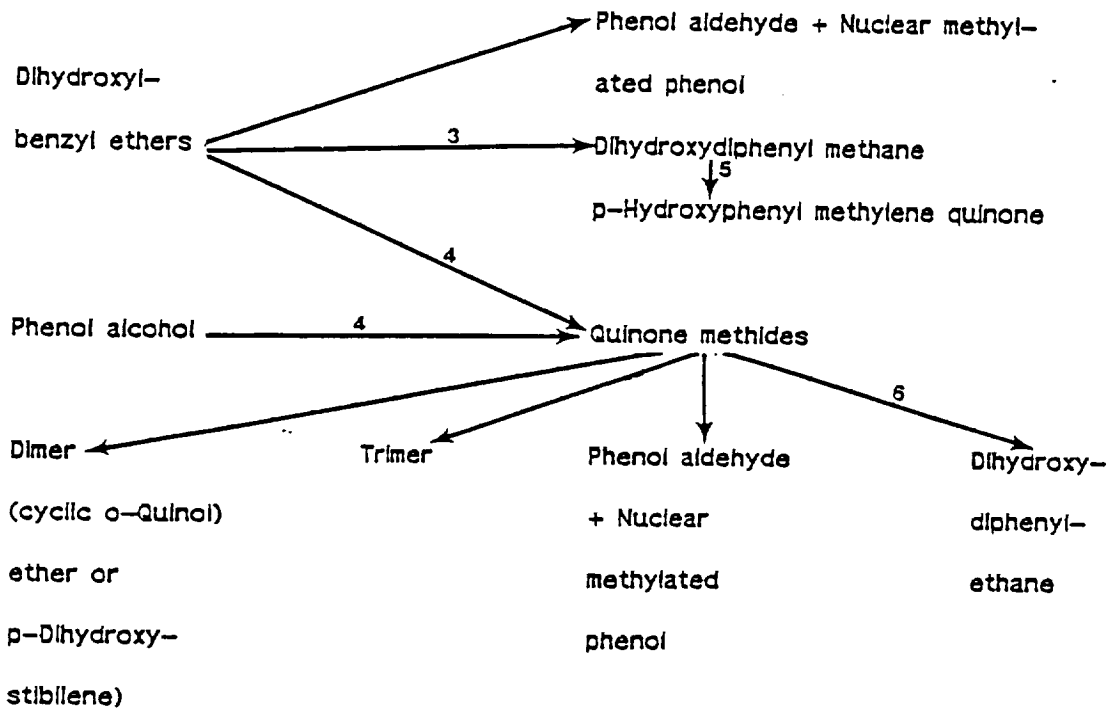


Fig. 1 - III - Hardening of Phenol Alcohols

The work of King et al is summarized in this report because it resembles to a great extent the work being done for this project. King et al studied the chemical structure and cure characteristics of a group of aldehyde-phenol resole resins by means of NMR, DSC and GPC. In particular, the effects on structure and reactivity of F/P ratio and specific types of reaction catalyst were studied. GPC was used to determine resins molecular weight distributions, and NMR to determine chemical structure features, and the DSC curing curves were interpreted in the light of the structural information provided by NMR. All resins were prepared from 90% pure phenol and 36% formaldehyde solution with either triethylamine (TEA) or sodium hydroxide as the catalyst. Table 5 shows the reactants used in terms of their mole ratios.

Resins 1 and 2 were prepared by refluxing the reactions, under vacuum at 75°C for 2 hrs., cooling and then vacuum distilling off the bulk of water below 50°C. Resins 3 and 4 were refluxed at normal boiling point (98°C) for different lengths of time: resin 3 for 40 min. and resin 4 for 30 min., then vacuum distilling at 50°C to remove the water.

NMR analysis revealed that the ortho/para ratio is higher for the two resins with F/P of 1.3 (3 and 4) than for those with F/P = 1.7 (1 and 2) and appears to be independent of the catalyst. The reaction with the most formaldehyde present (ie, 1 and 2, F/P = 1.7) favored production of a resole in which ether bridges outnumber substituted methanes. Reactions 3 and 4 with a F/P = 1.3 produced fewer ethers and more substituted methanes.

The number of free methylol groups was more or less the same for all four resins. For the same F/P ratio, the NaOH catalyst (resins 2 and 4) produces more diarylmethanes than does TEA (resins 1 and 3). The overall degree of condensation of benzyl alcohols is similar for both resins with F/P = 1.7 and is less than for the other pair with F/P = 1.3, especially for resins 4 in combination with NaOH. Thus resins 1 and 2 are similar in nature and consist predominately of methylol groups and ether links and are generally less condensed than resins 3 and 4. Resin 4 is in the most advanced state of condensation,

of benzyl alcohol and largely diarylmethanes. The difference in temperature levels, pressure and time intervals probably account for this.

GPC analysis shows that the resin with the higher F/P ratio (1 and 2) clearly have a much narrower molecular weight distribution than the lower F/P ratio (3 and 4) resins. For either pair of resins with the same F/P ratio, NaOH tends to lead to a much higher molecular weight polymer relative to TEA. The cumulative percentage of material by weight increases with increasing molecular weight for two resins (2 and 4) with the same catalyst but different amounts of formaldehyde.

The DSC results show that two separate reactions (two peaks) took place during resin scanning; the temperature range scanning was 50–200°C at 8°C per minute. The first peak occurred at 155°C and the second peak at 185°C. King et al found that NaOH preferentially catalyzes the reactions which correspond to the first peak and triethylamine catalyzes the second peak. The function of the catalyst presumably is to affect the relative numbers of sites available for the two processes which must have different activation energies. Lower temperatures and the alkali-earth (NaOH) catalyst tend to favor the formation of methylene bridge structure; higher temperatures and the organic base (TEA) tend to favor the formation of the ether structure. Of course the relative amounts of free methylol groups and the number of aromatic protons actually available will also influence the final number of methane bridges as compared to the number of ether structures.

There are a number of other uses for DSC and other instrumental techniques are described which may be applicable in studying the properties of aldehyde-phenol resins and prepreps; both cured and uncured. No attempt will be made to describe these in detail, but references are given for those who may find one or more of these of interest.

Leckenby, J. N. describes several thermal analysis techniques as applied to testing multilayer printed circuit boards (PCB). The techniques he describes are: (1) DSC, (2)

Thermo Mechanical Analysis (TMA), (3) Dynamic Mechanical Analysis (DMA), and (4) Thermo Gravimetric Analysis (TGA).

Taylor, R. E. et al has measured some thermo physical properties of a fairly wide variety of materials, from ammonium perchlorate to composite materials. The use of ramp heating for determining diffusivity and the heat conduction theory for strip heating, are described. Software has been developed for pulse heating in measuring diffusivity. Thermal diffusivity and specific heat measurements have been made on carbon/carbon composites. Heat flow through fibers (both length wise and across) as well as the matrix material have been measured.

Stenzenberger, H. et al has made use of DSC to study the curing of several polymers to control the quality of carbon fiber prepreps. TMA was used to develop post cure properties.

Moacanin, J. et al investigated a cure reactivity model for a resin system covering the temperature range of 153–177°C. DSC and Fourier Transform IR Spectroscopy were used to study the kinetics of the cure, attempting a correlation between total conversion, rates of conversion and disappearance of specific groups. They described the process in terms of two first order reactions.

May, C. A. et al made use of Dynamic Dielectric Analysis (DDA) and DSC in studying the cure of various polymers under a range of both temperature and pressures, up to the glass transition temperatures. The results indicated that a knowledge of the chemical structure of the matrix greatly aids in understanding the cure process.

Apicella, A. et al performed a curing process using DSC, high pressure chromatography, and both steady and dynamic viscosities to determine gelation limits, and the prediction of rheological behavior.

Wenz, S. M. et al used reverse phase liquid and IR chromatography, DSC, and rheological measurements to determine reaction enthalpy, viscosity, chemical structure, glass transition temperature, tensile strength, fracture toughness, fiber volume, and void

content. Data revealed that slower heat-up rates during curing produce higher reaction enthalpy, composites with higher resin content (lower voids), and higher glass transition temperatures.

IV. DIFFERENTIAL SCANNING CALORIMETRY (DSC)

Fiber reinforced composite materials are of increasing importance in many aerospace and aircraft applications as a result of the requirement for lighter weight structures. Carbon fiber composites are the accepted materials today, for many applications because they offer a very high strength to weight ratio and stiffness to weight ratio, as compared with conventional metallic structural materials. The usual technology required to mold complicated geometrically shaped parts require prepreg materials as precursors. They consist of the reinforcing fibers arranged either unidirectionally or as a woven fabric impregnated with a thermosetting resin formulation. The resin is sometimes B-staged, eg. polymerized to some degree to make it nonliquid, or semi-solid, at ambient temperature and suitable for further processing in a low pressure autoclave molding process. As a consequence of the rapid introduction of advanced resin composites into the production of structural components in aircrafts and spacecrafts, the development of advanced quality assurance criteria has become extremely important. During the early period, acceptance criteria for prepregs were based on performance tests such as mechanical and physical properties of molded test coupons, gel time, resin contents, flow properties and tackiness. Presently, it is accepted by the industry that the chemical composition of the resin used must also be part of the quality assurance control. Chemical analytical methods are being used more and more. One important technique is Differential Scanning Calorimetry (DSC), since this method provides information which is related to 1.) glass transition temperature (TG) of uncured prepreg or cured laminate, 2.) degree of cure of final product, 3.) heat of reaction during prepreg processing, 4.) resin reactivity kinetics, 5.) rheology studies, and 6.) gelation temperature, all of which have substantial bearing on strength and other mechanical properties.

The Du Pont 910 DSC system with the 1090 programmer/data analyzer was used for analysis in this work. Sixteen different specimens of Carbon Phenolic Prepreg, supplied by

Materials and Processes Laboratory, MSFC, NASA, Huntsville, Alabama were available for this study. Due to the proprietary nature of the resin and prepreg used, only limited data on the resin and prepreg physical and chemical characteristics were provided to the investigators. Resins used in this study were of the base-catalyzed resole types, supplied by U. S. Polymeric, only two were actually investigated 8625-01 and 8626-01.

The objective of this research was to evaluate Differential Scanning Calorimetry (DSC) as a tool to measure the quality and reproductibility of Carbon Phenolic Prepregs. This was only partially accomplished however. The heat of reaction under atmospheric pressure was measured in the curing process.

APPARATUS AND PROCEDURES (DSC)

The system's measuring unit is the plug-in DSC cell which uses a constantan (thermoelectric) disc as a primary heat transfer element. Schematic Figure 2 refers to the DSC cell, its isometric view and a cross section of the silver heating block, capped with silver, a vented lid encloses the constantan disc. A selected sample and an inert reference are placed in small pans which sit on raised portions of the disc. Heat is transferred through the constantan disc to both the sample pan and to the reference pan. Differential heat flow to the sample and reference is monitored by the chromel-constantan disc and the chromel wafers which are welded to the underside of the two raised portions of the disc. Chromel and alumel wires are connected to the chromel wafers at the thermocouple junctions to measure sample and reference temperatures. The alumel wire welded to the reference wafers is for thermal balance.

Purge gas enters the heating block through an inlet in the cell's base plate, is preheated to block temperature by circulation before entering the sample chamber through the purge gas inlet. Gas exits through the vent hole in the silver lid.

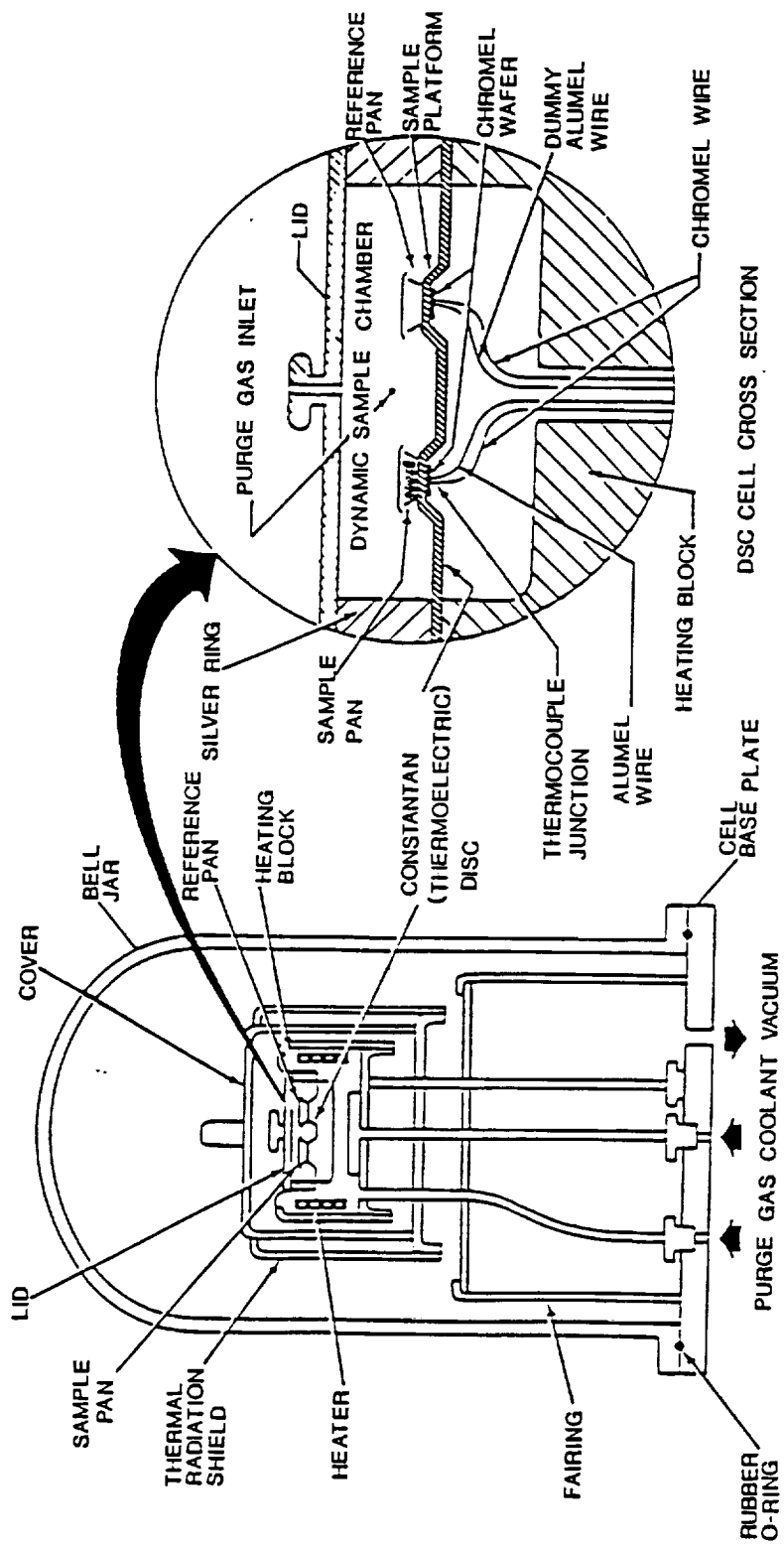


Fig. 1 - IV - DSC Cell and Cross Section

Vacuum and coolant ports on the cell base lead to openings in the cell but not directly to the sample chamber. A bell jar, placed over the cell and sealed with an o-ring, protects the user from evolved gases and permits cell evacuation.

Operating manuals for Du Pont 910 DSC and the Du Pont 1090 TA system and their interfaces will be needed.

Operation

This section describes all controls, indicators, and connectors normally used by the operator. It also contains normal operating procedures followed for these tests. (Refer to Instrument operators manual.)

Control, Indicators, and Connectors

The Operators Manual shows the location of operating controls, indicators, and connectors. Refer to operations manual for details for operation of both Du Pont 910 Differential Scanning Calorimeter and the Du Pont Thermal Analyzer.

DSC Operating Procedures

Install the DSC on the cell base module. Make sure that the cell switch is set to DSC.

CAUTION – Proper operation of the 910 Differential Scanning Calorimeter is dependent upon the use of a Du Pont Thermal Analyzer. A thorough knowledge of the 1090 TA programmer is essential and it is assumed that the user is completely familiar with the operation of the TA programmer before proceeding.

The following example involving a scan of carbon phenolic prepreg assumes a specific selection of INITIAL and FINAL TEMP., PROGRAM RATE. However, the steps are general and may be applied to any DSC scan. To operate 1090 TA/910 DSC system, proceed according to operating manual.

Error Codes

Numerous error codes are programmed into the 1091 which flash in the upper right-hand portion of the display when either an operator error is committed or the

Instrument malfunctions. When an error code is displayed, it continues to flash until one of the keys is pressed. Pressing the HELP key causes a display to appear which explains the error code. If the reason for the error code being displayed is not corrected, the error code will again display when the user tries to proceed with the experiment.

NOTE - If all routine corrective action does not eliminate reoccurring error codes, press the RESET switch (as last resort) to restore to normal operation.

Cell Cooling

If a DSC application requires operation below ambient temperature, programmed cooling or quench cooling may be used. For this test quench cooling was used as follows:

A. Quench Cooling Between Runs (Cooling Accessary)

.R 90 operation: (ref. Fig. 3.5 In Operators Manual)

1. Set the desired starting temperature by pressing the INITIAL TEMPERATURE button.
2. Press the SET UP button.
3. Place the metal cooling can over the cell and pour in the coolant (ice cubes were used). Use the open-top bell jar to minimize frost.
4. When ambient temperature is reached, remove the open-top bell jar and the cooling can and place the sample pan and the reference pan in the cell; then install the silver lid, cell cover, cooling can, and open-top bell jar.
5. Continue cooling to the INITIAL TEMPERATURE which is denoted by the READY light coming on.

NOTE - to prevent frost from forming on the disc, do not remove the silver lid when the temperature is below ambient.

6. Press the START button to start programming to the FINAL TEMPERATURE.

Experimental Details

A total of 16 carbon-phenolic prepregs systems were available from Materials and Processes Laboratory, MSFC, NASA, Huntsville, Alabama for study. But only two systems coded, numbered 8625-01 and 8626-01 were chosen for this work. Each sample was of

four ply and approximately 4 sq. cm in size, each sample was composed of eight sections identified as: A-sec. Edge, A-sec. Middle, C-sec. Edge, C-sec. Middle, E-sec. Edge, E-sec. Middle, G-sec. Edge, and G-sec. Middle. The specimen taken from each section was 10-15 mg. in weight using a single ply only.

After each DSC test, cell cooling is required. During cooling, normally cell temperature went below 17°C as ice cubes were used for quenching, hence time had to be allowed for the instruments return to ambient temperature. After each DSC test, a thermogram plot was made.

Table 1 and 2 showed the Peak Integration of 8625-01 and 8626-01 systems. Figures 1 and 2 showed the group of DSC Thermograms of 8625-01 and 8626-01 systems at 10°C/min under 14.7 psig Nitrogen. Heat of reaction (Delta H, J/gm) on the DSC under atmospheric pressure was found to be variable when run for eight different sections of 8625-01 systems, with values obtained from 12.1 to 15.5. The variability was attributed to the volatilization of reaction products and residual solvent, and natural variability of the material. This caused an endothermic response which competed with an exothermic heat of reaction and contributed to the variability of results. An additional source of variability was due to foaming of the resin which resulted in poor and variable contact of the resin with the sample pan, resulting in inconsistent values for Delta H. The heat of reaction (Delta H) values for the 8626-01 system varied from 12.8 to 14.0.

The higher the amount of heat evolved (i.e. higher Delta H), results from the increased crosslinking and polymerization which occurred. It could be concluded that the specimen 8625-01 Edge-G had the highest crosslink density after complete cure and therefore offered better high temperature properties. This may or may not be the reason however.

Considering the nature of the samples it would seem that the spread of the data is not particularly wide. In the case of 8625 the spread is 24%, in the case of the 8626

and the average of the seven points is 13.7 which agrees well with the average for sample 8626, which was 13.3.

Data for sample 8625 shows 3 data points outside of one Standard Deviation: A-Sec. Edge, C-Sec. Middle, and G-Sec. Edge, but only one outside of two Standard Deviations. Data for sample 8626 shows only one data point outside of one Standard Deviation: A-Sec. Edge and none outside of 2 standard Deviations.

TABLE 1 PEAK INTEGRATION OF 8625-01 SAMPLE

Sample No.	Heat of Transition			Calc. for St. Dev.		
	Onset temp., °C	Peak temp., °C	Delta, H Joules/gm	(x-x)	(x-x) ²	(x-x) ²
1 A-Sec. Edge	173.4	198.7	12.1	1.6	2.56	2.56
2 A-Sec. Middle	172.5	198.0	13.4	0.6	0.36	0.36
3 C-Sec. Edge	171.3	196.2	14.0	0.3	0.09	0.09
4 C-Sec. Middle	172.6	198.0	12.6	1.1	1.21	1.21
5 E-Sec. Edge	172.6	198.4	14.0	0.3	0.09	0.09
6 E-Sec. Middle	171.9	198.2	14.4	0.7	0.49	0.49
7 G-Sec. Edge	171.5	197.8	15.5	1.8	3.24	-
8 G-Sec. Middle	172.4	197.7	13.8	0.1	0.01	0.01
Average of Data			13.7			
Average omitting G-Sec. Edge			13.5			
Standard Deviation			1.003			
Standard Deviation (omitting 7)			0.945			

It was of interest to note that all sixteen specimens provide DSC-profiles (heating rate 10°C/min) with a single maximum peak temperature in the range of 196.2 to 198.7°C (Table 1 and 2) as can be seen in Fig. 1 and 2. It has to be noted at this point that the characteristic temperatures of the DSC-profile can change slightly with variations in the ratios of the reactants, (F/P) in the resin.

TABLE 2 PEAK INTEGRATION OF 8626-01 SAMPLES

Sample No.	Heat of Transition			Calc. for St. Dev.		
	Onset temp., °C	Peak temp., °C	Delta, H Joules/gm	(x-x)	(x-x) ²	(x-x) ²
1 A-Sec. Edge	172.3	196.7	14.0	0.7	0.49	-
2 A-Sec. Middle	173.5	197.2	12.8	0.5	0.25	0.25
3 C-Sec. Edge	172.4	197.3	13.4	0.1	0.01	0.01
4 C-Sec. Middle	172.2	196.9	13.1	0.2	0.04	0.04
5 E-Sec. Edge	173.5	197.1	13.2	0.1	0.01	0.01
6 E-Sec. Middle	173.1	197.7	13.6	0.3	0.09	0.09
7 G-Sec. Edge	173.6	198.2	13.0	0.3	0.09	0.09
8 G-Sec. Middle	173.0	197.8	13.0	0.3	0.09	0.09
Average of Data			13.3			
Average omitting A-Sec. Edge			13.1			
Standard Deviation			0.3657			
Standard Deviation (omitting 1)			0.2878			

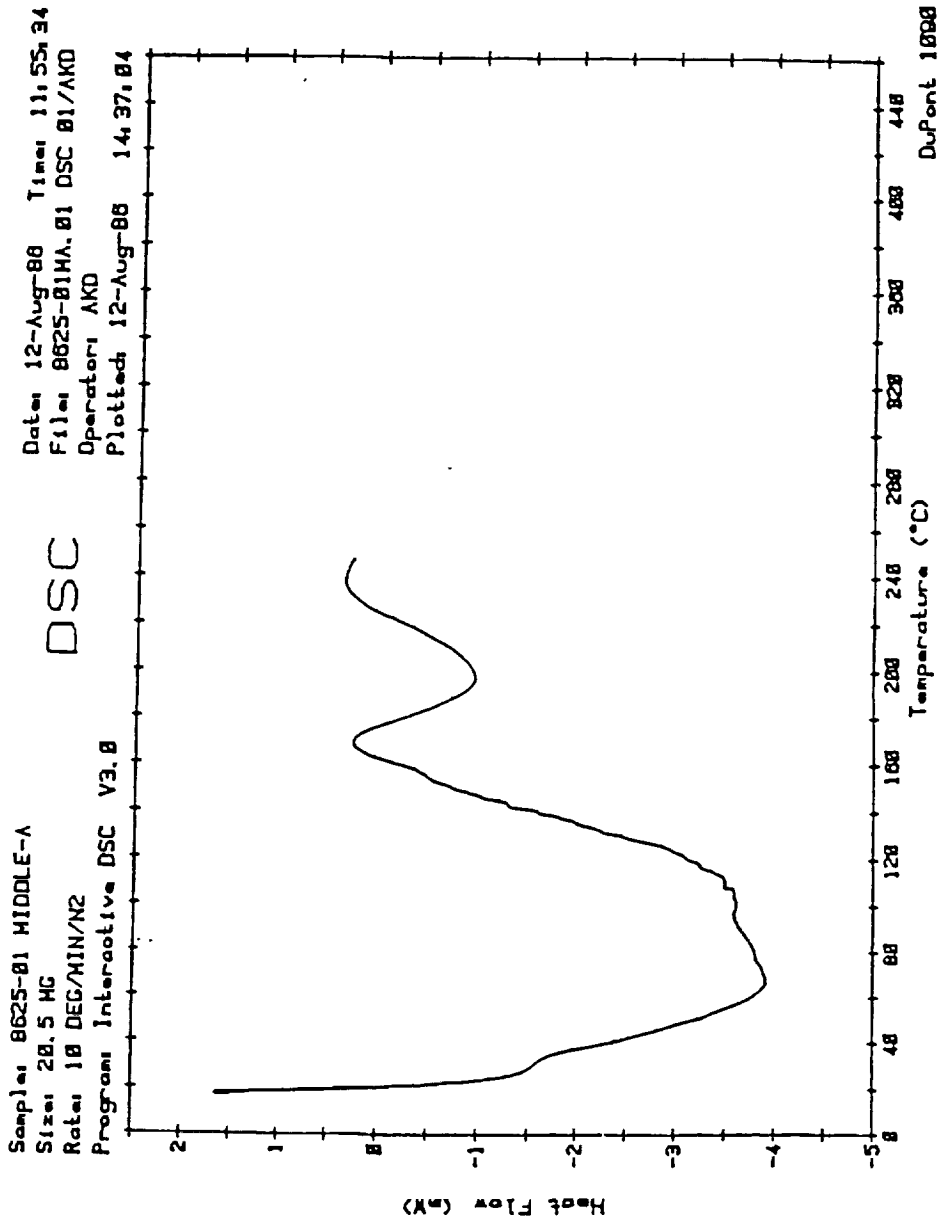


Fig. 2 - IV - Typical Peak Integration of 8625-01 System

ORIGINAL PAGE IS
OF POOR QUALITY

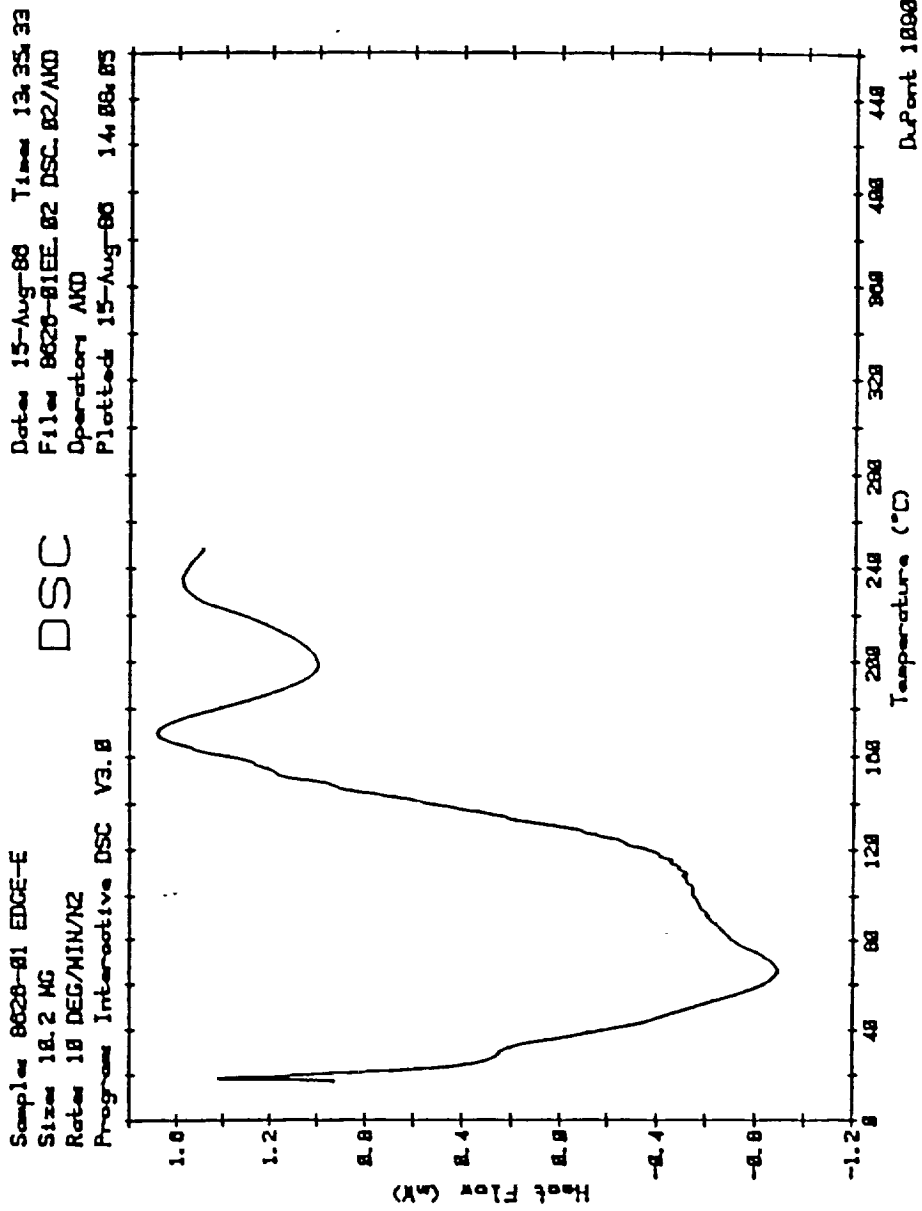


Fig. 3 - IV - Typical Peak Integration of 8626-01 System

The following conclusions are made concerning the research presented in this study:

1. Heat of reaction determination on the DSC under atmospheric pressure were found to be variable when run under identical conditions. The variability of results was partially attributed to the variability of specimens. Additional sources of variability were due to foaming of the resin which resulted in poor and variable contact of the resin with the sample pan, and experimental error. 8625-01 G-Sec. Edge system provided highest crosslink density after complete cure and therefore offered best high temperature properties. If one leaves out the specimen G-Sec. Edge, the spread of the data is not bad, and probably lies within acceptable limits when taking into consideration the character of the specimens and the possible experimental errors.

2. The Differential Scanning Calorimetry (DSC) method can be used as a tool for research in the early stages of polymerization development, to be followed by and defining the cure behavior of thermosetting resins and prepregs. DSC data is applicable as a quality control assurance method for both resins and prepregs.

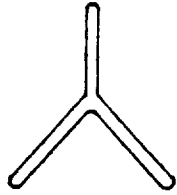
V. CARBON CLOTH

Thomas Edison was the first to use carbon fibers. In 1880 he used them as filaments in his first successful incandescent lamps. He made the carbon fiber by "baking threads in an oven". Until the late 1950's, however, there was not much interest in carbon fibers research because of the later development of tungsten filament lamps. The rocket age brought about the increased interest in carbon fibers because of the need for an ultra-refractory material which could reinforce certain rocket components. Composite materials made with carbon fibers have almost unlimited potential because of the superior physical and mechanical properties of the fibers, imbedded in an appropriate matrix.

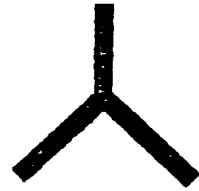
In the early 1960's, the United States Air Force developed the use of boron fibers as a reinforcement material for composites, with a high strength to weight and a high stiffness to weight ratio. Boron's low density is derived from its atomic structure and its low atomic number. Its high Young's modulus is derived from its electronic configuration which produces strong covalent bonds between the boron atoms. Carbon was discovered to have some characteristics similar to boron, because of its location adjacent to boron in the Periodic Table. Carbon fibers have almost completely replaced boron fibers in composite technology because of technological advantages in fabrication and ease of composite manufacture. In 1959, Union Carbide developed carbon fibers from rayon which is chemically similar to cellulose, the basic chemical constituent in the material that Thomas Edison used for the electric lamp filament. Two other precursors were discovered to be useful in the production of carbon fibers. Polyacrylonitrile (PAN) discovered by Y. Tsunoda in 1960 and mesophase pitch (MPP) discovered by S. Otani in 1965 both initially produced carbon fibers with low strengths and low tensile moduli, but new manufacturing techniques developed for these precursors have produced carbon fibers with much higher strengths and higher tensile moduli.

A fiber should be viewed as a mini-composite in itself because it is not a homogeneous anisotropic entity, but a collection of linked anisotropic units. Therefore, the moduli depend on the details of axial preferred orientation in each fiber structure, and the strength is a function of axial and radial textures and gradients as well as both surface and internal flaws. The most important mechanical properties of carbon fibers are strength, elasticity, and deformability. These properties depend upon the type of precursor, manufacturing conditions, subsequent processing methods, and other factors. The main morphological features of carbon fibers are the shape of the cross section and type of fiber surface, and these features are also dependent upon the precursor and manufacturing conditions. Fibers with circular cross sections are achieved by spinning from a melt. Other shapes of cross sections are achieved by dry or wet spinning the chemical fibers from a polymer solution, through various shaped spinnerettes (Fig. 1). Carbon fibers have other superior properties such as high thermal and chemical stability except in a gaseous and oxidative condition. The fiber properties do not change significantly when wetted by water.

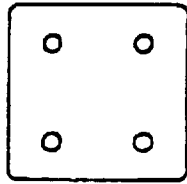
There are three process steps in fiber production: spinning of precursor fiber, stabilization (transformation into non-melting intermediate products), and carbonization. PAN and mesophase pitch (MPP) are the precursors most widely used today for carbon fiber production. The rayon precursor is still in wide use in the aerospace industry because of its known properties, capabilities, and functionality. Carbon fibers come in various forms: long and continuous, short, and fragmented, directionally or randomly oriented. Continuous fiber, directionally oriented are more useful in composites where the ultimate in performance and weight reduction is required, and these come in various forms: yarns (tows), individual filaments, unidirectional prepreg tapes, and fabrics with different weights and weaves. The most commonly used woven fabric is the eight-harness satin which retains most of the fiber characteristics in the composite and can easily be draped over complex mold shapes.



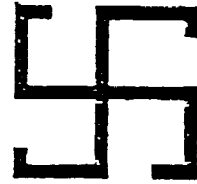
Trilobal shaped fiber



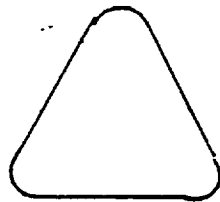
Spinnerette hole for Trilobal shaped fiber



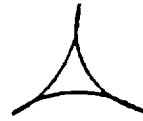
Square fiber



Spinnerette hole for Square fiber



Triangular fiber



Spinnerette hole for Triangular fiber

Fig. 1 - V - Typical Non-Circular Synthetic Fiber and Corresponding Spinnerette Hole Shapes

There is a difference between "carbon" and "graphite" when relating to fibers. Carbonization, which produces fibers of unusually high tensile strength, involves heating the fibers in a furnace to temperatures of 1000 to 1500 degrees C. To graphitize the material, the fibers must be heated to temperatures of 2000 to 2800 degrees C, and this is done when a high tensile modulus is more important than high tensile strength. It is important to note that none of the carbon fibers are ever converted into classic graphite regardless of the heat treatment, hence the term "graphitization" may be somewhat misleading.

With tensile strengths as high as three million psi and Young's modulus values as high as 148 million psi, graphite whiskers are one of the strongest materials known, but mass production of graphite in this form is impractical. Throughout the remainder of this paper, the work modulus refers to Young's modulus, or tensile modulus. A whisker may be defined as a single crystal with a large but finite length to thickness ratio, and it has a very smooth surface and possesses high strength and high modulus. The carbon atoms in a perfect single graphite crystal are arranged in hexagonal arrays, and these atoms in the basal plane are held together by very strong covalent bonds. The hexagonal layers themselves are held together by much weaker van der Waal forces and are stacked on top of each other in a regular ABAB.. pattern. The basal planes have to be aligned parallel to the axis of the fiber to obtain the highest modulus and greatest strength. The stacking arrangement in a graphite fiber is not the same as that of a perfect graphite crystal. The layers are slightly displaced, thus forming "turbostratic" graphite, but the orientation of the layers is still more or less parallel to the fiber axis. The degree of perfection of this alignment determines the strength modulus and it varies with the manufacturing process and conditions. Transverse properties, shear properties, and flaw properties of the fibers are affected by the arrangement of the layer planes. Graphite is weak and compliant in the direction perpendicular to the basal plan, which makes graphite a good lubricant and strong and stiff in the two directions of the basal plane. Even a slightly

misoriented layer plane will cause some amount of shear which will drastically lower the fiber modulus value, hence the need for correct alignment.

Because the mass production of graphite whiskers is impractical, much effort has been made to develop high strength, high modulus carbon fibers from the various precursors. There are three main ways to produce graphite fiber from precursors with proper preferred orientation, and preferred orientation simply means the extent to which the carbon-layer planes are oriented parallel to the fiber axis and to each other. The processes are: orientation of the polymer precursor by stretching, orientation by spinning, and orientation during graphitization. In the production of carbon fibers from rayon, the carbonized fibers are "graphitized" by a heat-treatment at approximately 2800 degrees C. The graphitized fibers consist of tangled ribbons of layer planes which must be strained or oriented properly to produce high modulus fibers, and this orientation is done by stretching. To create the preferred orientation in PAN, the fibers are restrained from shrinking during graphite conversion which is achieved at temperatures of greater than 2000 degrees C. There is a distinct advantage in the graphitization process applied to mesophase pitch as compared to the processes using rayon or PAN. In the Pan and rayon precursor processes, tension is required to achieve high modulus and high strength by developing or maintaining the necessary molecular orientation. The MPP process does not require this tension because the anisotropic liquid crystal nature of the pitch allows the molecular orientation to be achieved in the spinning process, and the tension is not needed to preserve or enhance the orientation.

To achieve high Young's modulus values, fibers need to be treated at temperatures of more than 2500 degrees C; however, maximum tensile strengths and breaking strain values are obtained with heat treatments between 1200 and 1500 degrees C. All "real" materials have an imperfect structure to some degree which always reduces physical and mechanical properties, but the perfect solid has a theoretical tensile strength which is approximately one-tenth the value of the theoretical Young's modulus. Because of the

actual imperfections, the tensile strengths are lower than that which is theoretically possible. During the rayon precursor graphitization step, a high degree of preferred orientation is achieved which results in fibers that have a Young's modulus approaching the theoretical values of the single graphite crystal. The tensile strengths of these same fibers, however, are well below those of graphite whiskers. The measured strengths of the best formed graphite fibers are twenty times less than the theoretical strength of graphite. It can also be seen that the Young's modulus increases continuously with heat-treatment temperature in the PAN precursor process. It is very important to note that as the heat-treatment temperature increases, the tensile strengths reach a maximum and then begin to decrease. As a rule of thumb, it is safe to say that as the temperature increases, the strength reaches a maximum, further increases in the temperature bring about decreases in strength while the modulus continues to increase. Higher temperatures bring about increases in the modulus, but decreases in strength. Carbon fibers (fibers which have not been graphitized) have a higher strain to failure reflex than high modulus graphite fibers. These carbon fibers may be chosen over the graphite fibers in some aircraft applications because composite parts are continually stressed and flexed so a higher strain to failure value would be needed.

Carbon fibers formed from rayon and PAN precursors are brittle and flaws usually control the strength of brittle materials. As gauge length, which is the length of the sample between clamps, is decreased in tensile tests of fibers containing flaws, the tensile strength increases, because of reduced number of flaws. In cases of low-modulus "carbon" fibers (heated to approximately 1300 degrees C) which may contain other than carbon and the carbon may not be completely graphitized, and of high modulus "graphite" fibers (heated to approximately 2800 degrees C), more completely decomposed and almost all graphite, a distribution of flaws is present along the length of each fiber. These flaws cause stress concentrations and reduce the fiber strength below the theoretical flaw-free fiber strength. The dependence of relative strength on gauge length is similar in

both the high-modulus fibers and low-modulus fibers even though the high modulus fibers are three to four times stronger.

As fibers are treated at higher and higher temperatures for the purpose of increasing Young's Modulus, the tensile strength also increases up to some maximum value, but begins to fall off or decrease as further increases in temperature are applied. The modulus continues to rise however.

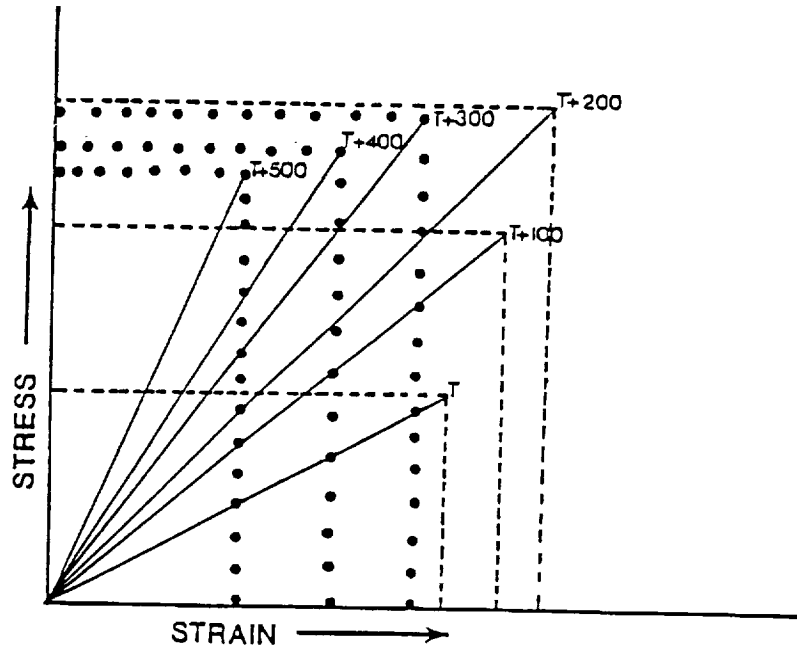


Fig. 2 - V - Stress-Strain Diagram

In the diagram above a series of carbon fibers are heated at various temperatures. A fiber treated at a temperature (T) develops a stress-strain curve as shown with the end of the line being the point of fracture. Increases in treatment temperature brings about increases in modulus, (as indicated by increasing slope) increases in fracture point, and increases in strength. Young's modulus being defined as the ratio of stress to strain. Continued increases in temperature however will produce continued increases in modull, some maximum fracture strength is reached and above that temperature the fracture point falls off, showing decreases in the tensile strength. From

above diagram fracture point increases from T to $T + 200$, and decreases from $T + 200$ to $T + 500$.

Expressing this another way, as the slope of the above curves increase (increasing modulus and strength) the ductility of the specimen decreases. It will become more brittle, until such time as brittleness dominates and after this point the specimens break at ever lower fracture points due to brittle failure rather than ductile failure.

There are several causes for the flaws or defects that limit the strength of the fiber. One cause for flaws in the carbon fibers is the use of too high a stretch ratio which will cause polymer ribbons (matrix) to pull away from the fiber surface during spinning. Carbon fibers of low strength may be formed by the incomplete oxidation of PAN fibers before carbonization which would cause a sheath/core structure to develop or it may cause cavities with the fibers. Also, cavities in the precursor fiber may be caused by gas dissolved in the fiber spinning solution or irregular flow of the spinning solution through the spinnerette nozzles. Internal voids or cavities may also be formed by the evaporation of foreign matter during thermal processing.

Another strength limiting defect is interfilament fusing which may occur in the precursor spinning process or in thermal processing. Contaminants in the original spun fiber are the cause of foreign particle inclusions and these may cause the fiber to fracture. Severe oxidation treatments may cause pits on the surface of the fibers and other types of fiber surface contaminations will reduce the strength. Radial cracks and longitudinal splits are defects often noted in carbon fibers. Misaligned crystallites are often associated with fiber fractures especially after high-heat treatments. There are several ways to improve strengths of carbon fibers by removing or modifying surface flaws: oxidative etching treatments, application of carbon coatings, and neutron radiation. Process improvements have also decreased the number of fiber defects which have improved the strength of the fibers. It is highly probable that different types of defects affect high-strength carbon fibers and high-modulus graphite fibers in different ways.

Internal defects are more damaging to the high-modulus fibers; whereas, surface defects are more damaging to the high-strength carbon fibers.

Stress is uniform over the entire length of the filament in a tensile test so the strength is determined by the worst flaw, or concentration of flaws, within the gauge section. For low-modulus carbon fibers made from rayon, the strength increases fifty percent for each tenfold decrease in gauge length. For instance, a decrease from 2 inches to 0.2 inches. There is a corresponding forty percent increase in strength for high-modulus graphite fibers with Young's modulus of fifty-five million psi, and a twenty-five percent increase in strength for graphite fibers with Young's modulus of seventy-four million psi. Stretching is the factor which causes the increased fiber modulus; therefore, the reduction in fiber strength dispersion is probably also caused by stretching. For fibers made from PAN precursor, there is a thirty percent strength increase for a tenfold reduction in gauge length regardless of heat-treatment temperature. Because there is no stretching involved in the heat-treatments, no changes in flaw sizes or shapes occur.

The shape of the cross section of the fibers may or may not be a strength limiting factor. Figure 1 shows typical non-circular shaped cross sections. Mesophase pitch fibers are melt spun so different non-circular cross sectional shapes may easily be produced. Depending upon the rate of evaporation as compared to the rate of diffusion in the spinning process, PAN-based carbon fibers will either be circular or dogbone-shaped. The strength and susceptibility to flaws are different for the two shapes. The circular fibers are used in the production of the high-modulus fibers therefore it is probable that these fibers are more susceptible to thermally induced flaws.

A precursor may be defined as something that precedes another. There have been several polymeric fibrous materials that have been tested, evaluated, and used as potential precursors for the production of carbon fibers. Two processes for the production of carbon fibers are the growing of graphite whiskers in an arc or the chemical

vapor deposition (CVD) of pyrolytic carbon on appropriate substrates. These processes, however, are less feasible and more costly than the pyrolysis of organic precursor fibers into carbon fiber which is a practical method for producing large quantities of graphite fibers that have reproducible and desirable properties. Other advantages of the pyrolysis technique over the other two methods are as follows: long, fine-diameter, flexible carbon fibers are more easily produced, it is less expensive, the process is faster, and meticulous control of the system atmosphere and pressure is not as critical. The fine (small diameter) flexible fibers are necessary for the production of composites.

Rayon, polyacrylonitrile, and mesophase pitch are the precursors that are most widely used in the production of carbon and graphite fibers. These three organic materials have satisfied the requirements for the production of carbon fibers with good properties. The requirements or criteria for the precursors are listed below:

- 1) Proper strength
- 2) Will not melt
- 3) Must not completely volatilize
- 4) Inexpensive

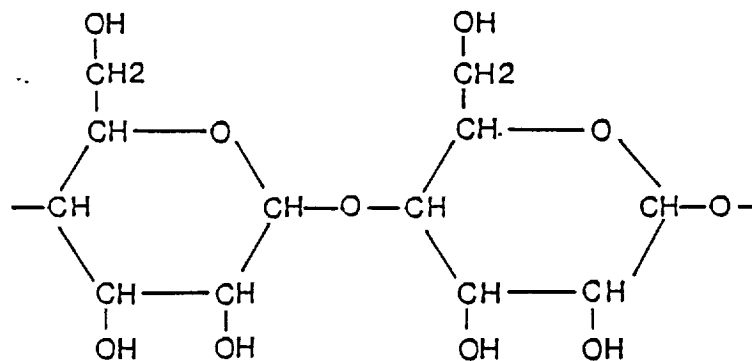
The proper strength is important so that the fibers will hold together during all stages of the conversion process to carbon. To prevent melting during the conversion process, a thermoplastic precursor must be thermoset prior to the conversion process or infusible precursor materials should be selected. There should be an appreciable amount of carbon yield of the precursor left after pyrolysis to justify its use on an economic basis, and this could not be accomplished if the precursor were to completely volatilize during pyrolysis. Cost of raw materials are always an important factor and the less expensive they are, the less expensive the final product may be, dependent on the process. The precursor should also possess good mechanical properties which result in the amount of preferred orientation of the carbon atoms during pyrolysis.

Since 1959, rayon has been used in the production of high-strength, high modulus carbon fibers for use in composite materials. Other than its use in the aerospace industry, the rayon precursor is practically obsolete because of the high cost of stretching and the uncertainty of the continued supply of rayon. Rayon has been supplanted by other plastics for most commercial uses. The carbon fibers produced from rayon have a higher strain to failure value than those produced from other precursors; therefore, the fibers are still in demand in aerospace applications where the composite parts are continually stressed and flexed and a high strain to failure value is necessary.

The schematic diagram for the rayon precursor process for the production of carbon fibers can be seen in Figure 2, and the steps for the rayon conversion process are listed below:

- 1) Spinning of Fiber
- 2) Stabilization
- 3) Carbonization
- 4) Stretch-graphitization

The rayon fiber is a thermoset polymer composed of cellulosic chains. The molecular structure of rayon is



During the stabilization step, the rayon is oxidized to increase carbon yield by cross-linking and cyclizing the cellulosic chains. Stabilization occurs at a low-temperature heat treatment, at temperatures up to 400 degrees C. Stabilization can be done in an inert atmosphere which requires long process times or it can be conducted in a reactive

atmosphere which reduces the process time considerably. The carbon yield, along with process time, is another important aspect of the stabilization step. Another method which results in high carbon yield and low processing times is chemical preimpregnation.

During the carbonization step, the rayon is converted to carbon by slowly heating to 950 degrees C temperature. Other sources cite ranges from 1000 to 1500 degrees C. This process is conducted in an inert atmosphere and the process time is fairly short. To increase the mechanical properties of the resulting fibers, tension may be applied during this step to improve the preferred orientation of the layer planes.

To graphitize the fibers, they are heat-treated at temperatures greater than 2800 degrees C. Graphitized fibers consist of tangled ribbons of layer planes which must be strained or oriented properly to produce high-modulus fibers. To compare the difference in modull for stretched and nonstretched fibers resulting from the graphitization step, one compares one-hundred million psi for the stretched fibers with ten million psi for nonstretched fibers. One of the disadvantages of using rayon-base graphite fibers is the high cost of stretching during the stretch-graphitization step.

Fibers produced from rayon have a relatively disordered micro structure of fine grain. The structure remains intact after heat-treatments up to 3000 degrees C. The individual layers have small diameters and are highly cross-linked which results in high intrinsic strength because there is very little room for slippage of the basal planes.

Polyacrylonitrile (PAN) is one of the most widely used precursors today, and one source cites that it has been found to be the most suitable precursor for high performance carbon fibers. This precursor came into existence two decades ago when a wide range of organic fibrous materials were being examined for use as carbon fiber reinforcing material. Rayon-based carbon fibers had already been in existence and use. In regard to carbon fibers, the following characteristics of PAN are important:

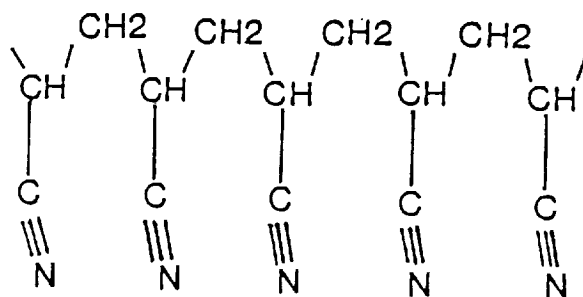
- 1) Structure and crystallinity
- 2) Orientation of molecular chains

3) molecular weight and its distribution

4) Co-monomer type and its content

These characteristics may play just as an important a role in the final properties of the carbon fibers as the processing parameters during pre-oxidation and carbonization. The Young's modulus of the carbon fibers is greatly affected by the primary Young's modulus of the precursor PAN.

The structure of an ideal PAN molecule is shown below:



PAN is a linear, atactic carbon-hydrogen polymer with polar nitrile (carbon-nitrogen) pendant groups attached. The physical properties of the polymer are greatly affected by the polarity of the nitrile groups. This polarity causes a high glass transition temperature in PAN; therefore, it is frequently co-polymerized with other monomers so as to reduce the glass transition temperature. The chemical composition (i.e. co-monomer type and ratio of each) has a major effect on the process ability of PAN-fibers in at least the early stages of carbon fiber manufacture; therefore, the exact chemical composition is a proprietary item for most PAN-fiber producers. The polarity of the nitrile groups also affects the solubility characteristics of the polymer so that only highly polar solvents can be used to solubilize PAN, and the strong ionic bonds causing this polarity may cause the fiber to decompose before it melts. The dissolving of PAN is done prior to the spinning step shown below.

The schematic diagram for the PAN precursor process for the production of carbon fibers can be seen in Figure 3. It may be observed that during the stabilization step,

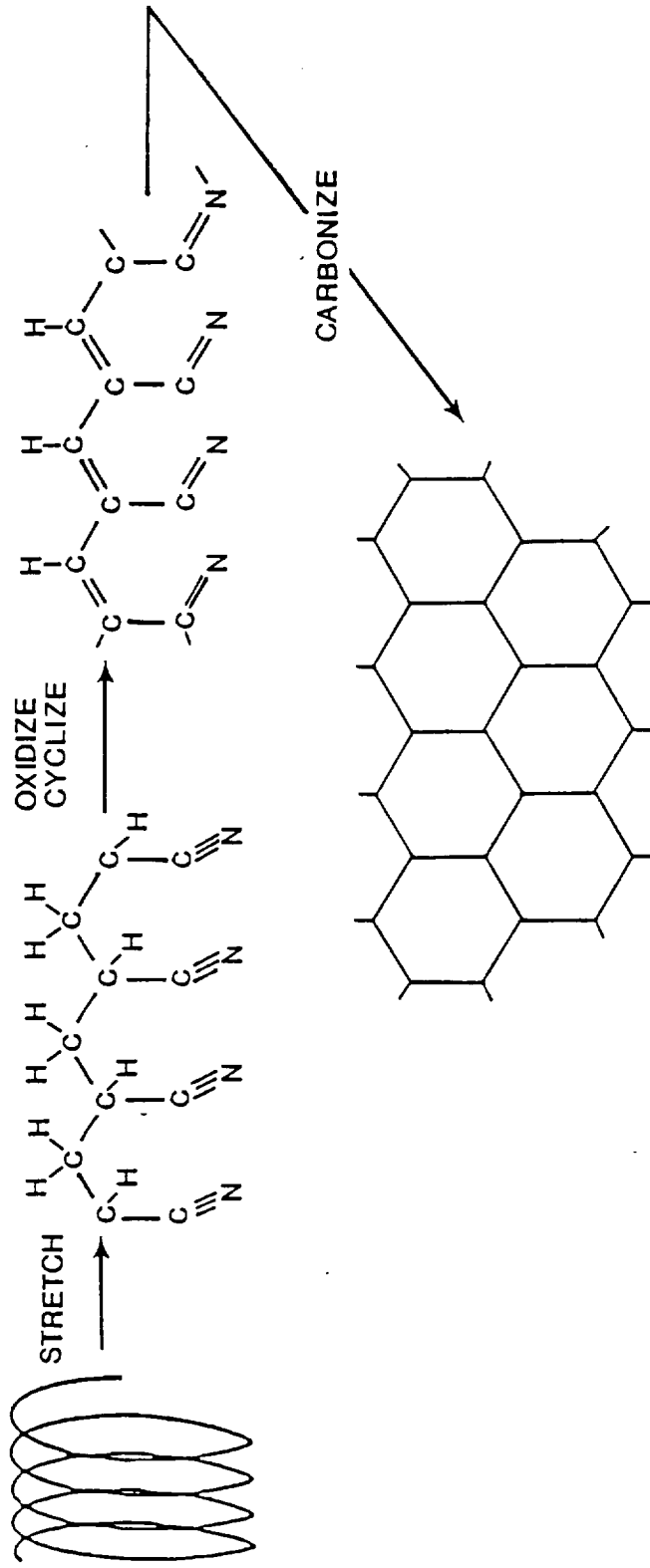
where oxidation takes place hydrogen is removed and expelled in the form of water. There are five steps in the PAN conversion process, Fig. 3. They are as follows:

- 1) Spinning precursor
- 2) Stretching precursor
- 3) Stabilization
- 4) Carbonization
- 5) Graphitization

There are two types of spinning techniques used in the precursor spinning step. Because of the danger of decomposition of the PAN fiber before it melts, the precursor is combined with a solvent (polar) and spun into filamentary form using either a "wet" or "dry" solution spinning technique. In dry spinning, the solvent must diffuse through the filament and then evaporate into the spinning chamber; in wet spinning, the solvent must also diffuse through the filament, but it will enter the coagulating bath solution, rather than evaporating. The shape of the cross section of the filaments is determined in the spinning process (Fig. 1). If the solvent evaporates or enters the bath solution slower than it diffuses through the PAN filament, the filaments will have a circular cross section because they will dry uniformly. However, if the rate of solvent evaporation is faster than the rate of solvent diffusion through the filament, then a dog-bone shaped fiber will result because the surface of the filament will harden faster than the core causing collapse. Wet-spun PAN fibers are the most suitable for the production of multi-filament carbon fiber yarn.

The initial stretching step of the precursor is done to help increase the axial alignment of the polymer molecules. This stretching can be accomplished in the coagulating bath or in boiling water, and it is done simply to enhance the mechanical properties of the fiber.

Stabilization of the fibers is necessary to prevent relaxation of the preferred orientation achieved in the stretching step. Stabilization is actually an oxidation process



POLACRYLONITRILE PROCESS

Fig. 3 - V - Polacrylonitrile Process

carried out in air at temperatures of 200 to 220 degrees C. During oxidation, the fibers are held in tension to maintain alignment of the polymer as it is transformed into a ladder or cyclic structure.

The fourth step of PAN conversion is carbonization which is simply the method of transforming the PAN-base fibers into carbon fibers. During this stage, turbostratic graphite-like fibrils are formed and oriented and these determine the high mechanical property levels of the carbon fibers. The non-carbon elements are driven from the precursor during oxidation in an inert atmosphere at temperatures from 1000 to 1500 degrees C. Extended hexagonal ribbon networks are the resulting form of the carbon atoms after carbonization.

To improve the Young's modulus of the fibers, it is necessary to heat-treat the fibers in temperatures in excess of 1800 degrees C. This is known as graphitization, but often as the modulus increases in this process, the tensile strength will decrease.

There are three categories of PAN-base carbon fibers based on modulus values. The "low" modulus fibers have values from 190-210 GPA and these are the commercial quality fibers. The "medium" modulus fibers have from 220 to 250 GPA and these are the fibers with the highest quality and best strength potential. The "high" modulus fibers have modulus values from 360 to 390 GPA and strength is usually sacrificed for the high modulus. The intermediate and high-modulus fibers are not widely used in aerospace applications because of their low strain to failure value.

There are two processes for the production of carbon fibers from pitch. Isotropic pitch and mesophase pitch are the precursors and they each have distinct properties and uses.

Isotropic pitch based carbon fibers are used for non-reinforcement purposes such as thermal insulation. The schematic diagram for the isotropic pitch precursor process for the production of carbon fibers can be seen in Figure 4. The process consists of four steps which are listed as follows:

High-Performance Carbon Fibers

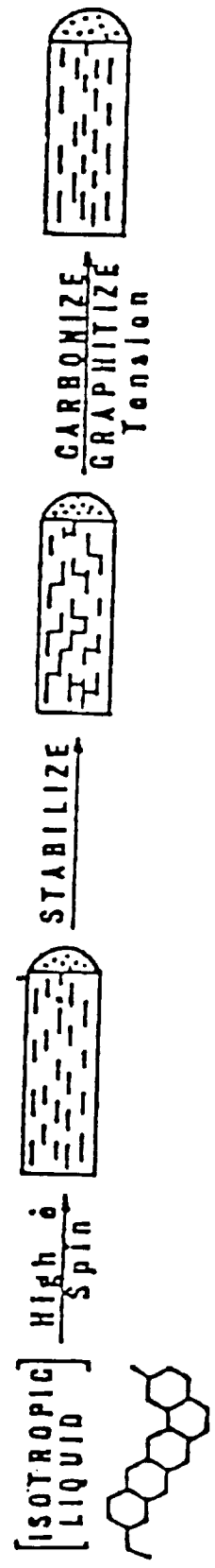


Fig. 4 - V - Isotropic Pitch Process for Carbon Fibers

- 1) Melt Spinning
- 2) Thermoset at low temperature
- 3) Carbonize
- 4) Stress-graphitize

This process is not very commercially significant due to the cost of the thermoset and stress-graphitize steps. The need for long time periods in the thermoset step, and the need for the high-temperature stress-graphitization are drawbacks to this process. The low-modulus fibers produced when the stress-graphitization is not employed do have limited uses. Carbon fibers produced from isotropic pitch will not be considered further in this paper.

Carbon fibers produced from mesophase pitch as the precursor have high modulus, moderate strength, high density, and can be graphitized into three-dimensional crystal order at high temperatures. These fibers have been available in continuous filament tow or yarn since 1974. Compared with rayon and PAN precursors, MPP precursor produces carbon fibers that are one of the least expensive high modulus types on the market. Process improvements have decreased the number of fiber defects which has led to increased strength and other properties of the resulting fibers. The schematic diagram for the MPP precursor process for the production of carbon fibers can be seen in Figure 5. The process is outlined below:

- 1) Mesophase transformation
- 2) Melt Spin
- 3) Thermoset
- 4) Carbonize
- 5) Graphitize

The advantage of this process over the isotropic pitch process is that long thermosetting times and stress-graphitization treatments are not needed.

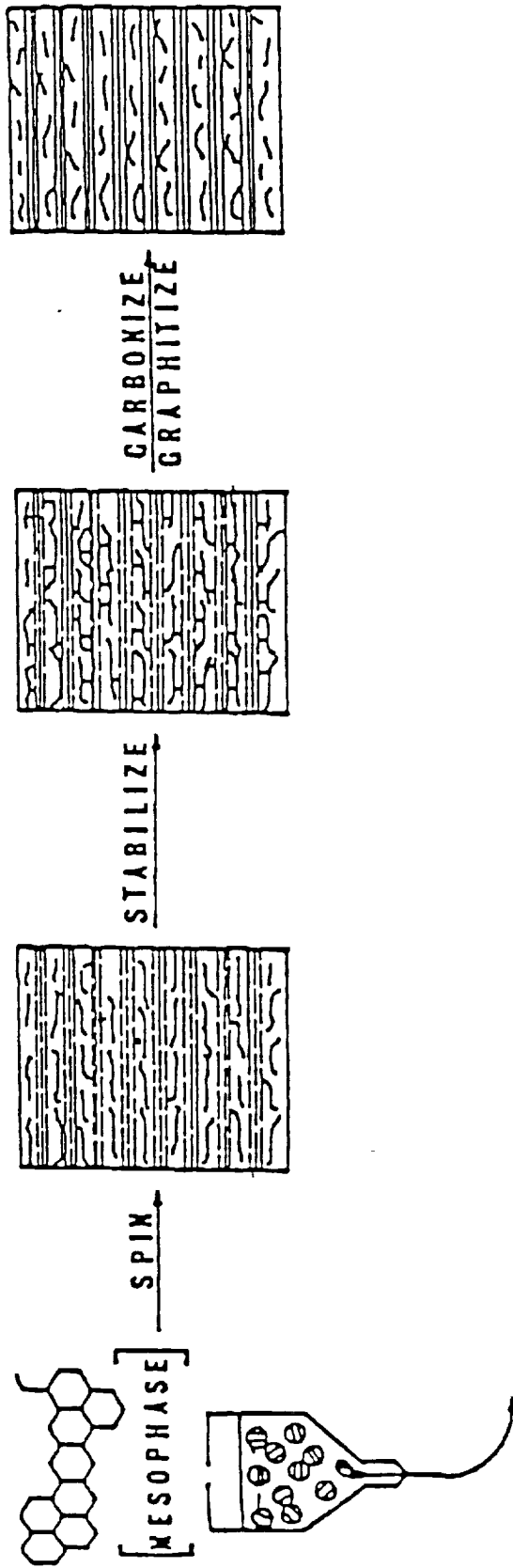


Fig. 5 - V - Mesophase Pitch Process for Carbon Fibers

In the first step, mesophase pitch which contains both isotropic and anisotropic material is converted from petroleum or coal tar pitch that is thermally treated to temperatures above 350 degrees C. Anisotropic simply means, liquid crystal phase, having different property values when measured along different axis. Fig. 5 shows the separation of the isotropic material being removed from the mixture in the first step.

The liquid mesophase state is then melt-spun in a conventional manner. The melt spinning operation gives excellent orientation in the as-spun filament because of the high extrusion velocity and fiber draw-down experienced in the process. "Green yarn" is produced when the mesophase pitch is melt spun through a multiple-hole spinnerette.

In the thermosetting step, the aromatic compounds have already been formed so the yarn must be oxidized at temperatures below its softening point to keep the filaments from fusing together.

The MPP is converted to coke, then carbon, and, ultimately, graphite. The fibers are carbonized at temperatures between 1500 to 3000 degrees C, usually around 2000 degrees C. Pitch results with around an eighty percent carbon yield as compared to a fifty percent yield for PAN and a theoretical carbon yield of fifty-five percent of rayon. However, tests show that the char yield for rayon is actually around ten to thirty percent which is quite low.

The graphitization step is conducted at the higher temperatures to provide the high modulus value graphite fibers. One advantage of this process step over the same process steps for PAN and rayon is that no tension is required to obtain the preferred orientation because the proper orientation is achieved during the spinning step.

MPP-base carbon fibers have high shear sensitivity and a low strain to failure value and these fibers are most advantageous in carbon-carbon composites.

Surface defects can be detrimental to the strength of a carbon fiber. There are many types of surface flaws which may affect this strength, a few of which are listed as follows: cavities, contaminants, cracks, and inclusions. The surface of both CCA-3 rayon

precursor fibers and SWB-8 PAN precursor fibers are shown in Figures 6-12. These photographs are taken at various magnifications by a JEOL JSM-35CF Scanning Electron Microscope (SEM).

The surfaces of different rayon-based carbon fibers can be seen in Figures 6, 7, and 8. The outer surface of the rayon fibers is marked by longitudinal grooves or striations. This is clearly shown in all three of the rayon photographs and in the cross section photograph, Figure 11.

A major surface defect can be seen in Figure 6 at a magnification of 1200 times the normal size of the fiber. The fiber appears to be torn on the surface which could have been caused by any number of things. Separating the fiber from the fiber bundle, touching the fiber with metal forceps, or damage caused during processing could be among the possible causes for the fiber damage. Figure 7 shows a rayon fiber at a magnification of 1527 times its normal size. Several particle inclusions can be seen in the longitudinal striations along the fiber. The rayon fiber shown in Figure 8 is magnified at 5100 times its normal size and a flaw can be seen in the right-hand portion of the photograph. Something, possibly a portion of another fiber, has fused or bonded to the fiber; also, several particles can be seen on the fiber.

Figures 9 and 10 are photographs of SWB-8 polyacrylonitrile-base carbon fibers shown at magnifications of 5100. The surfaces of the PAN fibers are smoother than the rayon fibers; however, these fibers also have shallow longitudinal striations on their surfaces. The fiber shown in Figure 10 has a rectangular pit in the upper right-hand portion of the photograph. Other than the pit and a few particles in the striations, this fiber is relatively flaw-free. The PAN fiber in Figure 9 has several contaminants within the striations and a small cavity can be seen on the right-hand side of the photograph.

The cross sections of both types of precursor fibers are shown in Figures 11 and 12 at magnifications of 5100. The rayon cross section is shown in Figure 11, and it is easily noted that the fiber cross section and the surface of the fiber appears to be

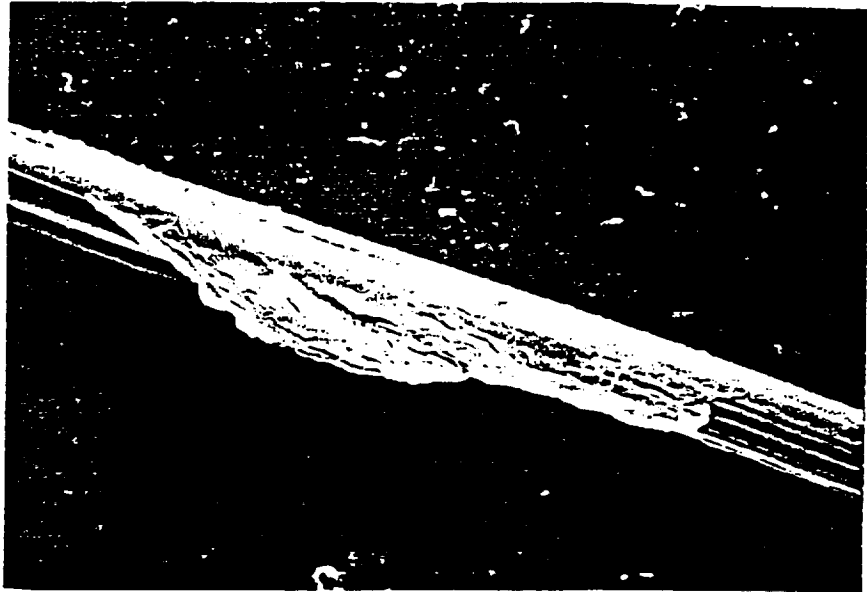


Fig. 6 - V - SEM Photograph of Surface of CCA-3 Rayon Precursor Fiber (x1200)

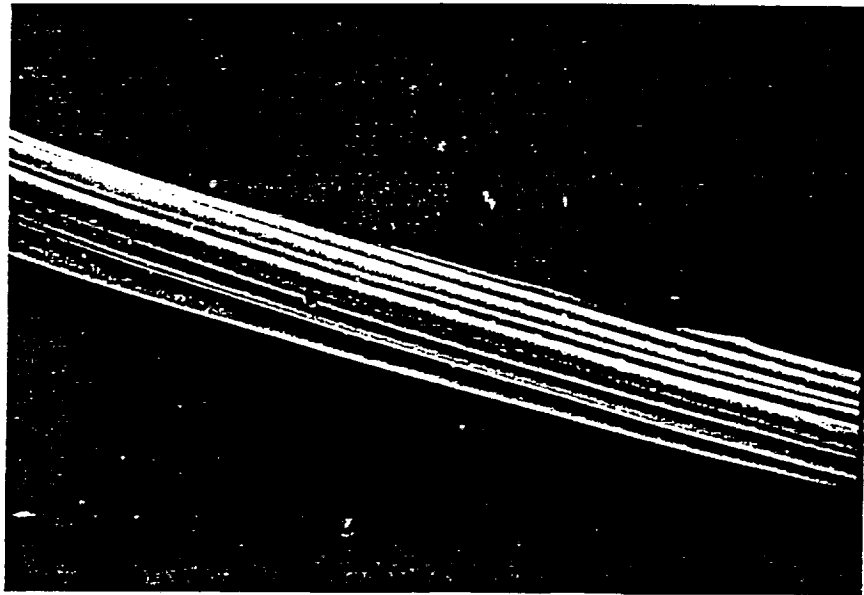


Fig. 7 - V - SEM Photograph of Surface of CCA-3 Rayon Precursor Fiber (x1527)

ORIGINAL PAGE IS
OF POOR QUALITY

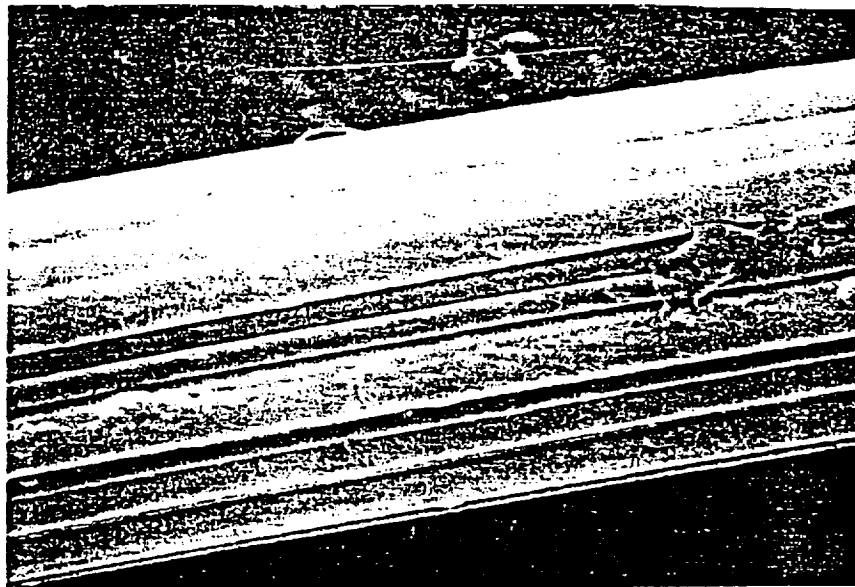


Fig. 8 - V - SEM Photograph of Surface of CCA-3 Rayon Precursor Fiber (x5100)

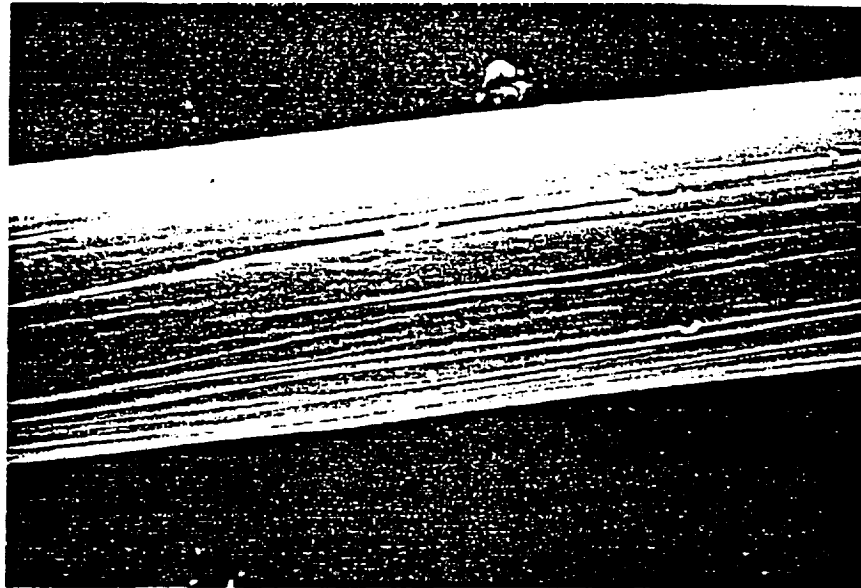


Fig. 9 - SEM Photograph of Surface of SWB-8 PAN Precursor Fiber (x5100)

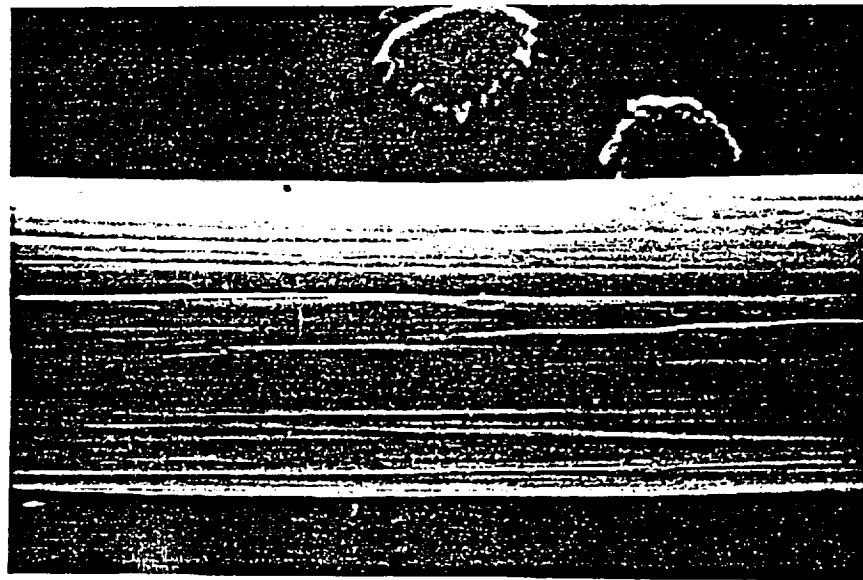


Fig. 10 - V - SEM Photograph of Surface of SWB-8 PAN Precursor Fiber (x5100)

ORIGINAL PAGE IS
OF POOR QUALITY

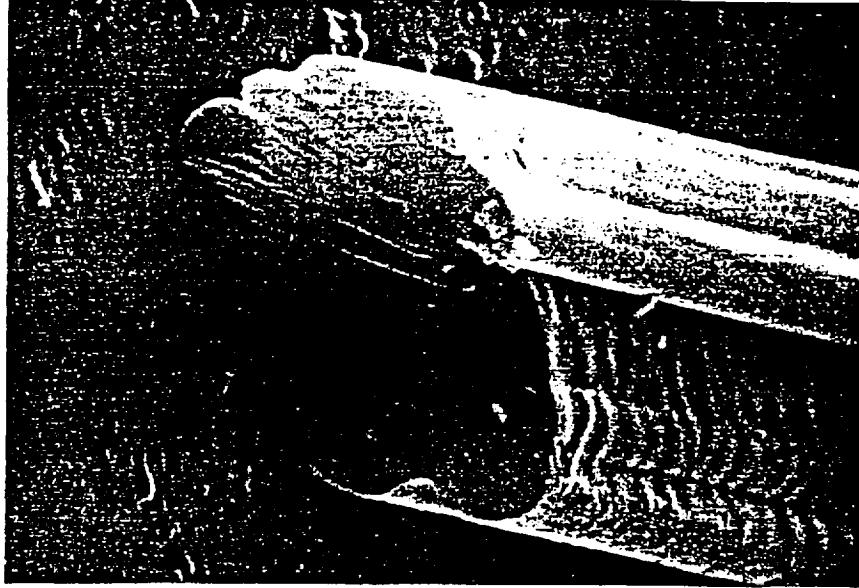


Fig. 11 - V - SEM Photograph of Cross Section of CCA-3 Rayon Precursor Fiber (x5100)

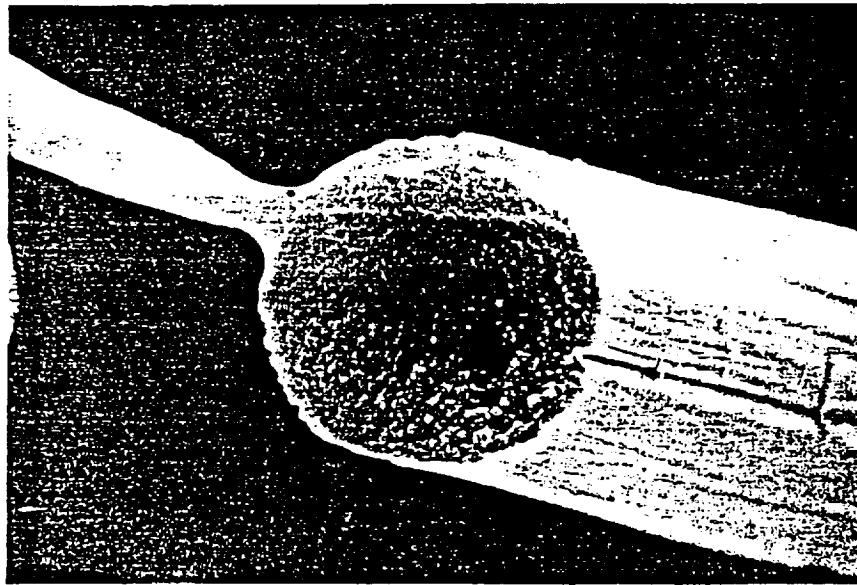


Fig. 12 - V - SEM Photograph of Cross Section of SW-8 PAN Precursor Fiber (x5100)

wrinkled. A few contaminants or particles are located on the fiber surface. The cracks are more than likely the result of mishandling during preparation of specimens for the SEM. Figure 12 shows the cross section of the PAN precursor. It can easily be seen that this fiber has a circular cross section and its surface is smoother than that of the rayon fiber. Cracks can be seen on the upper portion of the cross section and a particle is included on the surface of the fiber. All fiber samples shown in Figure 6-12 show several defects which may cause a decrease in tensile strength. These surface defects may be the result of spinnerette surface imperfections or they may be due to resin solids that were not homogenically blended, or other reasons. If they are not too numerous the decreases in physical and mechanical properties are not severe.

VI. BREAKING LOAD AND DEFLECTION TESTING EQUIPMENT

The Chatillon Model UTSE-2 tension/compression tester is located in the second floor laboratory in the Etheredge Chemical Engineering building. Drawings of the tension/compression tester and necessary external equipment are shown in Figures 1, 2, and 3.

The test stand shown in Figure 1 is designed to test the resiliency, yield points, and breaking strengths of various materials. The Model UTSE-2 is motor driven and can test materials up to strengths of 550 lb-f. The stand has a DC gearmotor which drives the tester at constant speeds and varying loads, the crossarm which maintains a constant speed at varying loads as it moves vertically is vertically adjustable, is attached to two one inch diameter stainless steel columns, and a steel strain gauge loadcell is mounted on the crossarm and has a capacity of 550 lb-f.

The power requirements of the test stand are 105-125 Vac, 50-60 Hz, and 5A. The force measurement of the low range is 0.0-110.0 lb x 0.01 lb, and the high range is 0.0-550.0 lb x 0.05 with an accuracy of ± 0.2 % F.S. and each range \pm one count.

The ON-OFF switch is illuminated when turned on. The MIN-VAR-MAX switch operates the speed of the ram. The MIN speed is one inch per minute, the MAX speed is 12 inches per minute, and the VAR speed adjusts the speed of the ram between the MAX and MIN speeds. The direction of travel of the ram and crosshead is controlled by the UP-DOWN switch, which provides for either tensile or compression testing.

Shown in Figure 2 is the circular grips assembly used to secure the fiber bundles during testing. The upper grip is attached to the loadcell of the test stand, and the lower grip is attached to the lower platform. The grips each contain a clamp for securing the end of the fiber and a circular head containing threads around which the fiber bundle may be wrapped.

Adjacent to the tensile testing equipment is a remote display cabinet shown in Figure 3, on which the breaking load and deflection measurements are recorded. This

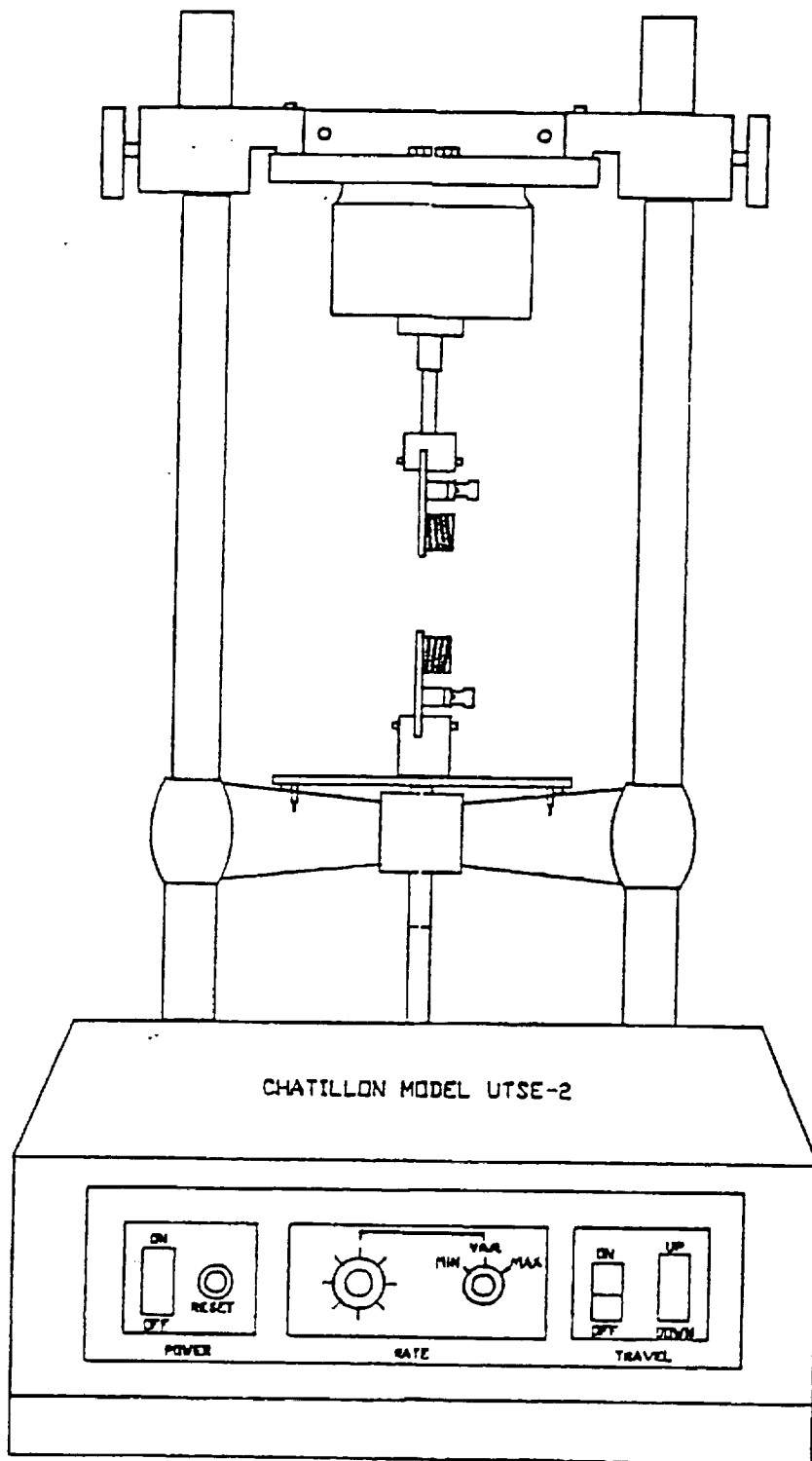


Fig. 1 - VI - Apparatus for Breaking Carbon Fibers

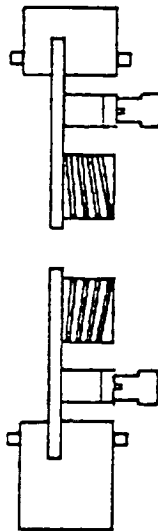


Fig. 2 - VI - Circular Grips for Holding Fibers

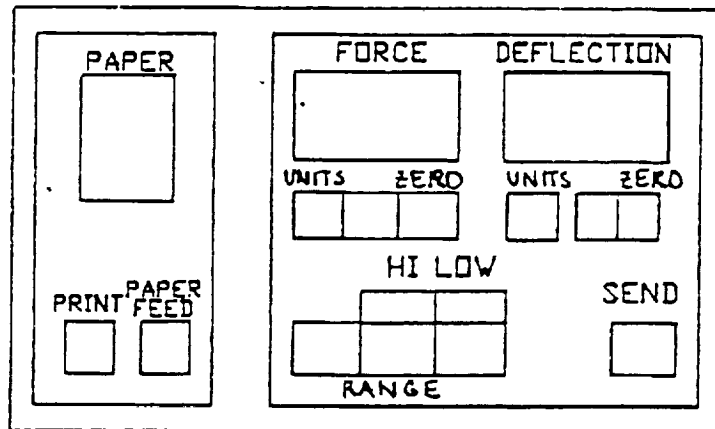


Fig. 3 - VI - Digital Recorder for Breaking Apparatus

recorder is connected to the test stand by an electrical cable. Contained within the display cabinet is an electronic signal conditioner, a microcomputer with associated digital displays, and a twenty-column thermal printer.

The signals from the loadcell and test stand are filtered and further amplified by the signal conditioner, and these amplified signals are then converted to digital equivalents. The microcomputer is basically a 6502 microprocessor governed by an E-PROM based program which can convert units. The microcomputer does the necessary digital manipulations of the amplified signals, and it also compensates for the deflection of the loadcell and the test stand frame.

The display console has many features which will be described. Two five-digit 9/16 inch LED displays continuously the test results of force and deflection. There are pushbuttons incorporated to zero force and deflection and to establish zero references. There is a MAX-HOLD button which allows the user to "freeze" the force display, or hold both the force and deflection together, at the maximum value. This is valuable when the yield or breaking points of the material need to be determined. The High Range (0-550 lb-f) or Low Range (0-110 lb-f) may be selected by pushbuttons on the cabinet. The units desired (lb, kg, or N) may be selected by the UNITS button on the display console.

Operating Procedure for the Tension/Compression Tester

The circular grips are mounted onto the test stand. The upper grip is attached to the loadcell and the lower grip is attached to the lower platform.

The Low Range (0-110 lb-f) and lb units selected by depressing the appropriate buttons on the display cabinet. The inch units are selected for the deflection measurements in the same manner. The test speed is set at minimum.

The test specimen is attached to the clamp of the upper circular grip and is then wrapped around the threaded circular head two times. Before the fiber bundle is attached to the lower grip, the weight of the fixture and test specimen must be tared out by depressing the ZERO button on the display cabinet. The fiber bundle is next connected to

the lower grip by wrapping it around the lower threaded circular head two times and then securing it in the clamp. The deflection ZERO button is then depressed to zero the deflection display. The MAX HOLD buttons for force and deflection are depressed to record the maximum force required to break the specimen.

The test is begun by depressing the travel switch in the down position with the speed set at MIN. The DOWN button must be continually held in the depressed position until the sample is broken. The force and deflection are then recorded from the display cabinet. The MAX HOLD buttons are then released, and the same procedure is repeated for each sample tested. The gauge length which is the distance between the upper and lower circular heads is measured by a ruler.

Test specimens are taken from two different types of materials, and fiber bundles are tested from five locations from each type of material. Ten samples are tested from each location in both the fill and warp directions at four different gauge lengths of 0.5, 1.0, 1.5, and 2.0 inches for a total of 800 test samples. The fibers in the warp direction are those fibers which run lengthwise with the fabric, and the fibers in the fill direction are those which run across the fabric and are perpendicular to the warp fibers.

VII. DETERMINATION OF BREAKING LOAD OF TEXTILE FABRICS USING THE RAVELED STRIP AND CUT STRIP METHODS.

SAMPLE PREPARATION

Take samples that extend the width of the fabric and 1½ yd. along the selvage (i.e. along the warp). Cut each specimen 1 inch wide; length shall be about 6 inches.

Raveled Strip Test - a strip test in which the specified specimen width is secured by raveling away yarns.

Cut Strip Test - a strip test in which the specimen width is secured by cutting the fabric.

PROCEDURE

Use clamps provided with jaws having smooth, flat, metallic faces (if the faces are not smooth, rubber pads may be used). Select the load range of the testing machine such that the break occurs between 10 and 90 percent of full scale load. Speed should be adjusted to 2 (high gear).

Secure the specimen centrally in the clamps of the testing machine, taking care that the long dimension is as nearly as possible parallel to the direction of application of the load. Be sure that the tension in the specimen is uniform across the clamped width.

Operate the machine and read the breaking load from the recording chart.

Calculate the average of the breaking load observed, that is, the maximum load to cause a specimen to rupture as read directly from the testing machine.

REFERENCE

ASTM - D1682 (1973).

VIII. CARBON FABRIC STUDIES

A large variation of fiber strength across a precursor fabric section will possibly cause variation in the final product. Two sample precursor fabrics are examined and tested in this report. Both the CCA-3 rayon-base and SWB-8 PAN-base carbon fiber samples are eight-harness satin weave fabrics. To find the breaking load variability at different fabric locations, data is taken from five sections of each precursor fabric sample. The locations are as follows: top left, top right, center, bottom left, and bottom right. Both fill and warp direction samples are tested at each location. The fill direction fibers are the fiber bundles or tows that run across the width of the fabric, and the warp direction runs down the length of the fabric. The tows from the fill direction are more crimped than the warp direction tows, and they usually contain less fibers per bundle than do the warp bundles.

Ten tows were tested for breaking load and deflection in both the fill and warp directions at the five locations on each fabric sample, and the raw experimental data is located in Appendix A in Tables 18-21. Ten tows of each gauge length of 0.5, 1.0, 1.5, and 2.0 inches were also tested at each of the above fabric-direction-location combination for a total of 800 different samples.

The results for the average breaking load of CCA-3 and SWB-8 in both the fill and warp directions at a gauge length of 0.5 inches can be seen in Table 1. The breaking load of CCA-3 in the fill direction ranges from 0.81 lb/tow at bottom right to 0.88 lb/tow at the center of the fabric. The average breaking load of these samples is 0.85 lb/tow with a standard deviation of 0.02. The breaking load of CCA-3 in the warp direction ranges from 1.16 lb/tow at bottom left to 1.46 lb/tow at the center. The average breaking load is 1.28 lb/tow with a standard deviation of 0.1. Both directions show that the fibers are strongest in the center of the fabric, and the strength distribution can be seen on the bar graph in Figure 1. For the fill direction of the SWB-8 PAN base fibers,

TABLE 1: Results for Average Breaking Load of 0.5" Gauge Length

	BREAKING LOAD (LB/TOW)			
	CCA-3		SWB-8	
	FILL	WARP	FILL	WARP
TOP LEFT	0.85	1.28	1.37	1.89
TOP RIGHT	0.85	1.22	1.76	1.27
CENTER	0.88	1.46	1.54	2.07
BOTTOM LEFT	0.87	1.16	2.26	1.65
BOTTOM RIGHT	0.81	1.28	1.55	1.74
AVERAGE (STD)	0.85 (0.02)	1.28 (0.10)	1.70 (0.31)	1.72 (0.27)

TABLE 2: Results for Average Breaking Load of 1.0" Gauge Length

	BREAKING LOAD (LB/TOW)			
	CCA-3		SWB-8	
	FILL	WARP	FILL	WARP
TOP LEFT	0.85	1.16	1.35	1.66
TOP RIGHT	0.78	1.59	1.61	1.52
CENTER	0.92	1.15	1.27	1.97
BOTTOM LEFT	0.74	1.18	2.29	1.38
BOTTOM RIGHT	0.80	1.29	1.74	1.97
AVERAGE (STD)	0.82 (0.06)	1.27 (0.17)	1.65 (0.36)	1.70 (0.24)

BREAKING LOAD VS LOCATION

for CCA-3 and SWB-8 (0.5" Gauge)

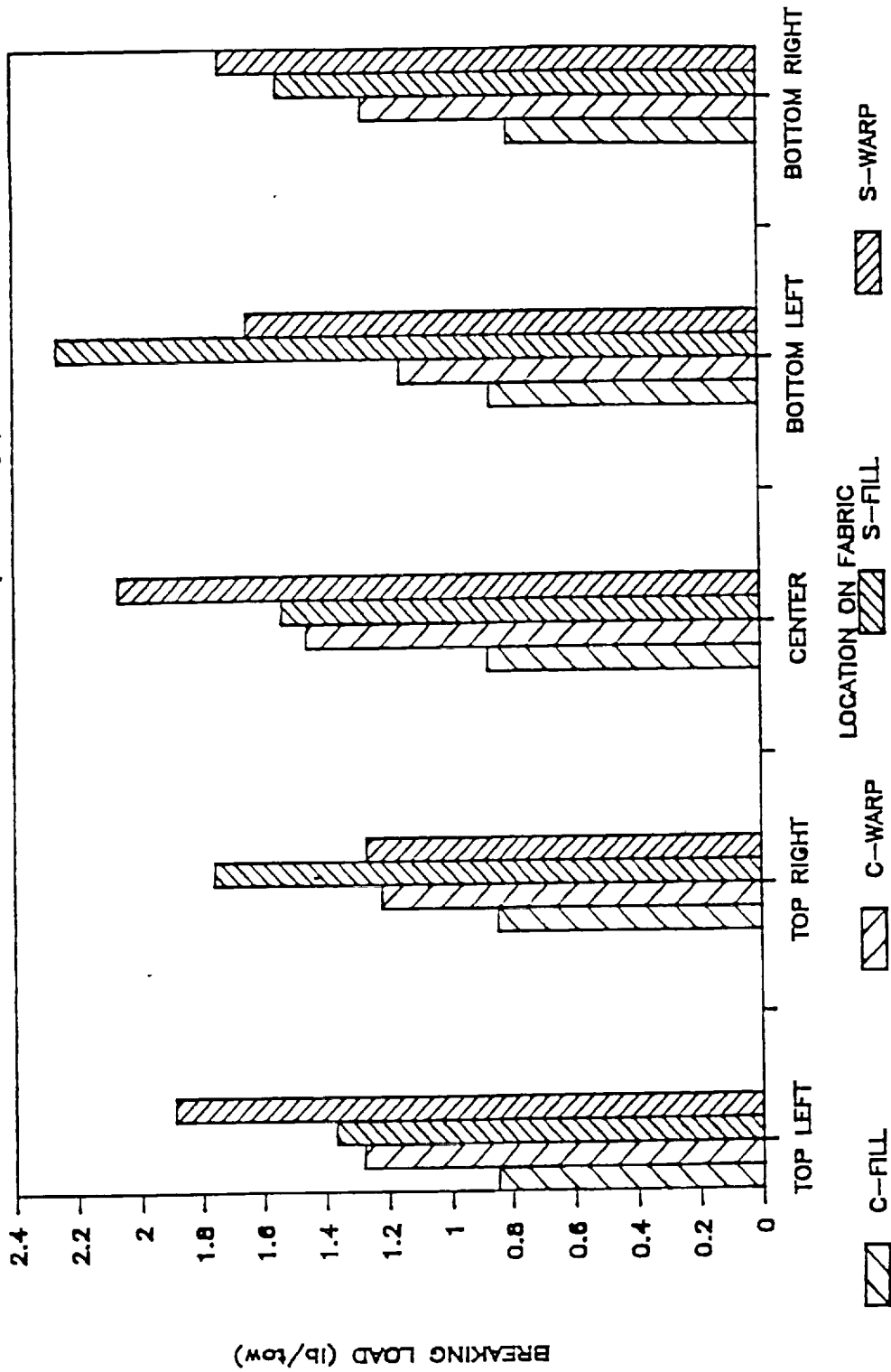


Fig. 1 -- VIII

the values range from 1.37 lb/tow at top left to 2.26 lb/tow at bottom left with an average breaking load of 1.70 lb/tow and a standard deviation of 0.31. For the warp direction, the largest value is 2.07 lb/tow at the center, and the smallest value is 1.27 lb/tow at top right. With a standard deviation of 0.27, the average breaking load is 1.72 lb/tow. It can easily be seen in Figure 1 that the SWB-8 samples are stronger than the CCA-3 samples at every location. The fill direction fibers of CCA-3 are the most uniform across the fabric as compared to the other three groups.

The results for the average breaking load of 1.0 inch gauge length for CCA-3 and SWB-8 at the different locations are tabulated in Table 2 and shown in Figure 2. The CCA-3 fibers in the fill direction range from 0.74 lb/tow at bottom left to 0.92 lb/tow at the center with an average breaking load of 0.82 lb/tow across the fabric. The warp direction fibers range from 1.15 lb/tow at the center to 1.59 lb/tow at top right with an average breaking load of 1.27 lb/tow across the fabric. The average breaking loads of the SWB-8 fibers in the fill and warp direction are 1.65 and 1.70 lb/tow, respectively. The fill direction values range from 1.27 lb/tow at the center to 2.29 lb/tow at bottom left, and the warp values range from 1.38 lb/tow at bottom left to 1.97 lb/tow at the center and bottom right. The fill direction of CCA-3 has the most uniform breaking load distribution across the fabric with a standard deviation of 0.06; whereas, CCA-3 - warp and SWB-8 - warp and fill have standard deviation of 0.17, 0.24, and 0.36, respectively.

Table 3 and Figure 3 show the results for the average breaking load of CCA-3 and SWB-8 fibers at a gauge length of 1.5 inches. The fill direction of CCA-3 ranges from 0.81 lb/tow at bottom left to 0.91 lb/tow at the center, and the warp direction ranges from 1.10 lb/tow at the center to 1.31 lb/tow at top left. The average breaking loads of these two direction are 0.83 and 1.19 lb/tow for the fill and warp, respectively. The values for SWB-8 in the fill direction range from 1.37 lb/tow at the center to 2.22 lb/tow at bottom left, with an average of 1.66 lb/tow. The values of the warp direction range

BREAKING LOAD VS LOCATION

for CCA-3 and SWB-8 (1.0" Gauge)

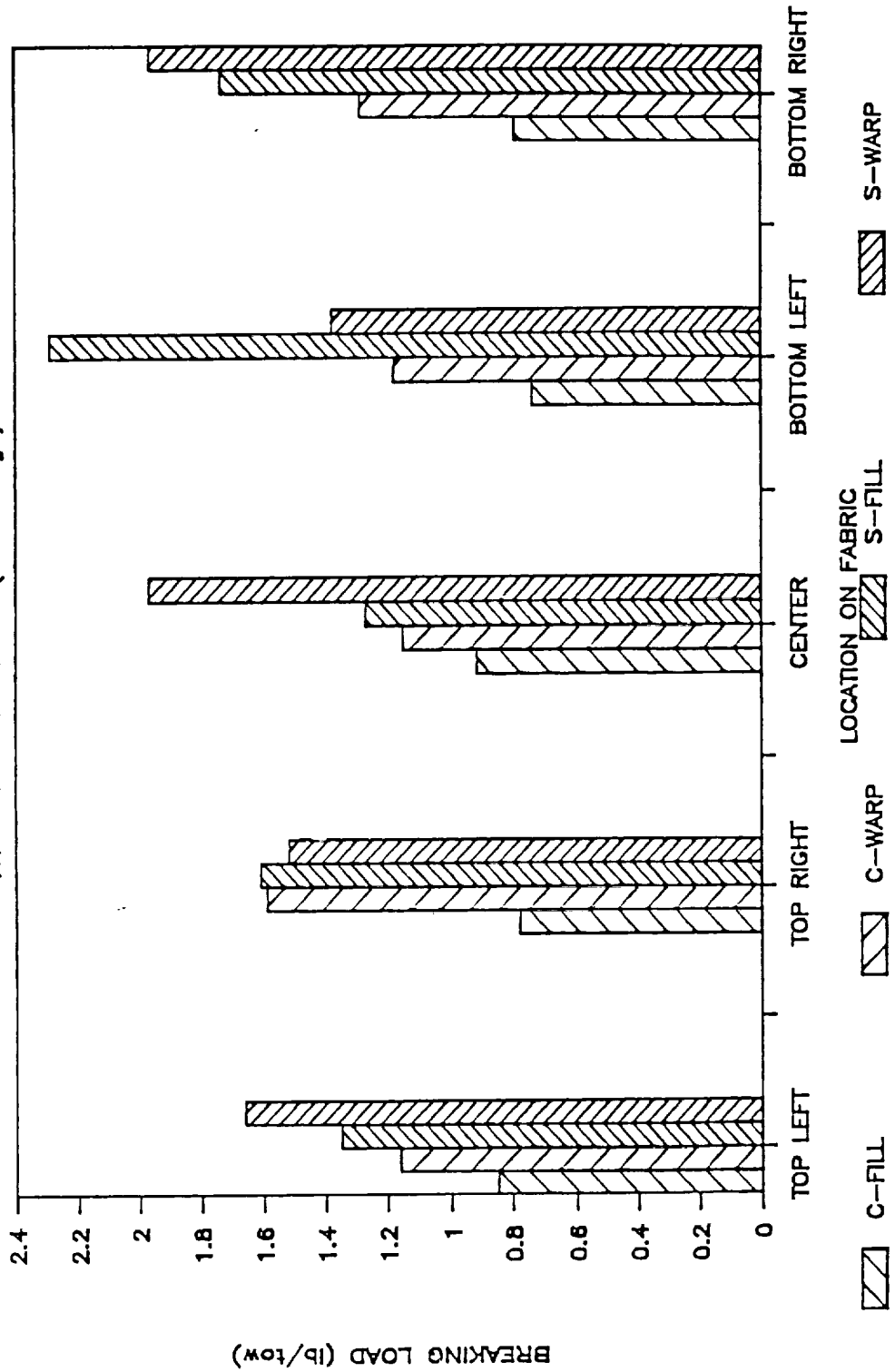


Fig. 2 - VIII

TABLE 3: Results for Average Breaking Load of 1.5" Gauge Length

	BREAKING LOAD (LB/TOW)			
	CCA-3		SWB-8	
	FILL	WARP	FILL	WARP
TOP LEFT	0.84	1.20	1.41	1.44
TOP RIGHT	0.77	1.17	1.55	1.45
CENTER	0.91	1.10	1.37	1.83
BOTTOM LEFT	0.81	1.15	2.22	1.19
BOTTOM RIGHT	0.84	1.31	1.77	2.16
AVERAGE (STD)	0.83 (0.05)	1.19 (0.07)	1.66 (0.31)	1.61 (0.34)

TABLE 4: Results for Average Breaking Load of 2.0" Gauge Length

	BREAKING LOAD (LB/TOW)			
	CCA-3		SWB-8	
	FILL	WARP	FILL	WARP
TOP LEFT	0.81	1.14	1.29	1.78
TOP RIGHT	0.89	1.12	1.83	1.38
CENTER	0.86	1.05	1.19	2.02
BOTTOM LEFT	0.78	1.15	1.99	1.21
BOTTOM RIGHT	0.78	1.04	1.61	2.11
AVERAGE (STD)	0.82 (0.04)	1.10 (0.05)	1.58 (0.31)	1.70 (0.35)

BREAKING LOAD VS LOCATION

for CCA-3 and SWB-8 (1.5" Gauge)

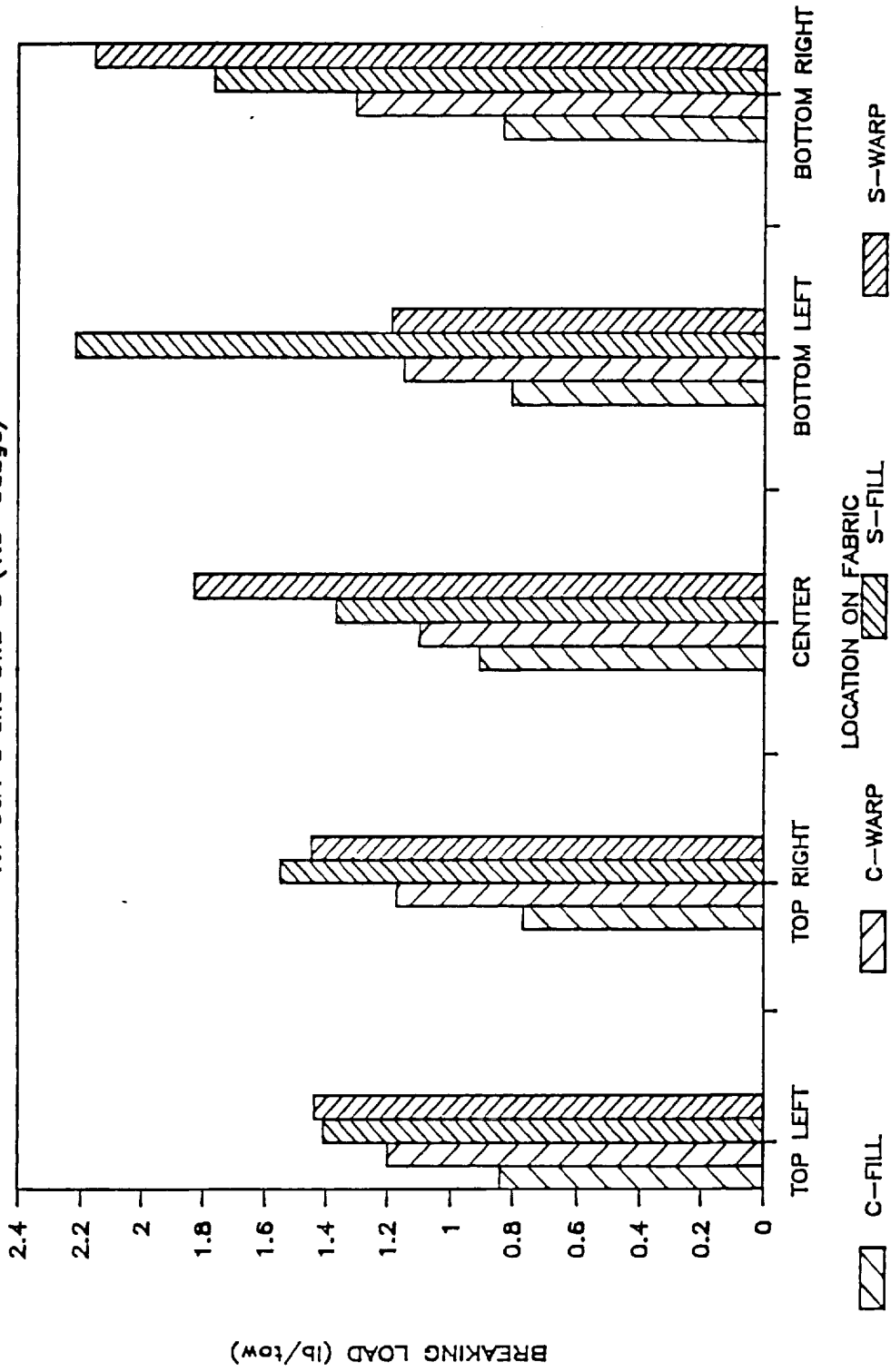


Fig. 3 - VIII

from 1.37 lb/tow at the center to 2.22 lb/tow at bottom left, with an average of 1.66 lb/tow. The values of the warp direction range from 1.19 lb/tow at bottom to 2.16 lb/tow at bottom right. For the fill and warp directions, the average breaking loads are 1.66 and 1.61 lb/tow, respectively. Once again, the fill direction of CCA-3 has the most uniform breaking load distribution across the fabric with a standard deviation of only 0.05. The warp direction of CCA-3 has a standard deviation of 0.07 so it also has a fairly uniform breaking load distribution across the fabric. The standard deviations of SWB-8 in the fill and warp directions are 0.31 and 0.34, respectively.

The 2.0 inch gauge length breaking load distribution results are tabulated in Table 4 and shown in Figure 4. The values for CCA-3 in the fill direction range from 0.78 lb/tow at bottom left and bottom right to 0.89 lb/tow at top right. The average breaking load distribution is 0.82 lb/tow with a standard deviation of 0.04. The warp direction values of CCA-3 range from 1.04 lb/tow at bottom right to 1.15 lb/tow at bottom left with an average breaking load of 1.10 lb/tow and a standard deviation of 0.05. The average breaking load of SWB-8 in the fill direction is 1.58 lb/tow and the standard deviation is 0.31. The values range from 1.19 lb/tow at the center to 1.99 lb/tow at bottom left. The values for SWB-8 in the warp direction range from 1.21 lb/tow at bottom left to 2.11 lb/tow at bottom right with an average breaking load of 1.70 lb/tow and a standard deviation of 0.35. The CCA-3 samples in the fill and warp directions have even breaking load distributions across the fabric.

The results for the deflection of CCA-3 and SWB-8 at a 0.5 inch gauge length are located in Table 5 and Figure 5. The values for CCA-3 in the fill direction range from 0.49 in/tow at bottom right to 0.77 in/tow at bottom left with an average deflection of 0.65 in/tow across the sample. The warp direction values of CCA-3 range from 0.26 in/tow at top right to 0.43 in/tow at bottom right with an average deflection of 0.35 in/tow. The average deflections for the fill and warp direction of SWB-8 are both 0.89 in/tow. The fill

BREAKING LOAD VS LOCATION

for CCA-3 and SWB-8 (2.0" Gauge)

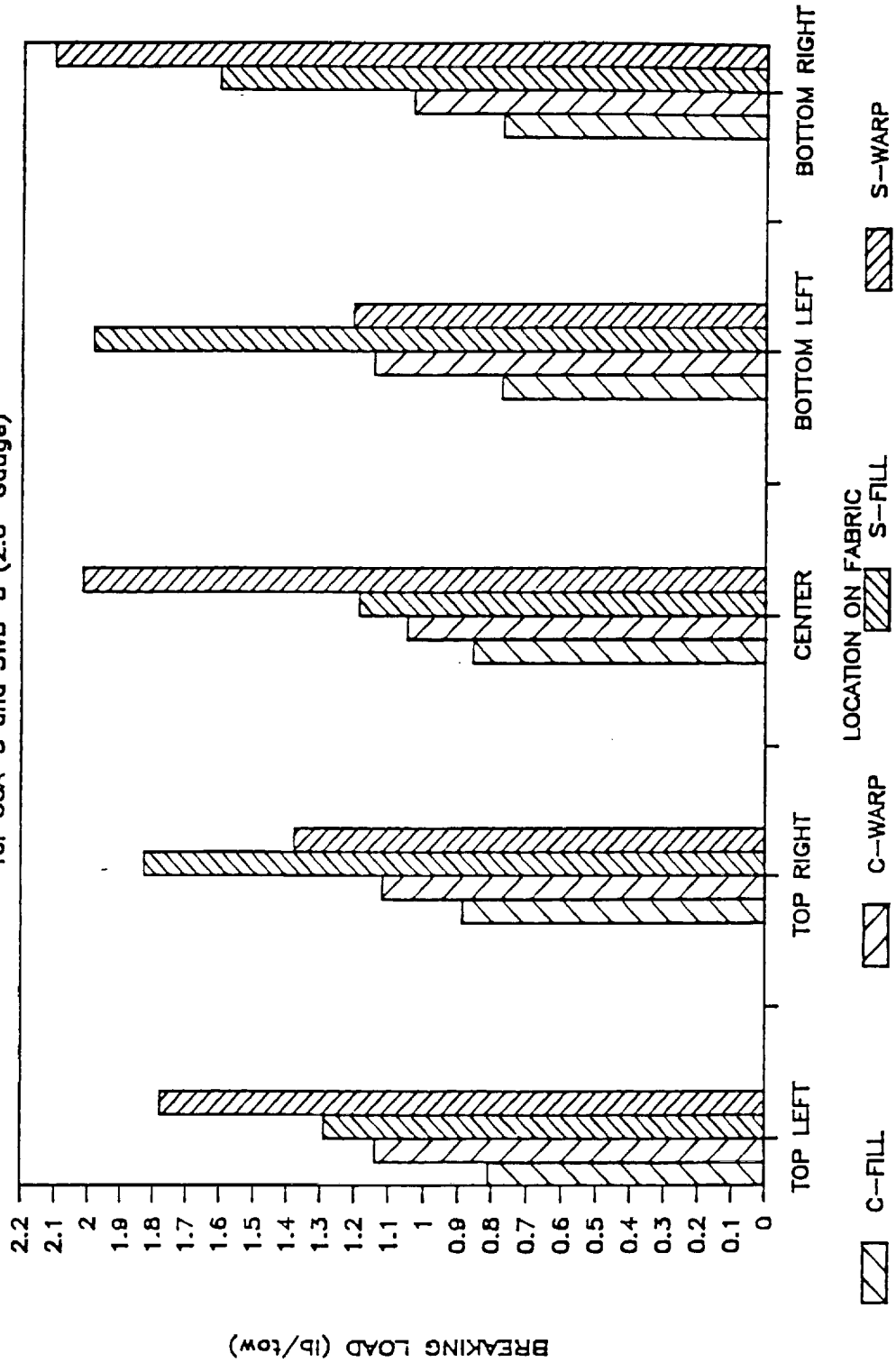


Fig. 4 - VIII

TABLE 5: Results for Average Deflection of 0.5" Gauge Length

	DEFLECTION (IN/TOW)			
	CCA-3		SWB-8	
	FILL	WARP	FILL	WARP
TOP LEFT	0.55	0.36	0.94	0.95
TOP RIGHT	0.71	0.26	0.88	0.85
CENTER	0.75	0.39	0.86	0.82
BOTTOM LEFT	0.77	0.31	0.95	0.95
BOTTOM RIGHT	0.49	0.43	0.81	0.89
AVERAGE (STD)	0.65 (0.11)	0.35 (0.06)	0.89 (0.05)	0.89 (0.05)

TABLE 6: Results for Average Deflection of 1.0" Gauge Length

	DEFLECTION (IN/TOW)			
	CCA-3		SWB-8	
	FILL	WARP	FILL	WARP
TOP LEFT	0.64	0.37	1.01	1.01
TOP RIGHT	0.65	0.36	0.94	1.05
CENTER	0.68	0.36	0.96	0.84
BOTTOM LEFT	0.58	0.39	1.00	0.93
BOTTOM RIGHT	0.58	0.30	0.90	0.93
AVERAGE (STD)	0.63 (0.04)	0.36 (0.03)	0.96 (0.04)	0.95 (0.07)

DEFLECTION VS LOCATION

for CCA-3 and SWB-8 (0.5" Gauge)

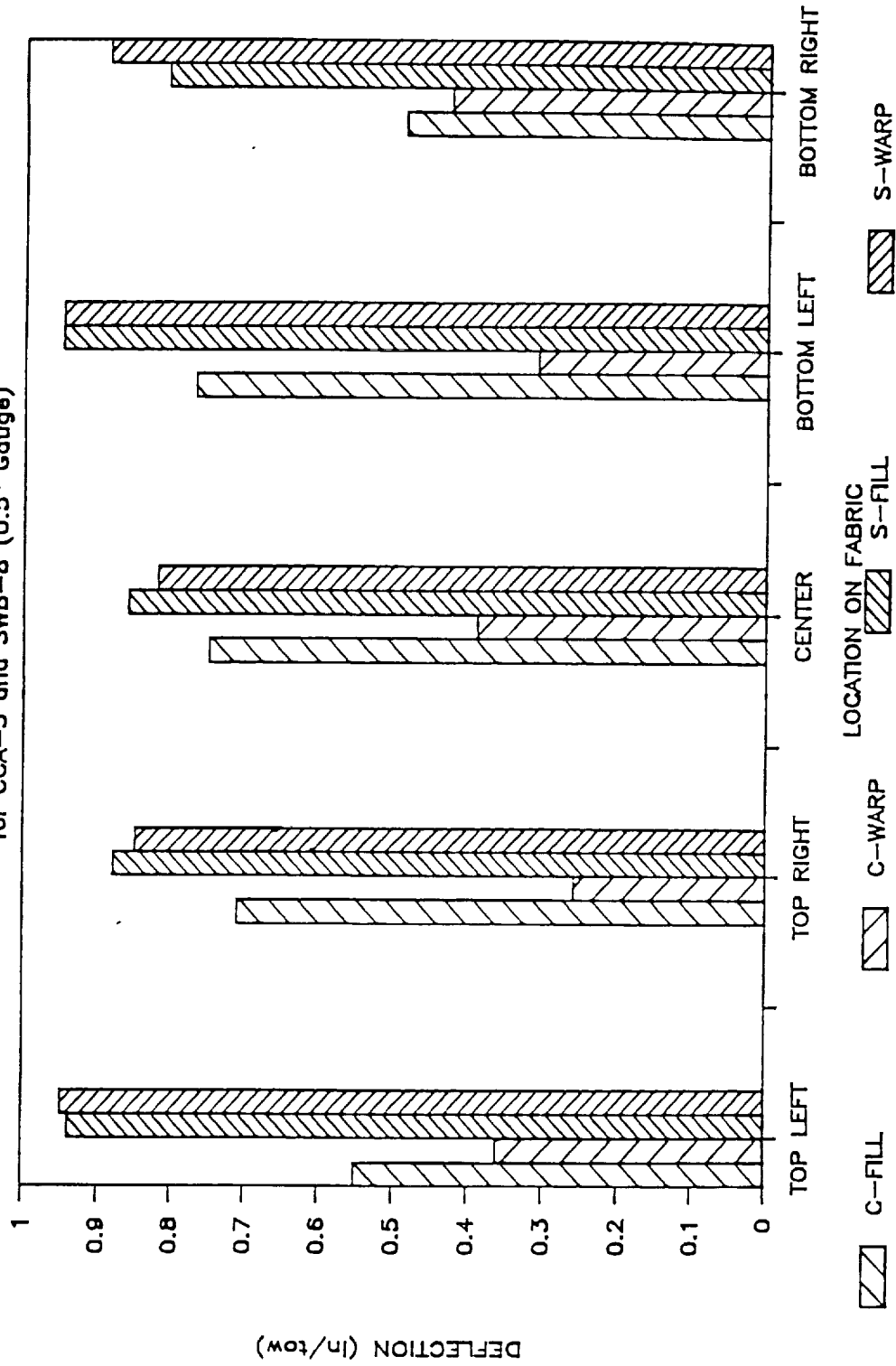


Fig. 5 - VIII

direction values range from 0.81 in/tow at bottom right to 0.95 in/tow at bottom left, and the warp direction values range from 0.82 in/tow at the center to 0.95 in/tow at top and bottom left. The standard deviations of the fill and warp directions of CCA-3 are 0.11 and 0.06, respectively, and the values for fill and warp of SWB-8 are both 0.05. All samples have uniform deflection distributions across the fabric.

The deflection values for 1.0 inch gauge length of CCA-3 and SWB-3 are located in Table 6 and are shown in Figure 6. The values of CCA-3 in the fill direction range from 0.58 in/tow at bottom left and right to 0.68 in/tow at the center. The average deflection distribution across the fabric is 0.63 in/tow with a standard deviation of 0.04. The CCA-3 warp direction values range from 0.30 in/tow at bottom right to 0.39 in/tow at bottom left with an average deflection of 0.36 in/tow and standard deviation of 0.03. The fill direction values of SWB-8 range from 0.90 in/tow at bottom right to 1.01 in/tow at top left. The average deflection distribution across the fabric is 0.96 in/tow with a standard deviation of 0.04. For the warp direction of SWB-8, the values range from 0.84 in/tow at the center to 1.05 in/tow at top right with an average deflection of 0.95 in/tow and a standard deviation of 0.07. All samples have a uniform distribution of deflection across the fabric.

The results for the deflection of CCA-3 and SWB-8 at a 1.5 inch gauge length are located in Table 7 and are shown in Figure 7. The average deflection values for CCA-3 in the fill and warp directions are 0.77 and 0.40 in/tow, respectively, and the average values for the fill and warp directions of SWB-8 are 1.01 and 1.03 in/tow, respectively. For the fill direction of CCA-3, the values range from 0.70 in/tow at top right to 0.84 in/tow at the center with a standard deviation of 0.05 from the average. The values of CCA-3 in the warp direction range from 0.36 in/tow at top left to 0.45 in/tow at top right with a standard deviation of 0.03 from the average deflection. The fill direction values of SWB-8 range from 0.95 in/tow at top right to 1.06 in/tow at top and bottom left with a standard

TABLE 7: Results for Average Deflection of 1.5" Gauge Length

	DEFLECTION (IN/TOW)			
	CCA-3		SWB-8	
	FILL	WARP	FILL	WARP
TOP LEFT	0.77	0.36	1.06	1.11
TOP RIGHT	0.70	0.45	0.95	1.21
CENTER	0.84	0.40	1.01	0.88
BOTTOM LEFT	0.80	0.41	1.06	1.02
BOTTOM RIGHT	0.72	0.39	0.98	0.95
AVERAGE	0.77	0.40	1.01	1.03
(STD)	(0.05)	(0.03)	(0.04)	(0.12)

TABLE 8: Results for Average Deflection of 2.0" Gauge Length

	DEFLECTION (IN/TOW)			
	CCA-3		SWB-8	
	FILL	WARP	FILL	WARP
TOP LEFT	0.74	0.39	1.21	1.06
TOP RIGHT	0.78	0.45	1.05	1.23
CENTER	0.77	0.49	1.08	1.07
BOTTOM LEFT	0.87	0.41	1.11	1.00
BOTTOM RIGHT	0.79	0.35	1.00	1.04
AVERAGE	0.79	0.42	1.09	1.08
(STD)	(0.04)	(0.05)	(0.07)	(0.08)

DEFLECTION VS LOCATION

for CCA-3 and SWB-8 (1.0" Gauge)

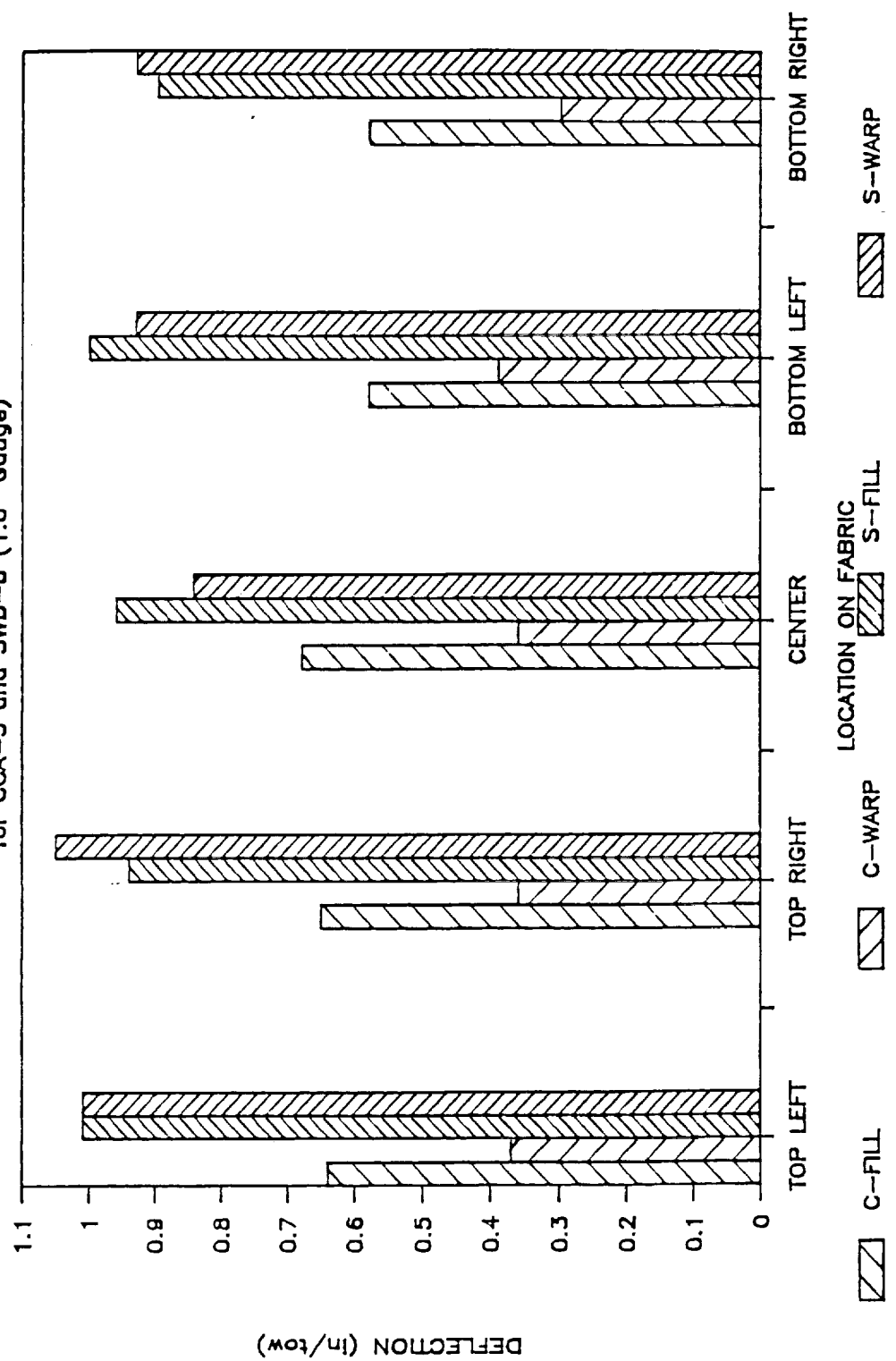


Fig. 6 - VIII

DEFLECTION VS LOCATION

for CCA-3 and SWB-8 (1.5" Gauge)

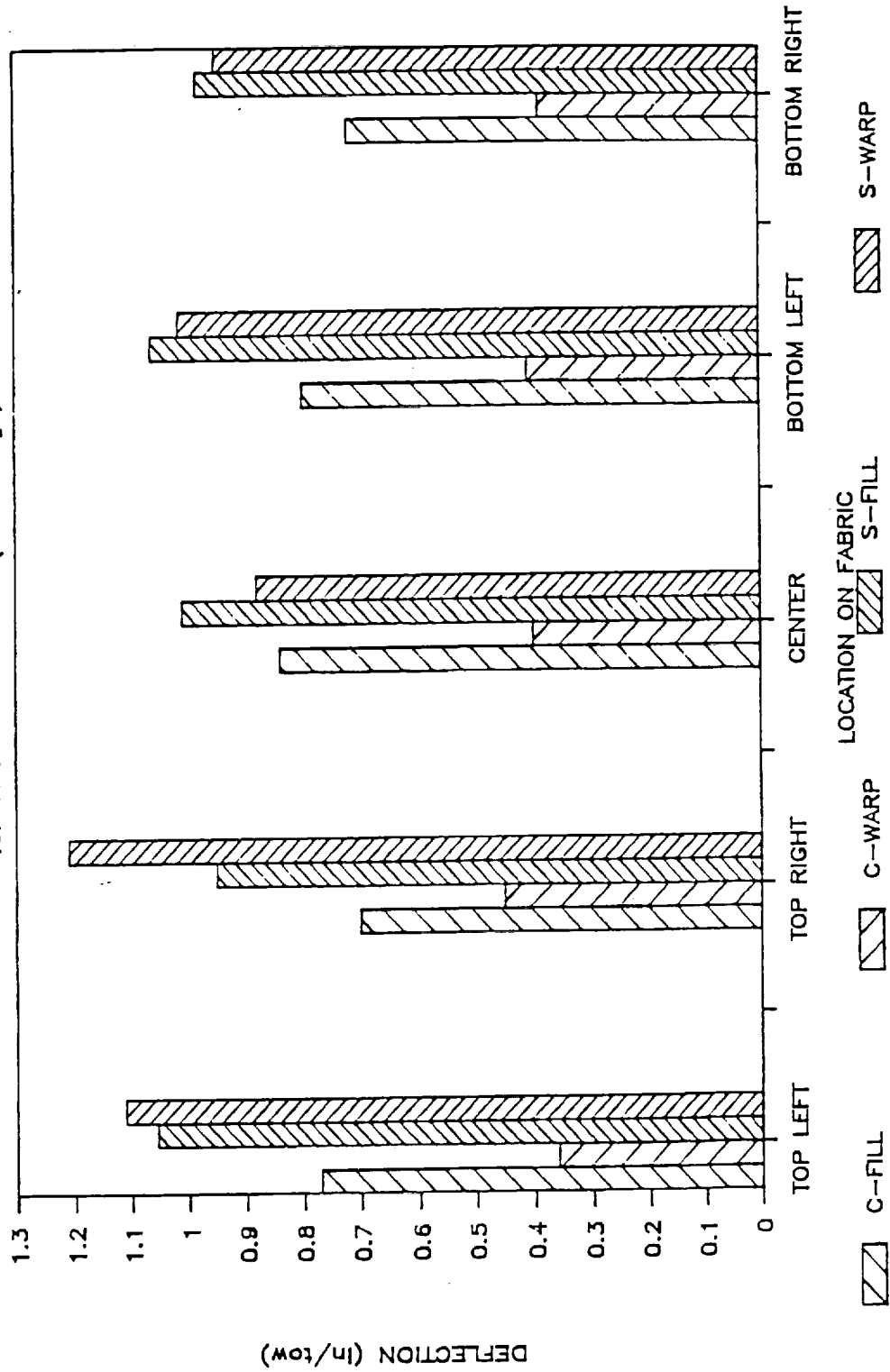


Fig. 7 - VIII

deviation of 0.04 from the average of 1.01 in/tow. The SWB-8 values in the warp direction range from 0.88 in/tow at the center to 1.21 in/tow at top right with a standard deviation of 0.12 from the average. The SWB-8 warp values have the most uneven distribution across the fabric.

The 2.0 inch gauge length results for the deflection of CCA-3 and SWB-8 fibers can be seen in Table 8 and Figure 8. The CCA-3 fill values range from 0.74 in/tow at top left to 0.87 in/tow at bottom left with an average of 0.79 in/tow and a standard deviation of 0.04. The warp direction values of CCA-3 range from 0.35 in/tow at bottom right to 0.49 in/tow at the center with an average deflection of 0.42 in/tow and a standard deviation of 0.05. The average values for deflection of SWB-8 in the fill and warp directions are 1.09 and 1.08 in/tow, respectively with standard deviations of 0.07 and 0.08, respectively. The SWB-8 fill values range from 1.00 in/tow at bottom right to 1.21 in/tow at top left, and the SWB-8 warp values range from 1.00 in/tow at bottom left to 1.23 in/tow at top right. All samples show a uniform deflection distribution across the fabric.

The results of breaking load vs gauge length for CCA-3 in the fill and warp directions are tabulated in Tables 9 and 10. These tables show the actual experimental results and the results calculated by linear regression. The actual results vs linear results are plotted in Figures 9 and 10. The actual values of breaking load for CCA-3 in the fill direction decreased from 0.85 lb/tow at 0.5 inch gauge length to 0.82 lb/tow at 2.0 inch gauge length. The linear results decrease from 0.842 lb/tow at 0.5 inch gauge length to 0.818 lb/tow at the 2.0 inch gauge length. The R squared value in the regression output is the degree of fit of the linear results to the actual results, and in this case, the value is 0.533333 which is not a good fit. This can clearly be seen in Figure 9 which compares the actual points to the linear regression results. The CCA-3 warp values for breaking load also decrease as gauge length increases. The actual

TABLE 9: Linear Regression Results for Breaking Load of CCA-3
Fill Direction

GAUGE LENGTH (in)	BREAKING LOAD (LB/TOW)	
	ACTUAL	LINEAR
0.5	0.85	0.842
1.0	0.82	0.834
1.5	0.83	0.826
2.0	0.82	0.818

Regression Output:

Constant	0.85	y int
Std Err of Y Est	0.011832	
R Squared	0.533333	
No. of Observations	4	
Degrees of Freedom	2	
X Coefficients(s)	-0.016	slope
Std Err of Coef.	0.010583	

TABLE 10: Linear Regression Results for Breaking Load of CCA-3
Warp Direction

GAUGE LENGTH (in)	BREAKING LOAD (LB/TOW)	
	ACTUAL	LINEAR
0.5	1.28	1.303
1.0	1.27	1.241
1.5	1.19	1.179
2.0	1.10	1.117

Regression Output:

Constant	1.365	y int
Std Err of Y Est	0.029832	
R Squared	0.915238	
No. of Observations	4	
Degrees of Freedom	2	
X Coefficients(s)	-0.124	slope
Std Err of Coef.	0.026683	

DEFLECTION VS LOCATION

for CCA-3 and SWB-8 (2.0" Gauge)

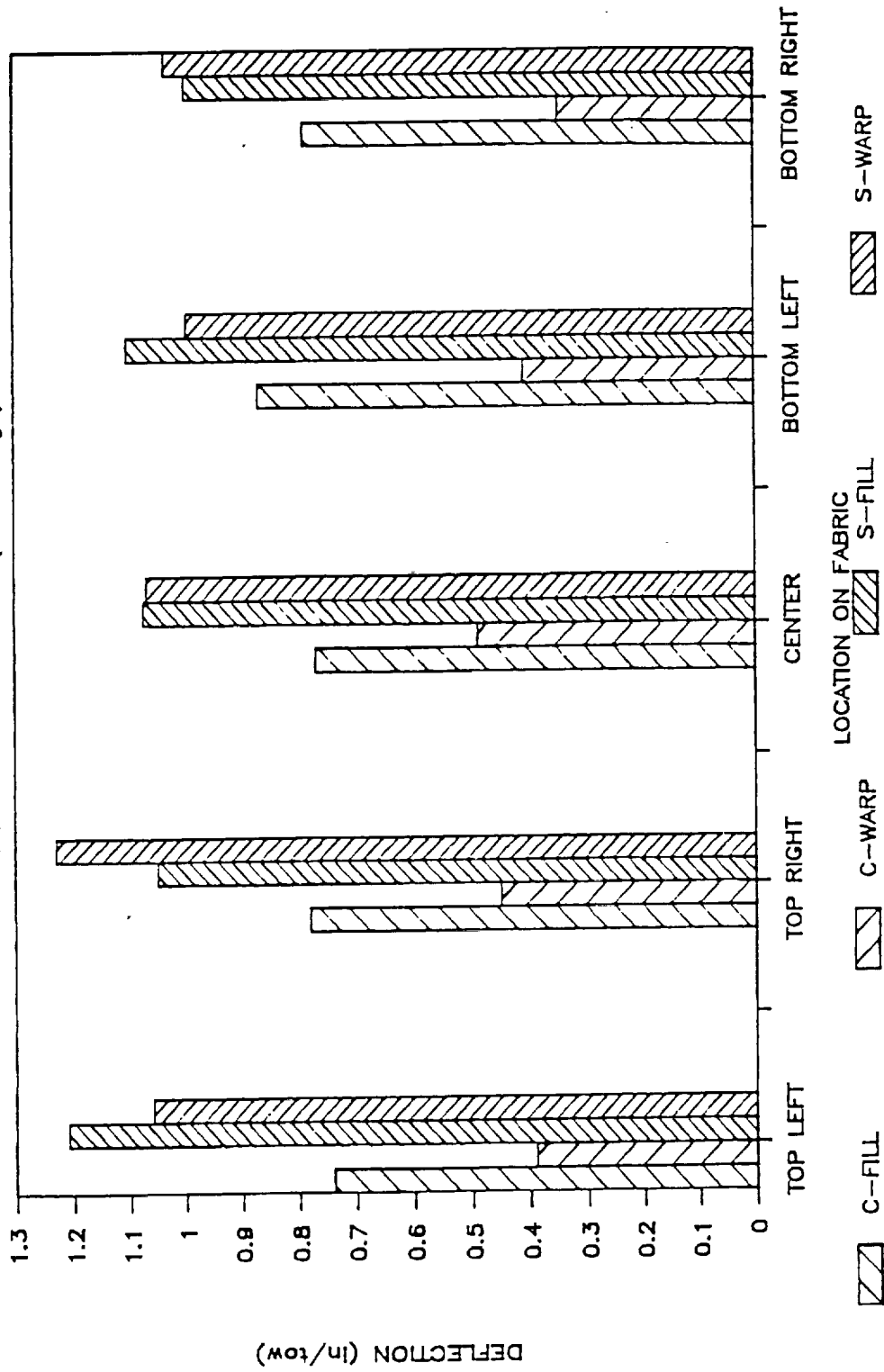


Fig. 8 - VIII

BREAKING LOAD VS GAUGE

Actual and Linear for CCA-3 (Fill)

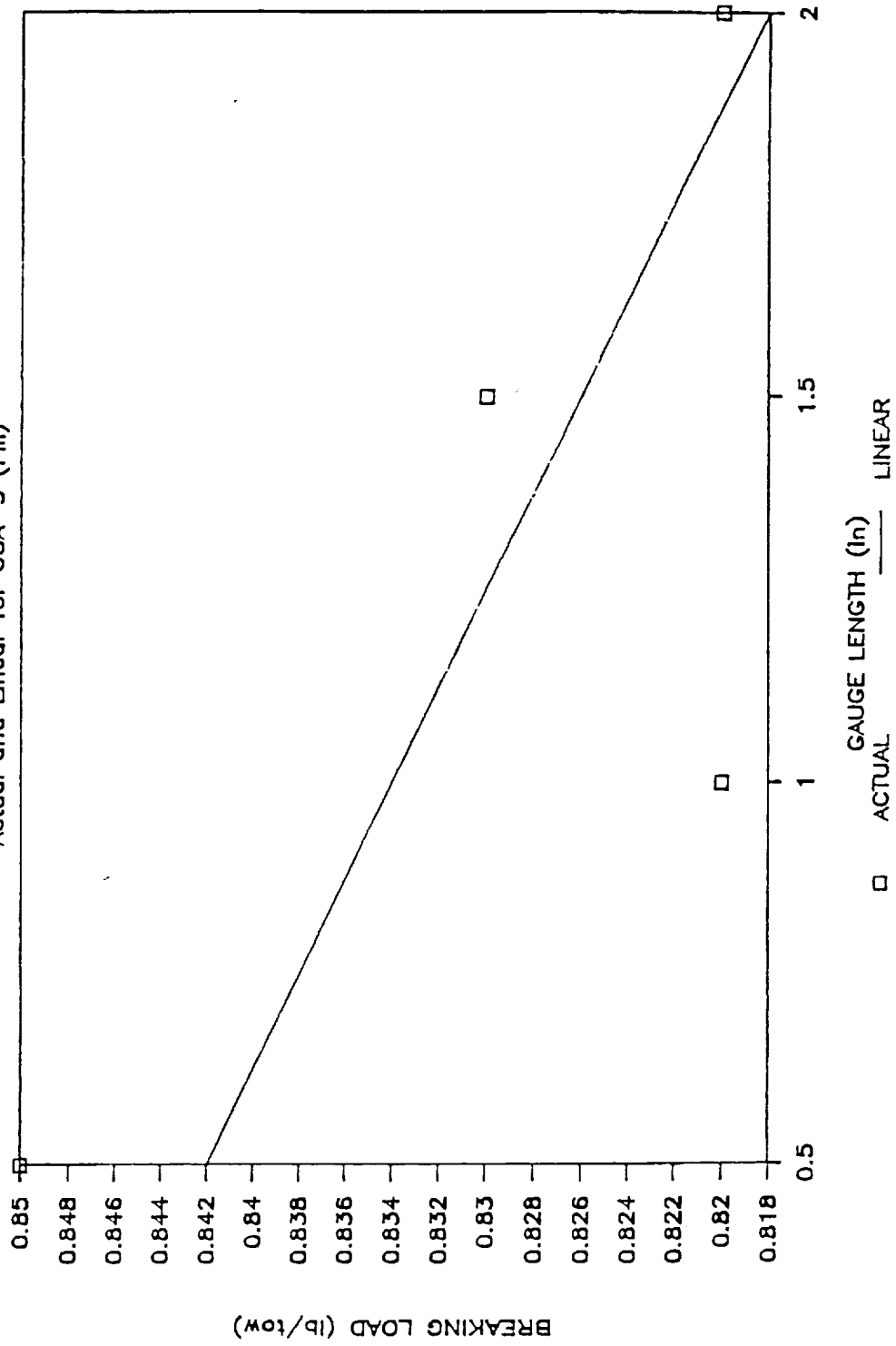


Fig. 9 - VIII

BREAKING LOAD VS GAUGE

Actual and Linear for CCA-3 (Warp)

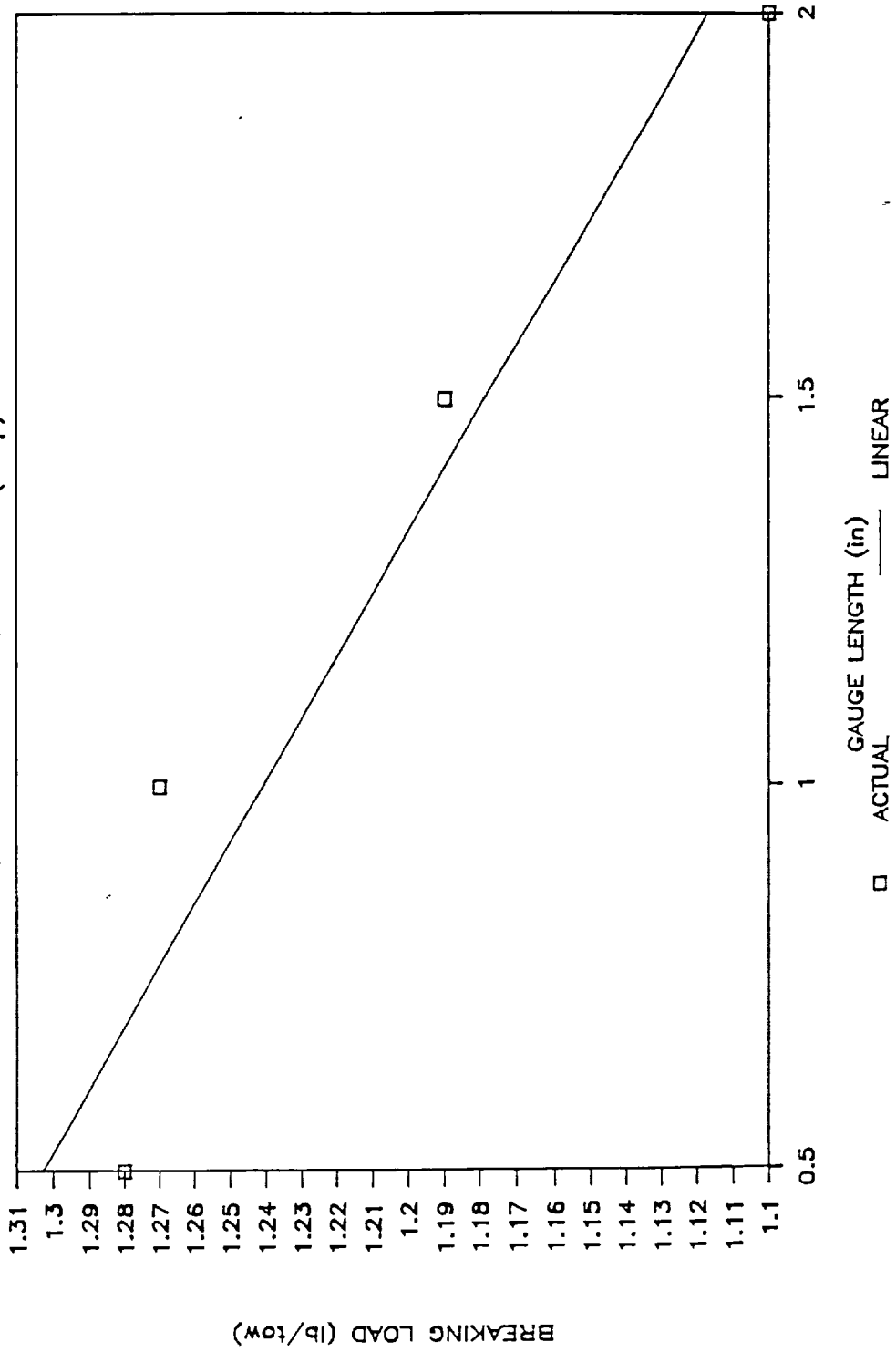


Fig. 10 - VIII

values decrease from 1.28 lb/tow at the 0.5 inch gauge length to 1.10 lb/tow at the 2.0 inch gauge length. The degree of fit of the linear results to the actual results is good in this case with a value of 0.915238. The linear results decrease from 1.303 lb/tow at the 0.5 inch gauge length to 1.117 lb/tow at the 2.0 inch gauge length. The comparison of actual to linear values can be seen in Figure 10.

The results for the comparison of breaking load vs gauge length for SWB-8 in the fill and warp directions are located in Tables 11 and 12. Both directions decrease in breaking load with an increase in gauge length. The actual values for the fill direction decrease from 1.70 lb/tow at the 0.5 inch gauge length to 1.58 lb/tow at the 2.0 inch gauge length, and the linear results decrease from 1.700 lb/tow to 1.585 lb/tow at the same gauge lengths. The degree of fit of the linear results to the actual results is 0.819397 which is a fair fit, and the plot can be viewed in Figure 11. The warp direction actual results decrease from 1.72 lb/tow at 0.5 inch gauge length to 1.70 lb/tow at 2.0 inch gauge length; however, the breaking load at 1.5 inches is 1.61 lb/tow which causes major error when linear regression is applied to the actual points. The linear results decrease from 1.705 lb/tow at 0.5 inches to 1.660 lb/tow at 2.0 inches. The degree of fit is very poor in this case with a value of 0.154639, and this can be seen in Figure 12. The poor fit is due to the abnormal actual value at 1.5 inches.

These results agree in all cases with the theory that strength decreases with an increase in gauge length. The longer the gauge length, the more flaws are present along the fiber; therefore, the strength weakens with an increase in gauge length.

The results for deflection vs gauge length for CCA-3 in the fill and warp directions are tabulated in Tables 13 and 14. For both directions, deflection increases as gauge length increases. The deflection values for CCA-3 fill increase from 0.65 in/tow at a gauge length of 0.5 inches to 0.79 in/tow at a gauge length of 2.0 inches. The linearized values increase from 0.626 in/tow at 0.5 inches to 0.794 in/tow at 2.0 inches.

TABLE 11: Linear Regression Results for Breaking Load of SWB-8
Fill Direction

GAUGE LENGTH (in)	BREAKING LOAD (LB/TOW)	
	ACTUAL	LINEAR
0.5	1.70	1.700
1.0	1.65	1.665
1.5	1.66	1.630
2.0	1.58	1.595

Regression Output:

Constant	1.735	y int
Std Err of Y Est	0.025980	
R Squared	0.819397	
No. of Observations	4	
Degrees of Freedom	2	
X Coefficients(s)	-0.07	slope
Std Err of Coef.	0.023237	

TABLE 12: Linear Regression Results for Breaking Load of SWB-8
Warp Direction

GAUGE LENGTH (in)	BREAKING LOAD (LB/TOW)	
	ACTUAL	LINEAR
0.5	1.72	1.705
1.0	1.70	1.690
1.5	1.61	1.675
2.0	1.70	1.660

Regression Output:

Constant	1.72	y int
Std Err of Y Est	0.055452	
R Squared	0.154639	
No. of Observations	4	
Degrees of Freedom	2	
X Coefficients(s)	-0.03	slope
Std Err of Coef.	0.049598	

BREAKING LOAD VS GAUGE

Actual and Linear for SWB-8 (FIII)

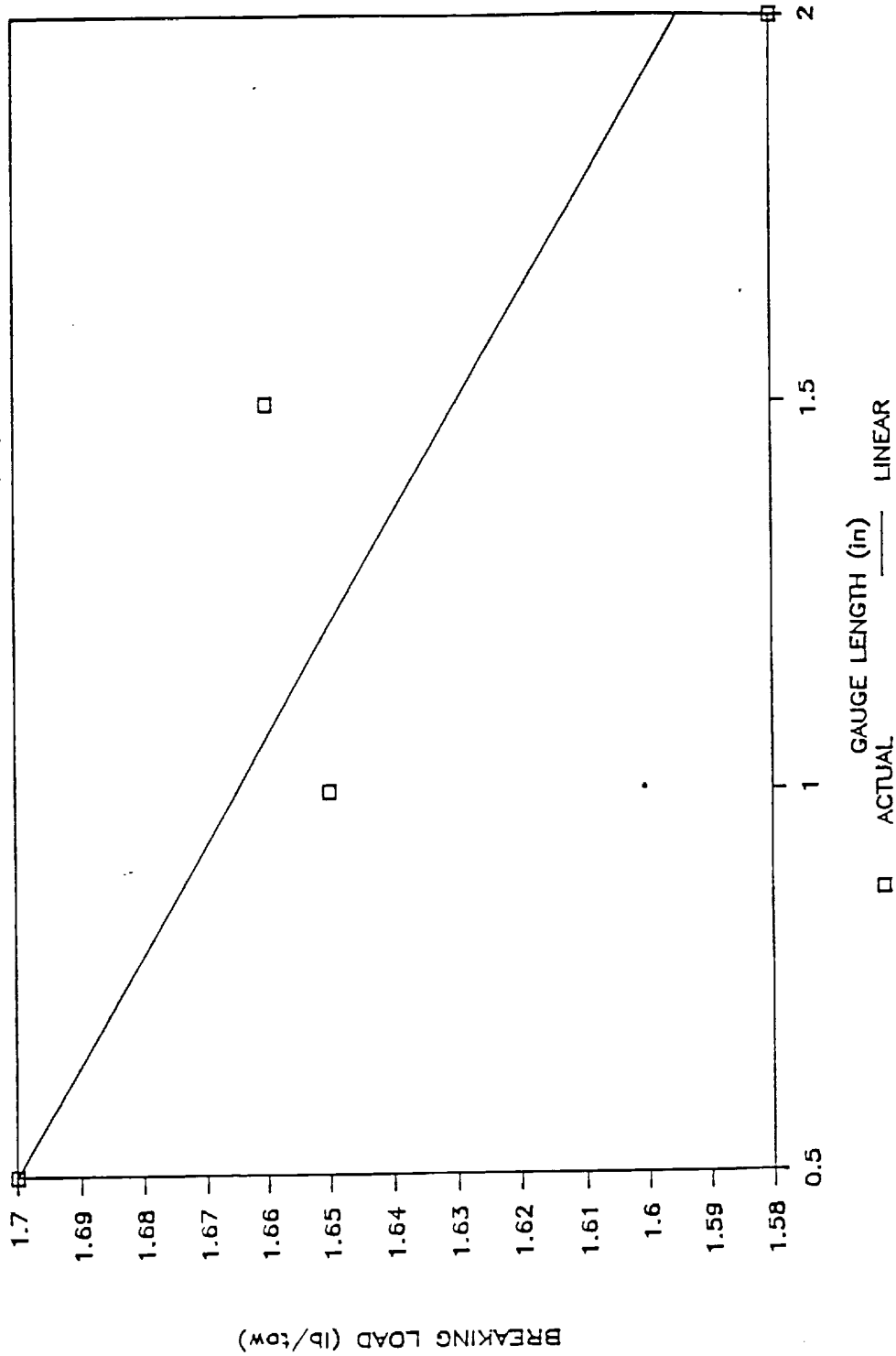


Fig. 11 - VIII

BREAKING LOAD VS GAUGE

Actual and Linear for SWB-8 (Warp)

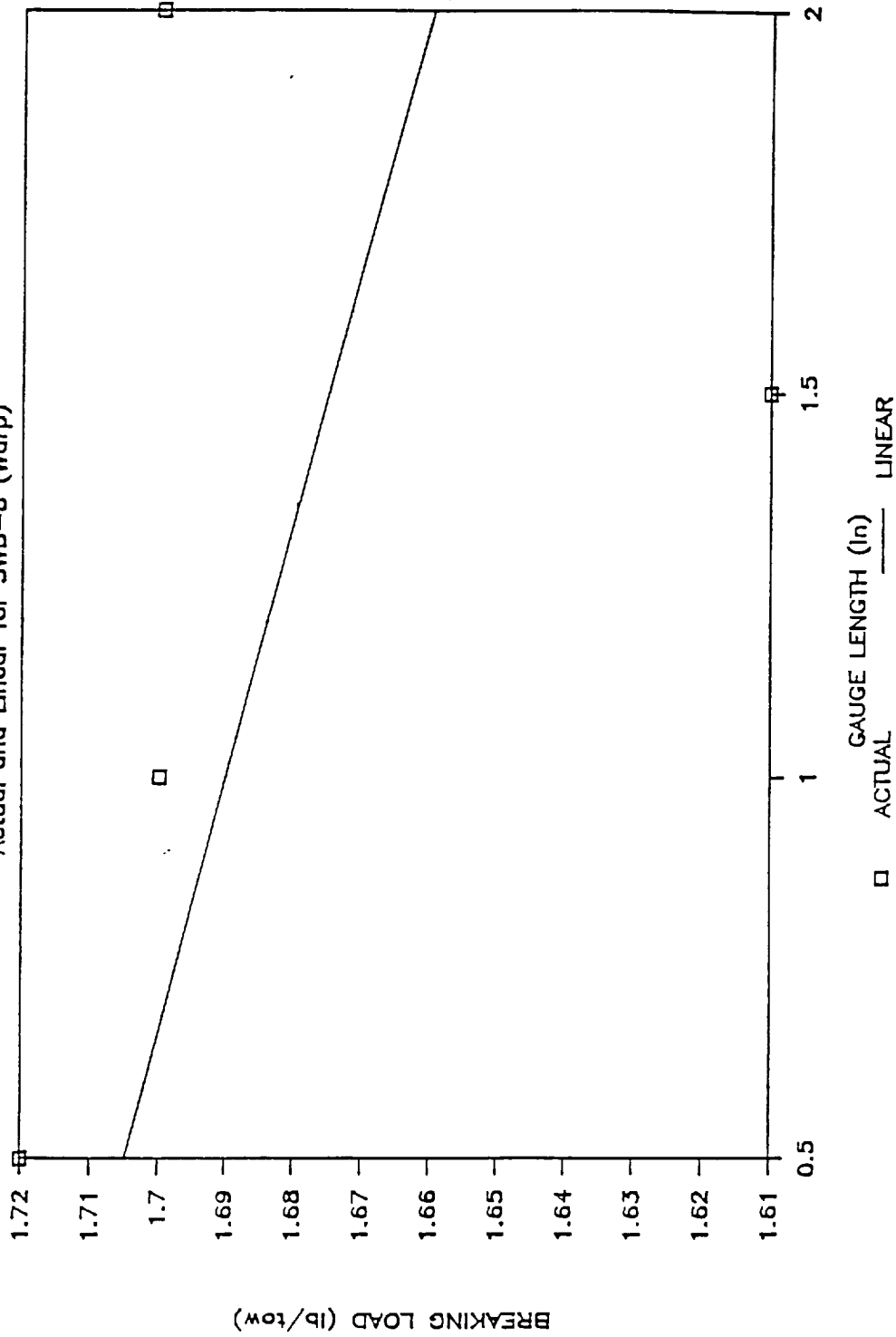


Fig. 12 - VIII

TABLE 13: Linear Regression Results for Deflection of CCA-3
Fill Direction

GAUGE LENGTH (in)	DEFLECTION (LB/TOW)	
	ACTUAL	LINEAR
0.5	0.65	0.626
1.0	0.63	0.682
1.5	0.77	0.738
2.0	0.79	0.794

Regression Output:		
Constant	0.57	y int
Std Err of Y Est	0.046475	
R Squared	0.784	
No. of Observations	4	
Degrees of Freedom	2	
X Coefficients(s)	0.112	slope
Std Err of Coef.	0.041569	

TABLE 14: Linear Regression Results for Deflection of CCA-3
Warp Direction

GAUGE LENGTH (in)	DEFLECTION (LB/TOW)	
	ACTUAL	LINEAR
0.5	0.35	0.435
1.0	0.36	0.370
1.5	0.40	0.395
2.0	0.42	0.420

Regression Output:		
Constant	0.32	y int
Std Err of Y Est	0.008660	
R Squared	0.954198	
No. of Observations	4	
Degrees of Freedom	2	
X Coefficients(s)	0.05	slope
Std Err of Coef.	0.007745	

DEFLECTION VS GAUGE LENGTH

Actual and Linear for CCA-3 (FII)

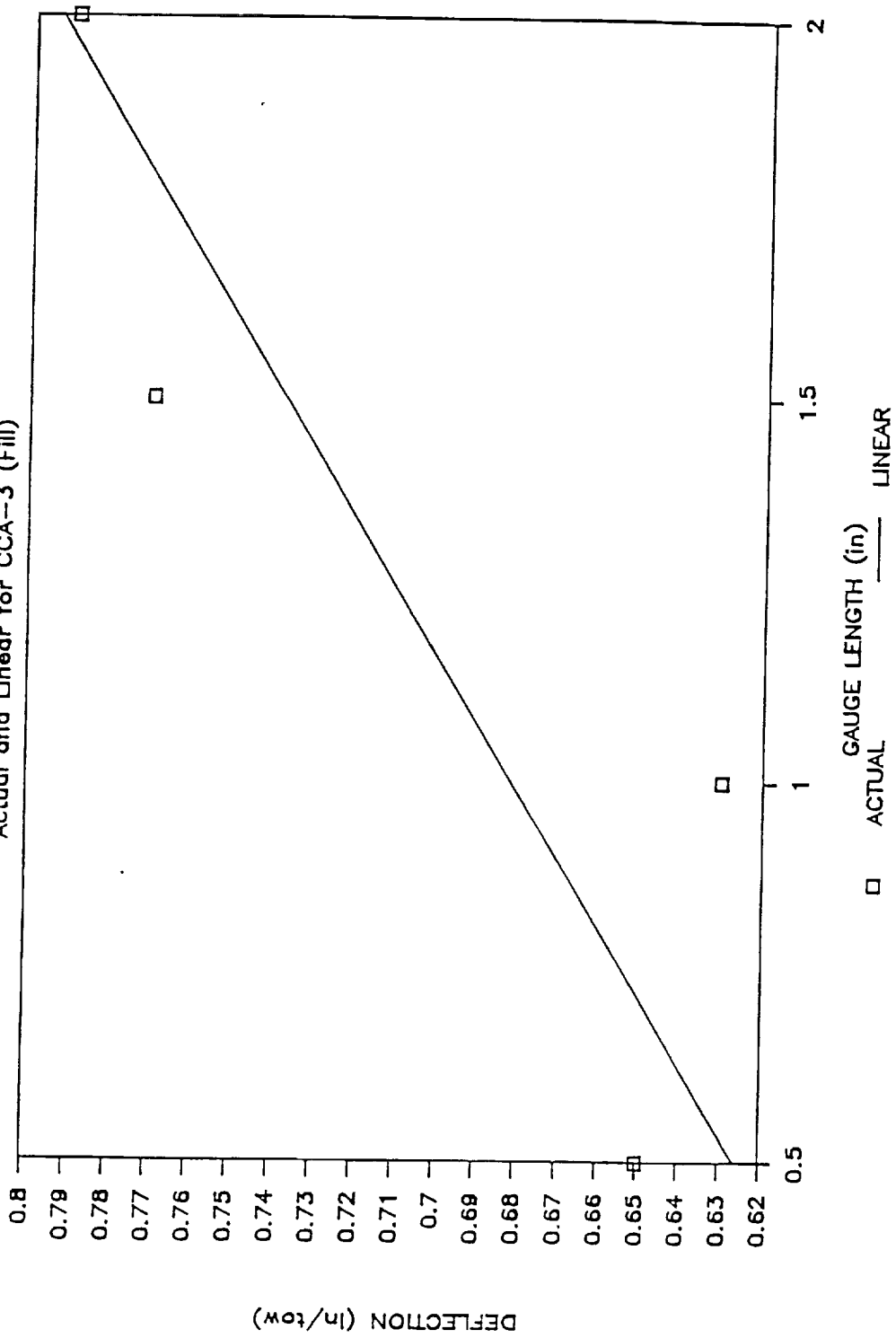


Fig. 13 - VIII

DEFLECTION VS GAUGE LENGTH

Actual and Linear for CCA-3 (Warp)

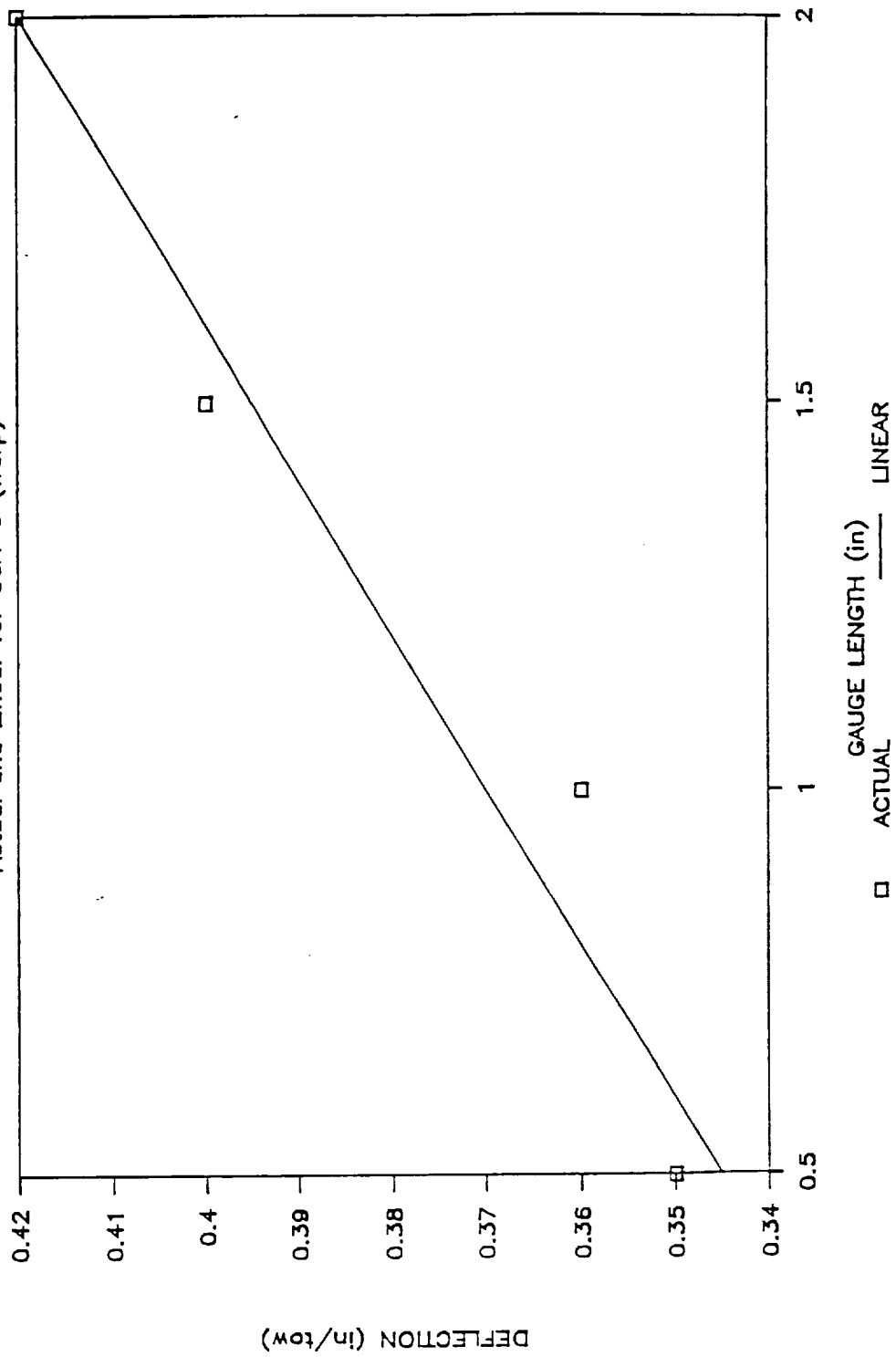


Fig. 14 - VIII

The actual value at 1.0 inches is lower than the value at 0.5 inches so the degree of fit of the linear values to the actual values is not as good as it should be. The R squared value for CCA-3 fill is 0.784, and the comparison of actual values to linear values is shown in Figure 13. The values for deflection of CCA-3 in the warp direction increase from 0.35 in/tow at 0.5 inches to 0.42 in/tow at 2.0 inches, and the linear values increase from 0.345 in/tow at the 0.5 inch gauge length to 0.420 in/tow at the 2.0 inch gauge length. The degree of fit in this case is 0.954198 which is a fairly close fit, and the comparison can be seen in Figure 14.

The results for the deflection vs gauge length for the fill and warp directions of SWB-8 can be seen in Tables 15 and 16. The degree of fit of the linear values to the actual values is very good for both directions. In both cases, the R squared term is 0.992949, and the comparisons of actual and linear values can be seen in Figures 15 and 16. The actual values increase from 0.89 in/tow at a gauge length of 0.5 inches to 1.09 in/tow at a gauge length of 2.0 inches for the fill direction, and they increase to 1.08 in/tow at 2.0 inches for the warp direction. For both directions, the linearized values increase from 0.89 in/tow at 0.5 inches to 1.085 in/tow at 2.0 inches.

As gauge length increases, the deflection increases in all cases because the fibers have longer to stretch.

The breaking load vs gauge length is plotted in Figure 17 for CCA-3 and SWB-8 in both the fill and warp directions. For CCA-3, the warp direction breaking load values are higher than the fill direction values. At a gauge length of 0.5 inches, the warp value is 1.28 lb/tow; whereas, the fill value is 0.85 lb/tow. The warp values decrease to 1.10 lb/tow, but they are still greater than the fill values which only decrease to 0.82 lb/tow. The warp fiber bundles usually contain more individual fibers than the fill fiber bundles; therefore, the warp tows are usually stronger than the fill tows.

TABLE 15: Linear Regression Results for Deflection of SWB-8
Fill Direction

GAUGE LENGTH (In)	DEFLECTION (IN/TOW)	
	ACTUAL	LINEAR
0.5	0.89	0.890
1.0	0.96	0.955
1.5	1.01	1.020
2.0	1.09	1.085

Regression Output:

Constant	0.825	y int
Std Err of Y Est	0.008660	
R Squared	0.992949	
No. of Observations	4	
Degrees of Freedom	2	
X Coefficients(s)	0.13	slope
Std Err of Coef.	0.007745	

TABLE 16: Linear Regression Results for Deflection of SWB-8
Warp Direction

GAUGE LENGTH (In)	DEFLECTION (IN/TOW)	
	ACTUAL	LINEAR
0.5	0.89	0.890
1.0	0.95	0.955
1.5	1.03	1.020
2.0	1.08	1.085

Regression Output:

Constant	0.825	y int
Std Err of Y Est	0.008660	
R Squared	0.992949	
No. of Observations	4	
Degrees of Freedom	2	
X Coefficients(s)	0.13	slope
Std Err of Coef.	0.007745	

DEFLECTION VS GAUGE LENGTH

Actual and Linear for SWB-8 (FII)

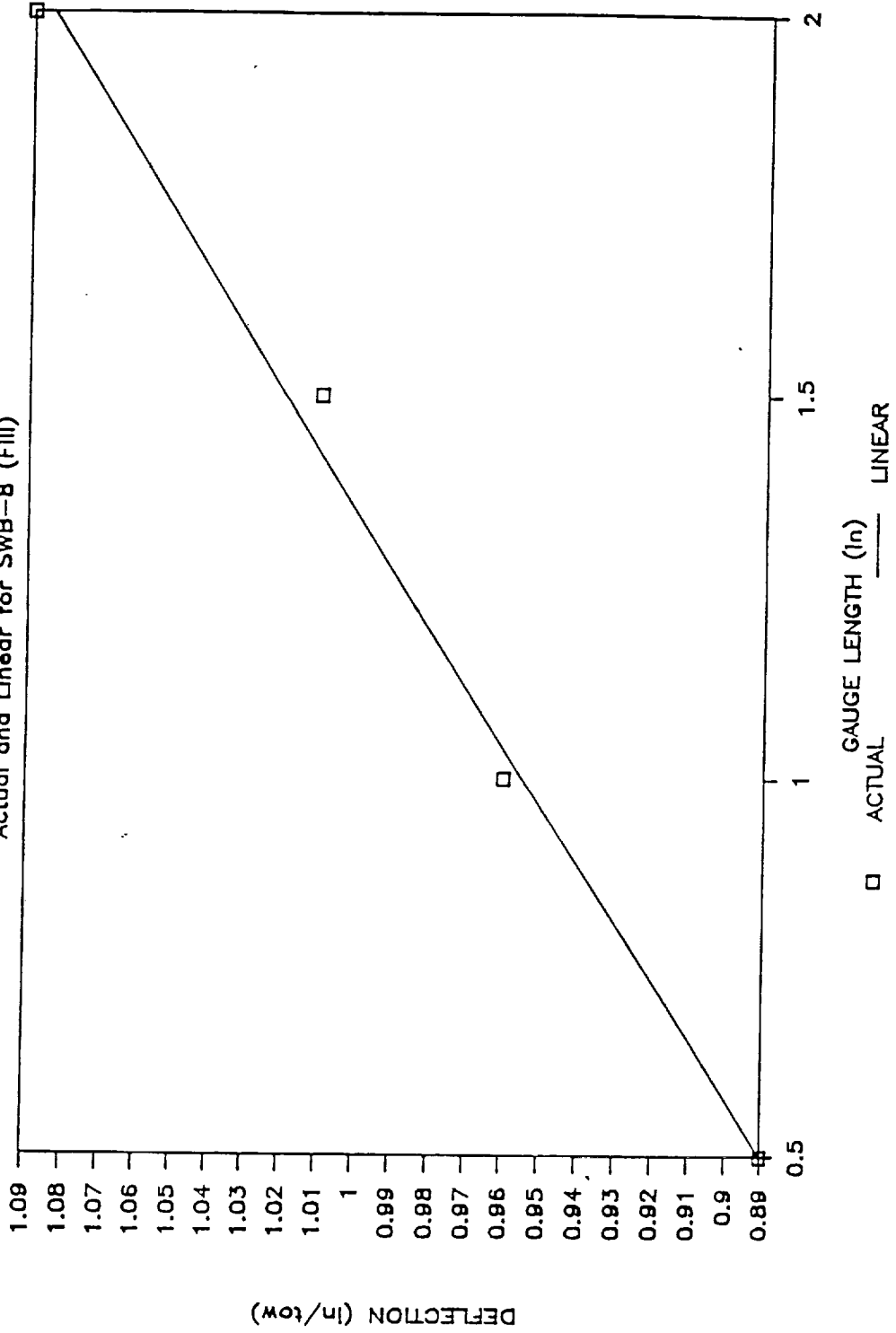


Fig. 15 - VIII

DEFLECTION VS GAUGE LENGTH

Actual and Linear for SWB-8 (Warp)

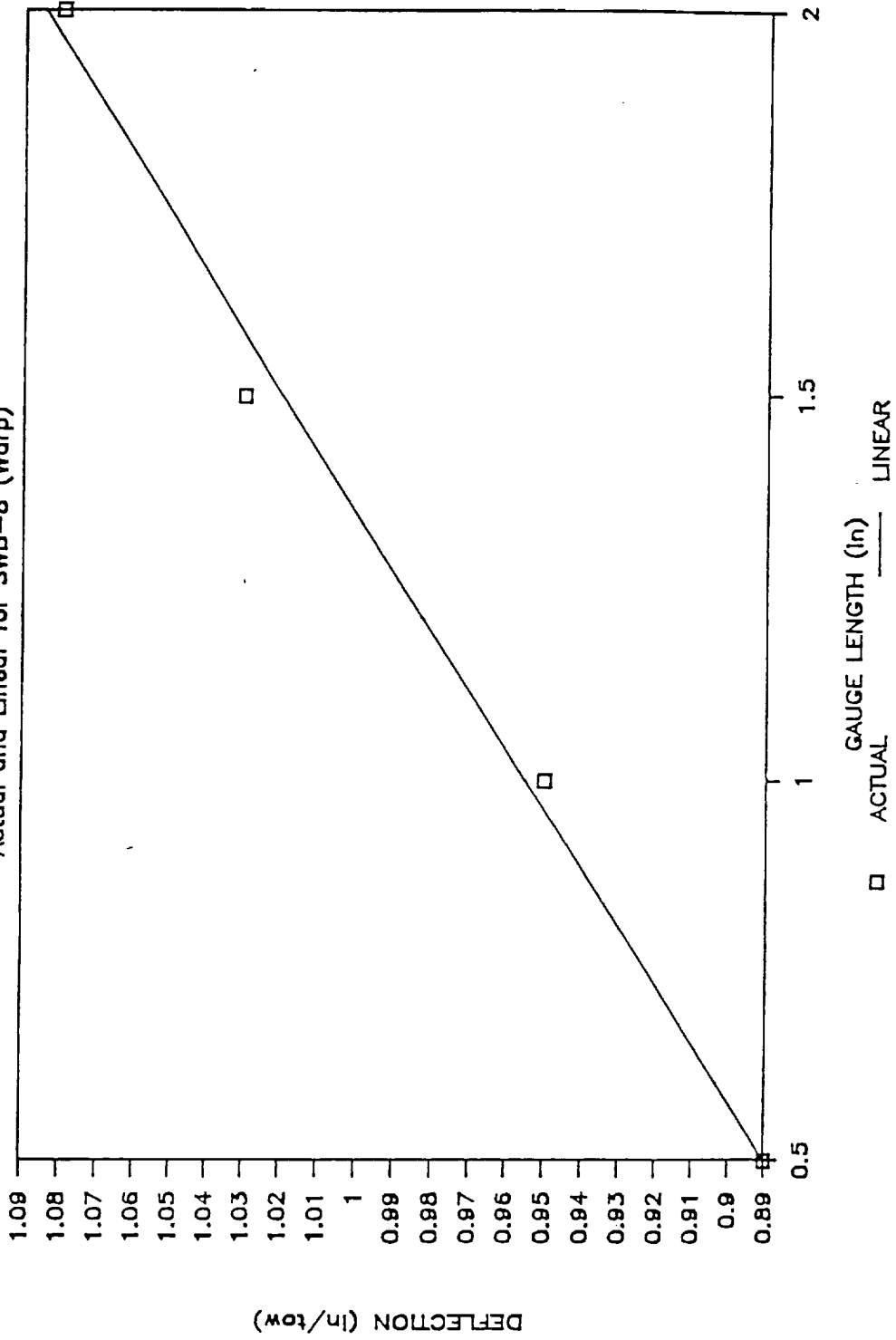


Fig. 16 - VIII

BREAKING LOAD VS GAUGE

Actual Values for CCA--3 and SWB--8

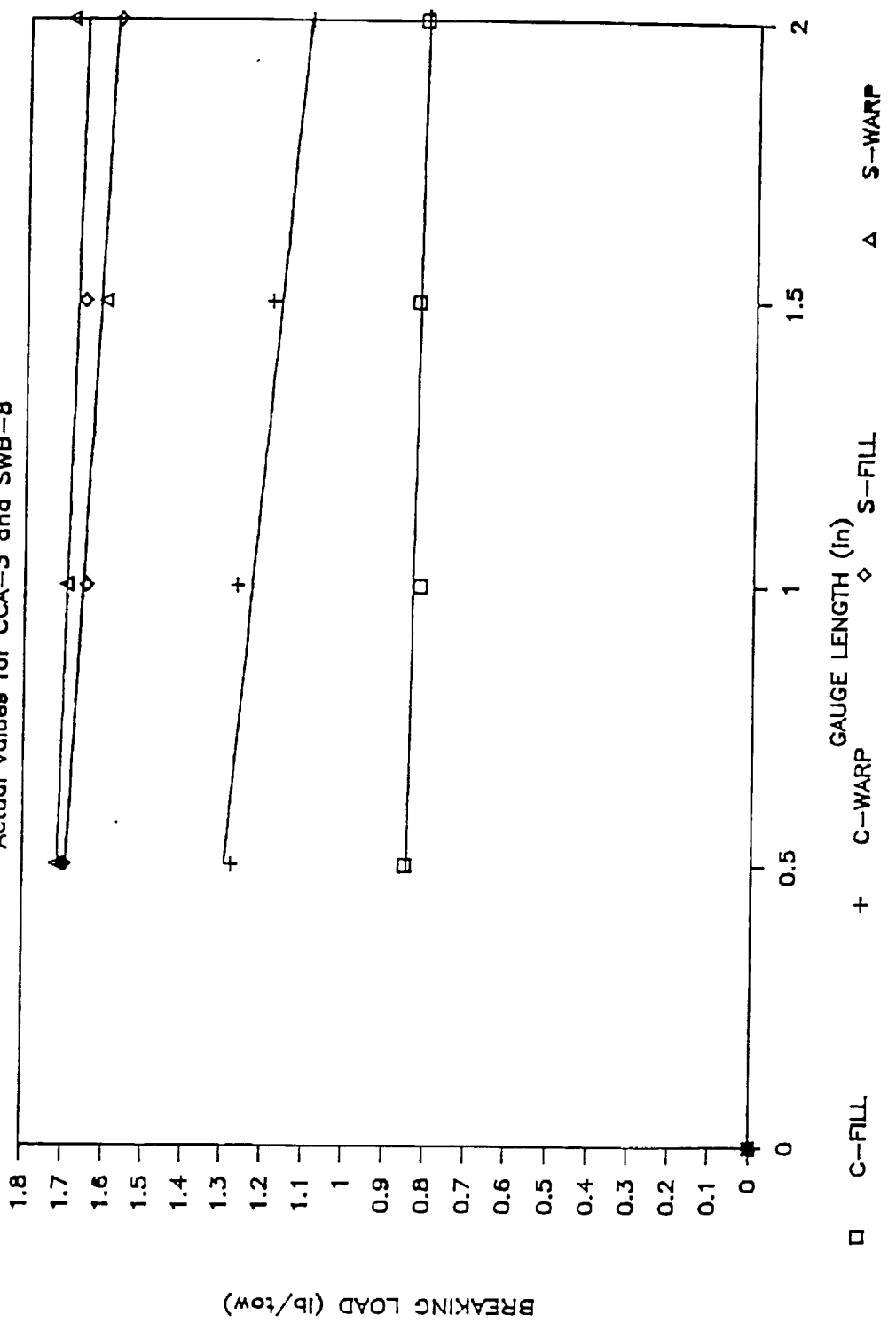


Fig. 17 -- VIII

For the SWB-8 samples, the warp values are also greater than the fill values, but the difference is not nearly as great as the difference between the warp and fill breaking loads of CCA-3. The SWB-8 fibers do not differ as much in their visual characteristics as do the CCA-3 fibers; therefore, it is not easy to distinguish between the fill and warp direction fiber bundles. At a gauge length of 0.5 inches, the warp value is 1.72 lb/tow and the fill value is 1.70 lb/tow. These values decrease to 1.70 and 1.58 lb/tow, respectively for the warp and fill directions.

The deflection vs gauge length for CCA-3 and SWB-8 in both the fill and warp directions is plotted in Figure 18. In all cases, the deflection increases as gauge increases. For the CCA-3 carbon fibers, the fill direction values are greater than the warp direction values. The values for fill increase from 0.65 in/tow at 0.5 inches to 0.79 in/tow at 2.0 inches; whereas, the warp values increase from 0.35 in/tow at 0.5 inches to 0.42 in/tow at 2.0 inches. The fill direction fibers are noticeably more crimped or wrinkled than the warp direction fibers; therefore, the fill fibers stretch more than the warp fibers before breaking. Another cause for the greater deflection in the fill fibers is that the warp fibers are stronger so they do not stretch as much as the weaker fill fibers.

The pattern for the SWB-8 fibers in the fill and warp directions is nearly identical. They both increase from 0.89 in/tow at a gauge length of 0.5 inches; however, the fill is slightly larger because it increases to 1.09 in/tow as compared to 1.08 in/tow for the warp direction at a gauge length of 2.0 inches. The fiber directions appear to be identical when looked at with the eye so one type is not more wrinkled than the other; therefore, the deflection patterns are very similar for the two directions. However, it can easily be seen from Figure 18 that the SWB-8 fibers have higher deflection values than the CCA-3 fibers, and this is because they are more crimped than the CCA-3 fibers so they stretch more at each gauge length.

DEFLECTION VS GAUGE LENGTH

Actual Values for CCA-3 and SWB-8

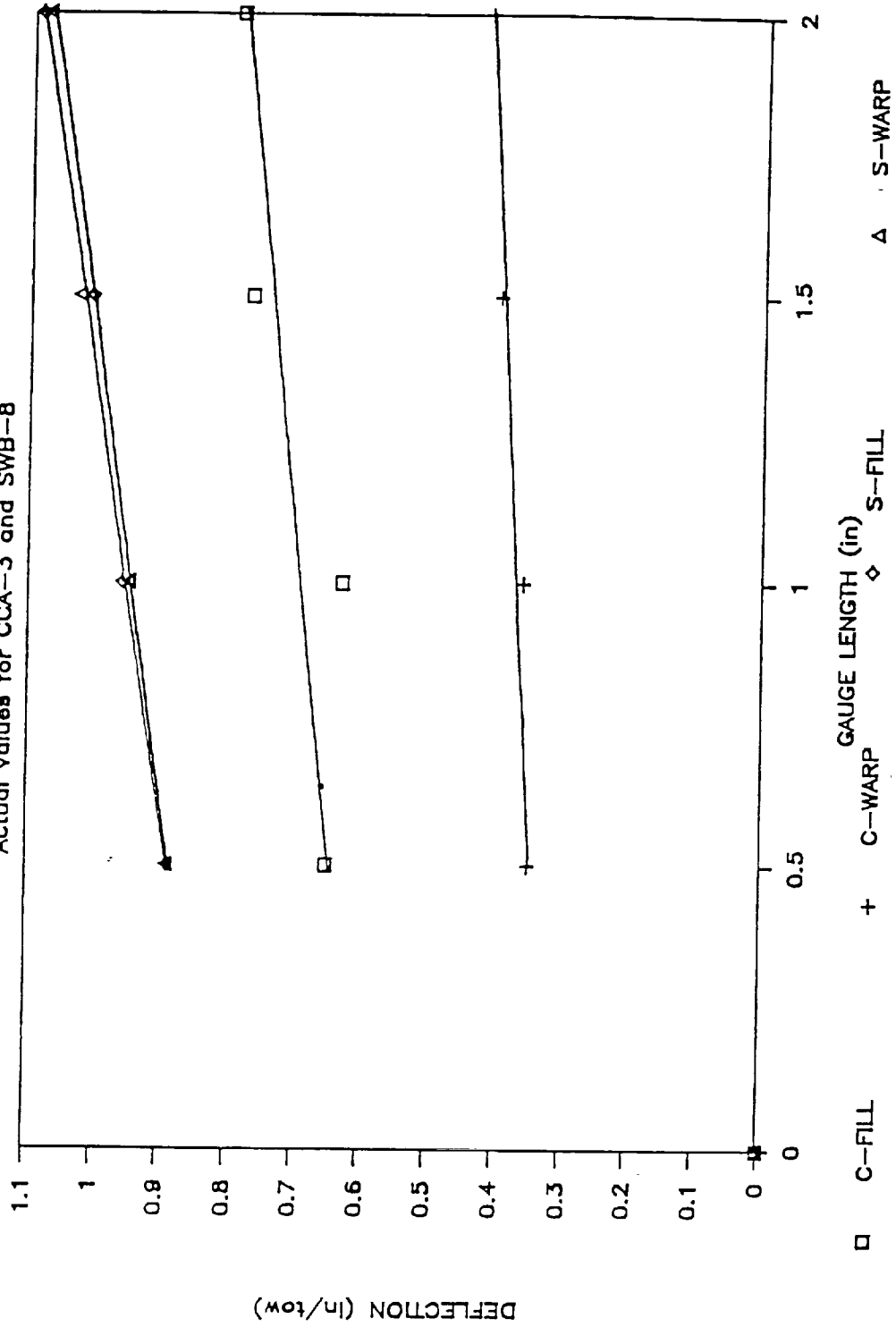


Fig. 18 - VIII

Table 17 and Figure 19 show the results for the Raveled and Cut Strip tests performed on the SWB-8 and CCA-3. For both tests and for both types of materials, nine different locations on the fabrics were tested for breaking load. The samples tested were one inch by six inch rectangles cut from the appropriate locations on the fabrics. The tests were performed at Redstone Arsenal in Huntsville, Alabama, and the procedure follows at the end of this section. For the CCA-3 carbon fiber samples in the Raveled Strip Test method, the values range from 31.0 lb/in at center right to 42.0 lb/in at bottom right with an average breaking load of 35.4 lb/in and a variance of 3.4. The values for CCA-3 in the Cut Strip Test method range from 30.0 lb/in at top right to 43.8 lb/in at top left with an average breaking load of 35.38 lb/in and a variance of 4.63. The values for SWB-8 in the Raveled Strip Test method range from 39.8 lb/in at center right to 47.4 lb/in at top right, and the values for the Cut Strip Test method range from 25.0 lb/in at center left to 45.2 lb/in at bottom right. The average breaking load values for the raveled and cut tests are 43.18 and 36.16 lb/in, respectively. The variances are 2.57 for the Raveled Strip Test method and 6.27 for the Cut Strip Test method. In both the CCA-3 and SWB-8 samples, the Raveled tests show higher breaking loads than do the Cut tests, and the SWB-8 fiber samples are stronger than the CCA-3 fiber samples.

The following conclusions are made concerning the research presented in this study.

1. The CCA-3 rayon-base carbon fibers and the SWB-8 PAN-base fibers contain surface defects which decrease the strength of the fibers. The CCA-3 fibers are non-circular in cross section; whereas, the SWB-8 fibers are circular in cross section.
2. The breaking loads of the carbon fibers from CCA-3 and SWB-8 do vary across the fabric; however, the distributions of breaking loads are fairly even in most cases.

TABLE 17
Results of Raveled and Cut Strip Test Methods for
CCA-3 and SWB-8

LOCATION	BREAKING LOAD (LB/INCH)			
	CCA-3		SWB-8	
	RAVELED	CUT	RAVELED	CUT
TOP LEFT	35.6	43.8	43.4	38.8
CENTER LEFT	35.6	32.2	44.8	25.0
BOTTOM LEFT	32.0	37.0	41.0	40.2
TOP CENTER	32.0	31.0	44.0	41.4
CENTER	36.0	31.6	40.6	36.4
BOTTOM CENTER	38.0	37.6	41.8	27.2
TOP RIGHT	36.0	30.0	47.4	33.2
CENTER RIGHT	31.0	41.6	39.8	38.2
BOTTOM RIGHT	42.0	33.6	45.0	45.2
AVERAGE	35.4	35.4	43.2	36.2
VARIANCE	(3.42)	(4.63)	(2.57)	(6.27)

BREAKING LOAD VS LOCATION

Ravel and Cut Tests for CCA-3 and SWB-8

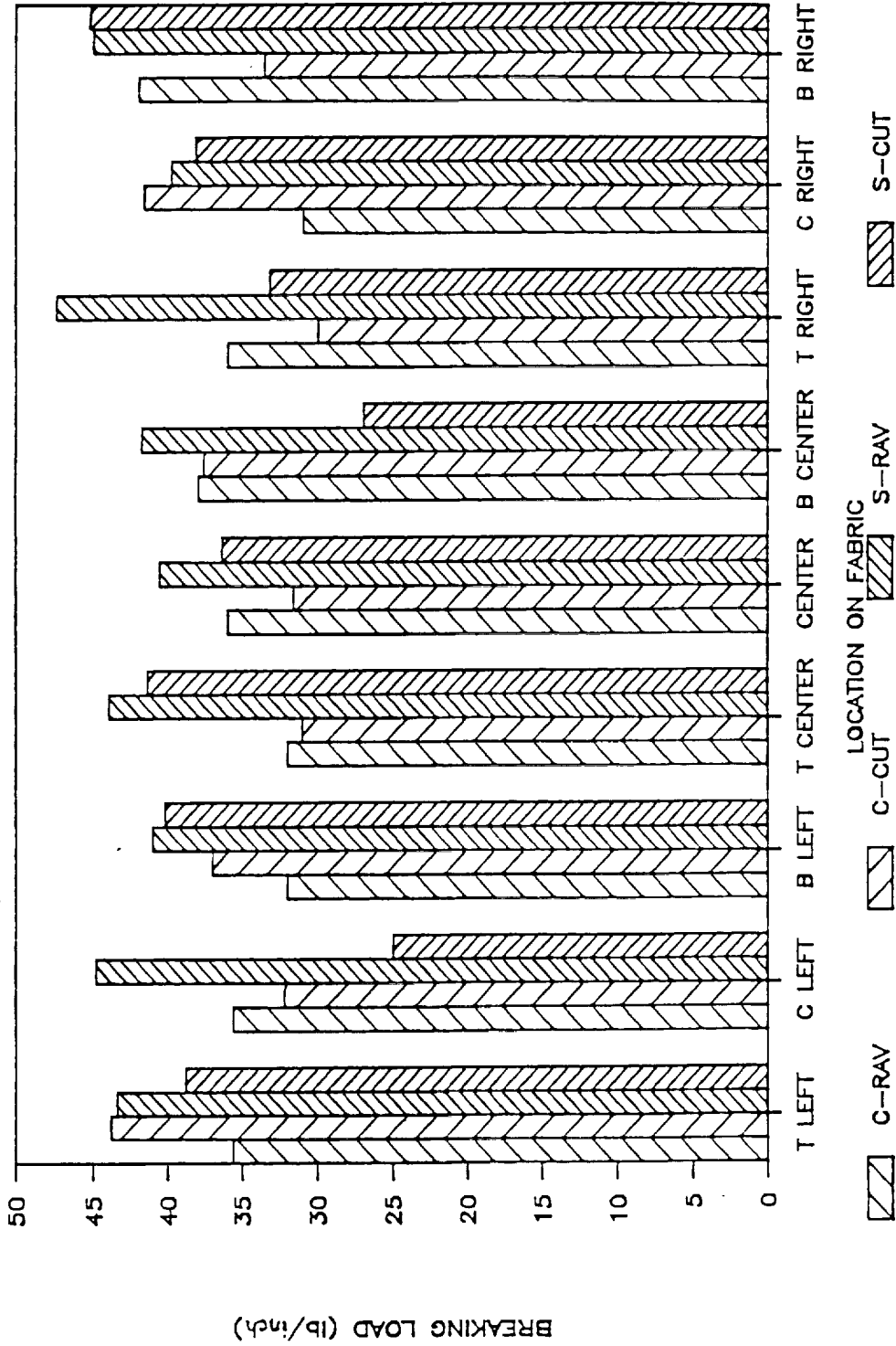


Fig. 19 - VIII

3. The SWB-8 PAN-base carbon fibers have greater breaking load variability across the fabric locations than do the CCA-3 rayon-base carbon fibers.
4. The deflections of the carbon fibers from CCA-3 and SWB-8 do vary across the fabric; however, the deflection distributions are extremely uniform with very small standard deviations.
5. The breaking loads for both the CCA-3 and SWB-8 fibers decrease as gauge length increases.
6. The deflections for both the CCA-3 and SWB-8 fibers increase as gauge length increases.
7. For both CCA-3 and SWB-8, the breaking loads of the warp direction fibers are greater than that of the fill direction fibers at the various gauge lengths.
8. The deflections of the fill direction fibers is greater than that of the warp direction fibers for both CCA-3 and SWB-8 at the various gauge lengths.
9. The SWB-8 carbon fibers have greater breaking loads and deflection values than do the CCA-3 carbon fibers at the various gauge lengths. The circular cross section of the SWB-8 fibers shown in the SEM photographs may account for the greater strength of the SWB-8 fibers as opposed to the non-circular cross section of the CCA-3 fibers.

Raw Data for Breaking Load and Deflection of CCA-3 and SWB-8 - Fill and Warp -
0.5" Gauge Length

RUN #	BREAKING LOAD (LB/TON)				DEFLECTION (IN/TON)				TOP LEFT				TOP RIGHT				BREAKING LOAD (LB/TON)				DEFLECTION (IN/TON)												
	CCA-3	FILL	WARF	SWB-8	CCA-3	FILL	WARF	SWB-8	CCA-3	FILL	WARF	SWB-8	CCA-3	FILL	WARF	SWB-8	CCA-3	FILL	WARF	SWB-8	CCA-3	FILL	WARF	SWB-8	CCA-3	FILL	WARF	SWB-8					
1	0.85	1.10	1.20	1.75	0.66	0.29	0.90	0.96	0.35	1.00	1.70	1.30	0.24	0.26	0.70	0.71	0.85	1.10	1.20	1.75	0.66	0.29	0.90	0.96	0.35	1.00	1.70	1.30	0.24	0.26	0.70	0.71	
2	0.80	1.00	1.20	1.75	0.47	0.29	1.44	1.05	0.30	1.25	1.40	1.60	0.62	0.20	0.65	1.21	0.80	1.00	1.20	1.75	0.47	0.29	1.44	1.05	0.30	1.25	1.40	1.60	0.62	0.20	0.65	1.21	
3	0.95	1.25	1.50	1.75	0.56	0.47	0.77	0.92	0.60	1.00	1.50	1.40	0.94	0.22	0.64	0.24	0.95	1.25	1.50	1.75	0.56	0.47	0.77	0.92	0.60	1.00	1.50	1.40	0.94	0.22	0.64	0.24	
4	0.70	0.75	1.00	2.05	0.34	0.44	0.93	0.98	0.55	1.40	2.00	1.40	1.05	0.17	0.70	0.85	0.70	0.75	1.00	2.05	0.34	0.44	0.93	0.98	0.55	1.40	2.00	1.40	1.05	0.17	0.70	0.85	
5	0.95	1.15	1.25	1.86	0.61	0.30	0.97	0.92	0.70	1.20	1.80	1.40	0.74	0.24	0.62	0.83	0.95	1.15	1.25	1.86	0.61	0.30	0.97	0.92	0.70	1.20	1.80	1.40	0.74	0.24	0.62	0.83	
6	0.70	1.15	1.25	1.86	0.49	0.43	0.83	1.03	0.55	1.60	1.65	1.70	0.93	0.22	1.04	1.09	0.70	1.15	1.25	1.86	0.49	0.43	0.83	1.03	0.55	1.60	1.65	1.70	0.93	0.22	1.04	1.09	
7	1.00	1.75	1.90	1.90	0.59	0.43	0.93	0.89	0.30	1.40	2.20	0.80	0.55	0.22	1.04	1.09	1.00	1.75	1.90	1.90	0.59	0.43	0.93	0.89	0.30	1.40	2.20	0.80	0.55	0.22	1.04	1.09	
8	1.00	1.75	1.90	1.90	0.66	0.29	0.89	1.01	0.35	1.40	2.35	1.40	0.48	0.22	1.18	0.69	1.00	1.75	1.90	1.90	0.66	0.29	0.89	1.01	0.35	1.40	2.35	1.40	0.48	0.22	1.18	0.69	
9	1.00	2.05	1.45	2.00	0.45	0.18	0.81	0.90	0.65	1.20	1.55	1.55	0.59	0.22	0.39	1.03	1.00	2.05	1.45	2.00	0.45	0.18	0.81	0.90	0.65	1.20	1.55	1.55	0.59	0.22	0.39	1.03	
10	0.35	1.10	1.70	2.50	0.39	0.30	1.10	0.92	0.80	1.45	2.35	2.35	0.92	0.21	0.87	1.13	0.35	1.10	1.70	2.50	0.39	0.30	1.10	0.92	0.80	1.45	2.35	2.35	0.92	0.21	0.87	1.13	
1	0.55	1.70	1.60	1.45	0.85	0.20	0.74	0.51	0.95	0.85	1.70	1.40	0.64	0.21	1.19	1.15	0.55	1.70	1.60	1.45	0.85	0.20	0.74	0.51	0.95	0.85	1.70	1.40	1.40	0.64	0.21	1.19	1.15
2	0.70	1.70	1.60	1.45	0.85	0.20	0.74	0.51	0.95	0.85	1.70	1.40	0.64	0.21	1.19	1.15	0.70	1.70	1.60	1.45	0.85	0.20	0.74	0.51	0.95	0.85	1.70	1.40	1.40	0.64	0.21	1.19	1.15
3	0.80	2.05	1.65	1.85	0.74	0.49	1.07	0.79	0.90	1.10	2.35	1.45	0.58	0.24	0.89	0.62	0.80	2.05	1.65	1.85	0.74	0.49	1.07	0.79	0.90	1.10	2.35	1.45	0.58	0.24	0.89	0.62	
4	0.90	1.95	1.30	2.40	0.75	0.55	1.07	0.79	0.90	1.10	2.35	1.45	0.58	0.24	0.89	0.62	0.90	1.95	1.30	2.40	0.75	0.55	1.07	0.79	0.90	1.10	2.35	1.45	0.58	0.24	0.89	0.62	
5	0.90	1.95	1.30	2.40	0.81	0.47	0.63	0.85	0.75	0.95	2.35	1.40	0.85	0.24	0.89	0.62	0.90	1.95	1.30	2.40	0.81	0.47	0.63	0.85	0.75	0.95	2.35	1.40	1.40	0.85	0.24	0.89	0.62
6	0.90	1.95	1.30	2.40	0.95	0.41	0.65	0.78	0.80	1.20	2.35	1.40	0.85	0.24	0.89	0.62	0.90	1.95	1.30	2.40	0.95	0.41	0.65	0.78	0.80	1.20	2.35	1.40	1.40	0.85	0.24	0.89	0.62
7	0.95	1.10	1.70	1.60	0.75	0.28	0.98	0.78	0.80	1.20	1.85	1.70	0.75	0.24	0.89	0.62	0.95	1.10	1.70	1.60	0.75	0.28	0.98	0.78	0.80	1.20	1.85	1.70	1.70	0.75	0.24	0.89	0.62
8	0.95	1.10	1.70	1.60	0.60	0.28	1.11	0.86	0.80	1.10	1.85	1.70	0.75	0.24	0.89	0.62	0.95	1.10	1.70	1.60	0.60	0.28	1.11	0.86	0.80	1.10	1.85	1.70	1.70	0.75	0.24	0.89	0.62
9	0.95	1.10	1.70	1.60	0.64	0.24	0.70	0.80	1.00	1.15	2.50	1.90	0.57	0.22	1.01	0.66	0.95	1.10	1.70	1.60	0.64	0.24	0.70	0.80	1.00	1.15	2.50	1.90	1.90	0.57	0.22	1.01	0.66
10	0.35	1.10	1.70	2.50	0.39	0.30	1.10	0.92	0.80	1.45	2.35	2.35	0.92	0.21	0.87	1.13	0.35	1.10	1.70	2.50	0.39	0.30	1.10	0.92	0.80	1.45	2.35	2.35	0.92	0.21	0.87	1.13	
1	0.95	1.25	1.90	2.20	0.36	0.40	0.78	0.89	0.89	0.40	2.20	2.20	0.89	0.40	0.78	0.89	0.95	1.25	1.90	2.20	0.36	0.40	0.78	0.89	0.89	0.40	2.20	2.20	0.89	0.40	0.78	0.89	
2	0.95	1.25	1.90	2.20	0.39	0.42	0.77	0.96	0.89	0.37	2.15	2.15	0.96	0.37	0.77	0.96	0.95	1.25	1.90	2.20	0.39	0.42	0.77	0.96	0.89	0.37	2.15	2.15	0.96	0.37	0.77	0.96	
3	0.90	1.45	1.25	2.00	0.49	0.33	0.63	0.81	0.89	0.41	1.90	1.90	0.81	0.41	0.63	0.81	0.90	1.45	1.25	2.00	0.49	0.33	0.63	0.81	0.89	0.41	1.90	1.90	0.81	0.41	0.63	0.81	
4	0.95	1.10	1.25	1.45	0.48	0.52	0.63	0.77	0.89	0.47	1.70	1.70	0.77	0.47	0.63	0.77	0.95	1.10	1.25	1.45	0.48	0.52	0.63	0.77	0.89	0.47	1.70	1.70	0.77	0.47	0.63	0.77	
5	0.90	1.60	1.85	1.65	0.78	0.47	0.85	0.91	0.89	0.47	1.65	1.65	0.91	0.47	0.85	0.91	0.90	1.60	1.85	1.65	0.78	0.47	0.85	0.91	0.89	0.47	1.65	1.65	0.91	0.47	0.85	0.91	
6	0.90	1.25	1.90	1.65	0.32	0.41	0.85	0.86	0.89	0.32	1.65	1.65	0.86	0.32	0.85	0.86	0.95	1.25	1.90	1.65	0.32	0.41	0.85	0.86	0.89	0.32	1.65	1.65	0.86	0.32	0.85	0.86	
7	0.90	1.25	1.90	1.65	0.54	0.31	0.76	0.92	0.89	0.31	1.60	1.60	0.92	0.31	0.76	0.92	0.95	1.25	1.90	1.65	0.54	0.31	0.76	0.92	0.89	0.31	1.60	1.60	0.92	0.31	0.76	0.92	
8	0.90	1.25	1.90	1.65	0.54	0.31	0.76	0.92	0.89	0.31	1.60	1.60	0.92	0.31	0.76	0.92	0.95	1.25	1.90	1.65	0.54	0.31	0.76	0.92	0.89	0.31	1.60	1.60	0.92	0.31	0.76	0.92	
9	0.90	1.25	1.90	1.65	0.54	0.31	0.76	0.92	0.89	0.31	1.60	1.60	0.92	0.31	0.76	0.92	0.95	1.25	1.90	1.65	0.54	0.31	0.76	0.92	0.89	0.31	1.60	1.60	0.92	0.31	0.76	0.92	
10	0.95	1.25	1.90	1.65	0.54	0.31	0.76	0.92	0.89	0.31	1.60	1.60	0.92	0.31	0.76	0.92	0.95	1.25	1.90	1.65	0.54	0.31	0.76	0.92	0.89	0.31	1.60	1.60	0.92	0.31	0.76	0.92	

Table 18

ORIGINAL PAGE IS
OF POOR QUALITY

Raw Data for Breaking Load and Deflection of CCA-3 and SWB-8 - Fill and Warp -
1.0" Gauge Length

RUN	BREAKING LOAD (LB/TON)			DEFLECTION (IN/TON)			TOP LEFT			TOP RIGHT			DEFLECTION (IN/TON)			
	CCA-3	FILL	WARP	CCA-3	FILL	WARP	CCA-3	FILL	WARP	CCA-3	FILL	WARP	CCA-3	FILL	WARP	
1	0.90	1.20	1.85	0.74	0.48	0.75	0.85	1.01	1.65	0.85	1.85	0.64	0.45	0.57	0.99	
2	0.95	1.50	1.85	0.74	0.48	1.14	0.65	1.02	1.25	0.65	1.40	0.64	0.25	0.94	1.19	
3	0.95	1.75	1.95	0.64	0.24	1.05	0.60	1.17	1.55	0.60	1.70	0.64	0.25	0.90	0.65	
4	0.95	1.25	1.95	0.75	0.24	1.29	0.70	0.98	1.60	0.70	1.60	0.91	0.25	1.11	0.65	
5	0.70	1.00	1.50	0.75	0.24	0.87	0.85	1.12	1.60	0.85	1.40	0.91	0.25	1.08	1.19	
6	0.95	1.00	1.85	0.62	0.22	0.82	0.90	1.12	1.25	0.90	1.50	0.55	0.25	1.01	1.19	
7	1.00	1.00	1.70	0.60	0.22	1.12	0.85	1.12	1.50	0.85	1.45	0.55	0.25	0.99	0.94	
8	0.90	1.05	1.75	0.43	0.40	1.03	1.00	1.24	2.25	1.00	0.85	0.45	0.44	0.97	1.05	
9	0.90	1.55	1.40	0.43	0.40	0.91	0.85	1.24	1.25	1.00	0.85	0.45	0.44	0.97	1.05	
10	0.90	1.05	1.60	0.46	0.42	1.15	0.70	0.98	1.66	0.70	1.45	0.72	0.41	0.95	1.30	
				CENTER												
1	0.90	1.00	0.85	0.60	0.26	0.82	0.95	0.70	1.25	0.95	1.75	0.53	0.43	1.18	1.25	
2	0.95	1.15	1.75	0.65	0.23	0.77	0.85	0.93	0.75	0.80	2.40	0.64	0.43	1.02	0.61	
3	0.95	1.25	2.00	0.79	0.34	0.94	0.70	0.94	1.50	0.70	2.25	0.56	0.22	0.83	0.65	
4	0.90	1.50	1.10	0.79	0.34	1.11	0.90	0.95	1.50	0.90	1.85	0.56	0.44	1.13	0.61	
5	0.95	1.55	2.05	0.61	0.31	0.89	0.90	0.80	0.85	0.90	1.55	0.56	0.51	0.53	0.82	
6	0.95	1.20	2.25	0.63	0.41	1.09	0.70	0.80	1.00	0.70	2.40	0.45	0.21	1.02	0.90	
7	1.05	1.25	2.25	0.53	0.26	0.91	0.65	0.80	1.00	0.65	1.95	0.51	0.21	1.02	0.91	
8	0.90	0.75	1.60	0.72	0.20	1.25	0.85	1.01	1.30	0.85	1.95	0.51	0.21	1.02	0.91	
9	0.90	0.75	2.25	0.62	0.45	0.92	0.80	0.88	1.15	0.80	2.40	0.51	0.21	1.02	0.91	
10	0.90	0.75	1.55	0.60	0.40	1.15	0.80	0.88	1.15	0.80	2.40	0.51	0.21	1.02	0.91	
				BOTTOM RIGHT												
1	0.90	1.15	2.05	0.65	0.24	0.98	0.95	0.98	1.25	0.95	1.75	0.87	0.23	1.05	1.00	
2	0.90	1.15	2.10	0.75	0.12	0.98	0.85	0.98	0.75	0.80	2.40	0.87	0.23	1.05	1.00	
3	0.95	1.60	1.95	0.55	0.23	0.92	0.75	0.92	1.50	0.75	2.25	0.87	0.23	1.05	1.00	
4	0.95	1.10	2.35	0.51	0.25	1.00	0.95	1.13	1.00	0.95	1.85	0.87	0.23	1.05	1.00	
5	0.75	1.10	1.95	0.60	0.25	1.02	0.95	0.95	1.00	0.95	1.85	0.87	0.23	1.05	1.00	
6	0.95	1.10	2.20	0.48	0.29	0.99	0.95	0.97	1.45	0.95	1.95	0.87	0.23	1.05	1.00	
7	0.95	1.15	1.80	0.67	0.29	0.99	0.95	0.97	1.75	0.95	1.95	0.87	0.23	1.05	1.00	
8	0.90	1.20	1.75	0.57	0.47	0.93	0.89	0.87	1.40	0.89	1.85	0.87	0.23	1.05	1.00	
9	0.90	1.15	1.90	0.70	0.39	0.93	0.89	0.87	1.40	0.89	1.85	0.87	0.23	1.05	1.00	
10	0.95	1.40	1.85	0.55	0.18	0.97	0.91	0.91	1.40	0.91	1.85	0.87	0.23	1.05	1.00	

Table 19

Raw Data for Breaking Load and Deflection of CCA-3 and SWB-8 - Fill and Warp -
1.5" Gauge Length

RUN	BREAKING LOAD (LB/TON)				DEFLECTION (IN/TON)				BREAKING LOAD (LB/TON)				DEFLECTION (IN/TON)			
	CCA-3	FILL	WARP	SWB-8	CCA-3	FILL	WARP	SWB-8	CCA-3	FILL	WARP	SWB-8	CCA-3	FILL	WARP	SWB-8
1	0.80	1.65	1.15	0.90	0.71	0.39	0.60	0.31	0.85	1.25	0.90	1.00	0.70	0.81	0.33	0.55
2	0.90	1.50	1.70	0.95	0.62	0.40	0.74	0.40	0.75	1.10	0.80	1.20	0.65	0.65	0.42	0.70
3	0.90	1.05	0.95	0.80	0.77	0.42	0.77	0.62	0.90	0.70	0.85	0.65	0.66	0.42	0.41	0.50
4	0.75	1.10	1.55	0.85	0.71	0.48	0.82	0.45	0.90	0.70	0.80	1.10	0.79	0.41	0.51	0.61
5	0.75	0.95	1.20	0.75	0.94	0.52	0.89	0.46	0.70	1.50	1.00	1.50	0.65	0.75	0.55	0.74
6	0.80	0.85	1.20	0.65	1.07	0.55	0.62	0.25	0.80	1.45	0.90	0.35	0.67	0.79	0.44	0.41
7	1.00	1.50	0.85	0.80	0.76	0.46	0.73	0.37	0.75	1.25	1.10	1.30	0.76	0.79	0.45	0.51
8	0.75	0.90	0.75	0.70	0.89	0.42	0.70	0.27	0.85	1.25	0.80	0.30	0.42	0.90	0.49	0.51
9	0.90	1.35	0.80	0.80	0.50	0.36	0.76	0.40	0.65	1.20	0.70	1.25	0.71	0.72	0.49	0.60
10	0.90	1.30	1.15	0.85	0.66	0.50	0.70	0.40	0.65	1.20	0.70	1.25	0.71	0.72	0.49	0.60
					CENTER								BOTTOM LEFT			
1	1.05	1.30	1.25	0.90	0.86	0.50	0.58	0.61	0.80	0.95	0.75	0.80	0.84	0.62	0.35	0.25
2	1.05	0.95	1.15	0.85	0.99	0.35	0.85	0.46	0.95	1.00	0.80	0.95	0.75	0.91	0.37	0.71
3	0.95	1.05	1.15	0.85	1.08	0.43	0.87	0.53	0.90	0.85	0.80	0.95	0.85	0.44	0.44	0.52
4	0.85	1.20	0.70	0.80	1.09	0.43	0.73	0.44	0.95	0.85	0.75	1.00	0.73	0.45	0.39	0.59
5	0.90	0.70	1.05	0.85	0.86	0.42	0.87	0.51	0.60	1.15	0.80	1.25	0.63	0.45	0.43	0.43
6	0.75	1.10	0.90	0.70	0.74	0.33	0.86	0.37	0.70	0.80	0.80	1.40	0.67	0.45	0.38	0.38
7	0.85	1.30	0.75	0.80	0.86	0.38	0.86	0.48	0.90	1.30	0.80	1.40	0.96	0.34	0.34	0.35
8	0.90	0.95	1.05	0.95	0.71	0.45	0.69	0.56	0.75	1.65	0.80	0.35	0.36	0.39	0.39	0.34
9	1.00	1.10	1.05	0.85	0.69	0.53	0.70	0.37	0.90	1.25	0.80	1.20	0.35	0.39	0.39	0.34
10	1.00	1.10	1.05	0.85	0.69	0.53	0.70	0.37	0.90	1.20	0.70	1.15	0.35	0.45	0.45	0.34
					BOTTOM RIGHT								BOTTOM LEFT			
1	0.80	1.70	1.10	0.85	0.86	0.38	0.80	0.44	0.80	0.95	0.70	0.80	0.78	0.80	0.47	0.64
2	0.85	1.35	1.15	0.70	0.68	0.40	0.77	0.27	0.80	1.00	0.80	0.95	0.78	0.80	0.47	0.64
3	0.90	1.00	0.80	0.75	0.66	0.33	0.83	0.41	0.80	0.85	0.70	0.95	0.78	0.80	0.47	0.64
4	0.85	1.35	1.15	0.75	0.77	0.23	0.72	0.25	0.80	0.85	0.70	0.95	0.78	0.80	0.47	0.64
5	0.95	1.60	1.25	0.75	0.70	0.44	0.72	0.21	0.80	0.85	0.70	0.95	0.78	0.80	0.47	0.64
6	0.90	1.50	1.05	0.75	0.73	0.54	0.69	0.11	0.80	0.85	0.70	0.95	0.78	0.80	0.47	0.64
7	0.85	1.20	1.00	0.90	0.86	0.45	0.75	0.29	0.80	0.85	0.70	0.95	0.78	0.80	0.47	0.64
8	0.75	1.15	0.95	0.75	0.68	0.45	0.75	0.21	0.80	0.85	0.70	0.95	0.78	0.80	0.47	0.64
9	0.80	1.35	1.10	0.70	0.62	0.15	0.77	0.23	0.80	0.85	0.70	0.95	0.78	0.80	0.47	0.64
10	0.80	1.35	1.10	0.70	0.62	0.15	0.77	0.23	0.80	0.85	0.70	0.95	0.78	0.80	0.47	0.64

Fig. 20 - VIII

IX. CARBON BLACK REINFORCING FILLER

Introduction

Carbon black is widely used as a filler agent in several resin formulations in prepreg materials. The term filler is misleading in that for this particular application, the filler is more than just an inert material which is added to the mixture to extend the resin and reduce costs. In this case, as with many carbon black applications, the filler has a great deal of surface activity which, when finely dispersed throughout the resin matrix, allows the carbon black to enhance certain physical properties of the matrix. Thus, carbon black filler is added to resin mixtures for its favorable contribution to the suitability and serviceability of the overall product.

The exact type of carbon black to perform a desired task can only be made through judicious selection and testing procedures. This section is not intended to serve as a guide to that selection procedure, but rather to present a condensed overview of theory relative to carbon black applications and carbon black nomenclature.

Background

Carbon black has been used ever since the early cave dwellers discovered that they could draw figures on their cave wall using recovered soot or charcoal. Ever since then, scientists and engineers have been making efforts to change the manufacturing and use of carbon black from a pure art form to a profession with a scientific basis (Gould, 1976). These efforts have been in part successful, however, there still remain many unknowns relative to carbon black applications.

The use of carbon black that the cave dwellers discovered was that of pigmentation. Indeed, we still use this discovery today in the form of pigmentation in inks, paints, and even in black colored mortar mixes. Inspection of a paint container may reveal that even brightly colored paints contain some amounts of carbon black which are used to adjust hue and tone of the color. Carbon black has become a major industrial chemical with many uses extending well beyond pigmentation applications (Gould, 1976). On a volume

basis, some of the largest uses include the use of carbon black as a filler to enhance the properties of rubber products or other resin based products. About 95% of the carbon black made is used in tire manufacture (Stokes, 1976).

Manufacture and Classification

To utilize carbon black in a product, we no longer have to scrape soot from a wall above an oil lamp, but rather, the carbon black is purchased from a vendor who specializes in the manufacture of carbon black. After a brief review of the vendor's literature, one may wonder if it would not be easier to go back to the cave. Modern technology has developed a myriad of hundreds of different types of carbon blacks. Each type of carbon black has advantages for a specific application.

Carbon blacks are classified into grades according to the particular method used for their manufacture and their specific physical properties. Almost all of today's commercial grades of carbon black are 99% pure carbon. The classifications by manufacturing methods are as follows (Mantell, 1976):

Type	Process Features	Raw Material Used
Channel	Impingement of flame on cool surfaces	Natural gas Hydrocarbons
Furnace	Controlled combustion inside a specially designed furnace	Natural gas Hydrocarbons
Thermal	Regenerative cracking at +1100°C in refractory brick work with no oxygen present	Natural gas
Lampblack	Confined partial combustion	Hydrocarbon liquids
Acetylene	Confined exothermic cracking with no oxygen present	Acetylene

Within each method of manufacture, the exact conditions of temperature, oxygen feed rate, combustor residence time, and combustor turbulence all have a direct effect on the

final physical properties of the carbon black. Even the amount of aromatic compounds in the feedstock for some of the processes can have a dramatic effect on the final product which means that the source of hydrocarbon feedstock is important in carbon black manufacture. Hence, a plant making channel black in the far west could produce a different grade channel black than a plant in the southeast if they were using feedstocks from different crude oil fields even though both plants were using identical equipment. The west coast U.S. feedstock may contain considerable aromatic chemicals, while southeast U.S. feedstocks are more likely to be mostly paraffinic.

The classical classification system for identifying carbon blacks is a system which alludes to the characteristics which they impart to a final product in which they are incorporated as a filler. The industrial area of greatest interest has historically been the rubber industry, hence, the classical emphasis has been on properties relating to tire wear, skid resistance, and effects of the filler on cure (rubber vulcanization) rates. Some of these classifications are as follows:

Classification by Abrasion resistance

HAF high abrasion furnace
ISAF intermediate super abrasion furnace
SAF super abrasion furnace

Classification by Level of reinforcement

SRF simireinforcing furnace

Classification by Vulcanization property

HMF high modulus furnace

Classification by rubber processing property

FEF fast extruding furnace

Classification by utility

APF all purpose furnace
GPF general purpose furnace

Classification by particle size

FF fine furnace
LPF large particle furnace
FT fine furnace
MT medium furnace

Or any group could also have subgroups

HAF-HS high aggregate subgrade
HAF-LS low aggregate subgrade

Even though this method of classification can quickly get out of hand for the hundreds of different carbon blacks, many vendors and users alike still use this classical system to some extent even today. To make some order out of chaos, the ASTM has developed a classification system (ASTM D1765). The first character of the classification relates to the effect the carbon black has on rubber cure rate

N normal cure rate
Furnace blacks which have had no special modifications will fall in this category
S slow cure rate
Channel blacks which have had no special modifications will fall in this category

The next character relates to the group number relating to the carbon black individual particle size. The groups are as follows:

Group No.	Typical average Particle Size, nm
0	1 to 10
1	11 to 19
2	20 to 25
3	26 to 30
4	31 to 39
5	40 to 48
6	49 to 60
7	61 to 100
8	101 to 200
9	201 to 500

The third and fourth digits are arbitrarily assigned digits.

By this method, thermal blacks have the designation (xxxx):

N880 Fine thermal
N990 Medium thermal
N907 Medium thermal nonstaining (MT-NS)

In addition to these classifications, one may often see a carbon black designated with an IRB number. IRB numbered carbon blacks are International Reference Blacks which are used to designate standard carbon blacks that are used in the laboratory for research or product development work. This classification is not used for general industry application.

After the carbon black has been produced, there is a certain amount of post production processing which is carried on. The carbon black is usually cooled with a water spray from its manufacturing temperatures to reasonable handling temperatures. After cooling, the carbon black, which at this point is a very fluffy powder, must be pelletized to some degree to increase its bulk density and to facilitate ease of handling. The two pelletizing processes used are the dry process and the wet process.

The dry process pelletizer agglomerates the carbon black particles without the addition of water whereas the wet process uses a small amount of water to assist the fine particles to stick together in a small clump. The dry process is used only in a few applications while the wet process is by far the most common form of pelletizing.

Application of Carbon Black as a Filler

The end user of the carbon black will select the particular grade dependent on the results of tests made to determine the enhancement (or degradation) of the physical properties. Thus, the purpose for the carbon black in a formulation is more than just being used as a filler. It will have an effect on the shear strength, tensile strength, flexural strength, and modulus of the finished product. In addition, the type of carbon black can have a dramatic effect on the viscosity and processibility of the resin mixture in which it is added, as well as the cure rate of the resin system.

To illustrate this point, a series of tests were done by Fiberite Incorporated to identify a replacement carbon black in MX-4926 prepreg. The carbon black that had been used was a carbon black designated as P-33 and the proposed replacement carbon black was F-1069. Both of these carbon blacks are thermal blacks and the numbers used are

designations assigned by the carbon black supplier. Table 1 shows the P-33 compared to the replacement carbon black F-1069.

Table 1
Carbon Black Properties

	P-33	F-1069
Feed Stock	Natural Gas	Natural Gas
Surface area, M ² /g	13	10
Particle size, nm	180	399
Oil Absorption, cc/gm	0.4	0.5
pH	9.0	9.0
Carbon Content, %	99.5	99.3
Volatile Content, %	0.5	0.7

Represented here are the most important physical properties of any carbon black. Beside feed stock source and particle size, a measurement of surface area, oil absorption, pH, carbon content, and volatile content are given in order that a comparison of the two carbon blacks can be made. Other possible characteristics can be mineral analysis for the elements sodium, potassium, or iron. These minerals can be introduced into the carbon black from the water that is used for cooling and pelletization during the manufacturing step, as well as from the raw material. For additional possible comparison, see details in ASTM D1765.

The two carbon black samples seem to be close in all physical properties except particle size. The P-33 might be classified as a FT whereas the F-1069 may be a MT.

Subsequent applications testing proved that the F-1069 carbon black was unsuitable as a replacement black in SRM nozzle filler service. Some of the investigative work which detailed reasons for the failure is as follows.

Table 2 shows the results of a series of tests made with the MX-4926 prepreg formulation by Fiberite. In this case, each of the important parameters were tested so

that a comparison could be made between the carbon black grades. The grades tested were the P-33, F-1069, two grades of SRF, and two additional MT grades. The results of Table 2 show variations of the effects of carbon black grade with the advantage going to the F-1069 replacement.

An additional consideration to be given for any resin formulation is the ease of handling or processibility of the resin as it is applied to the carbon cloth. No matter how good the physical properties, the resin will be of no value unless it can be applied to the cloth in such a way that it flows evenly into the pores of the fiber. Thus, viscosity and consistency become important. In the case of the Fiberite tests, the SRF black created resin mixtures which were too viscous to treat the fabric, whereas the F-1069 had a viscosity and consistency which allowed for good treatment of the carbon fiber cloth.

Even with the advantage in some physical properties and processing ease, the F-1069 failed when the cured matrix was tested in service conditions. A contributing cause may be seen when electron photo micrographs of the F-1069 carbon black and two other carbon blacks which became eventually successful replacements were studied. Figure 1 is the F-1069 carbon black and Figures 2 and 3 are the successful replacements. A comparison can be made in the photographs to determine similarities or differences between the unsuccessful F-1069 and the two replacements that did successfully replace P-33.

The two replacements shown in Fig. 2 and 3 are very similar and both materials have a very uniform texture. By comparison, the F-1069 carbon black of Figure 1 has an appearance that is much different. It seems to be agglomerated in lumps and have uneven particle size distribution.

In order to try to further quantify differences in the performance of a successful carbon black, an additional analysis was made of the F-1069 and a successful replacement. The results are shown in Table 3.

TABLE 2
MX-4926 PROPERTIES

Lot. No.	2488	2489	2501	2502	2500	2566
Fabric	CSA	CSA	CSA	CSA	CSA	CSA
Filler	P-33	SRF-1	SRF-2	MT-1	MT-2	F-1069
Resin Solids, %	35.5	34.4	34.2	35.5	34.6	35.4
Volatile, %	5.3	4.8	5.0	5.5	4.7	4.8
Flow, %@150 psi	20.5	4.5	15.7	19.0	17.4	15.9
Filler Con- tent, %	10.5	12.1	7.5	11.3	10.7	10.9
Sp. Gravity	1.46	1.46	1.45	1.46	1.46	1.43
Cured Ply, in.	0.0134	0.0149	0.0140	0.0133	0.0141	0.0134
Barcol	66	71	71	74	69	74
Residual Vol, %	1.58	1.49	1.47	1.52	1.55	1.64
Shear, psi	4,690	4,430	3,690	3,150	2,640	3,803
Tensile, psi	24,740	23,120	24,200	24,330	23,430	24,300
Ten. Mod, 10^6 psi	3.18	2.76	2.78	2.95	2.51	2.77
Ten. Elong, %	1.24	1.39	1.45	1.35	1.39	1.42
Flexural, psi	36,140	36,110	39,740	39,900	36,360	40,330
Flex. Mod. 10^6 psi	2.43	2.08	2.67	2.14	2.55	2.54
Compression, psi	35,640	48,530	43,580	41,620	43,280	41,520
Thermal Con- ductivity, BTV/hr-°F.	0.67	---	---	---	---	0.69
Thermal Exp. $\times 10^6$ in/in Parallel	3.82	---	---	---	---	3.85

ORIGINAL PAGE IS
OF POOR QUALITY

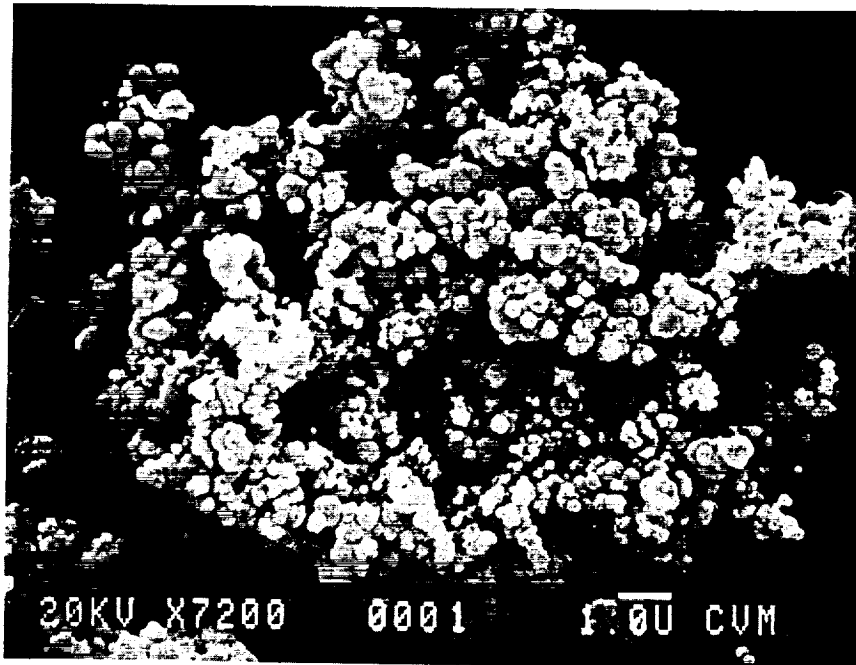


Fig. 1 - IX - Past Filler, Vendor B

ORIGINAL PAGE IS
OF POOR QUALITY

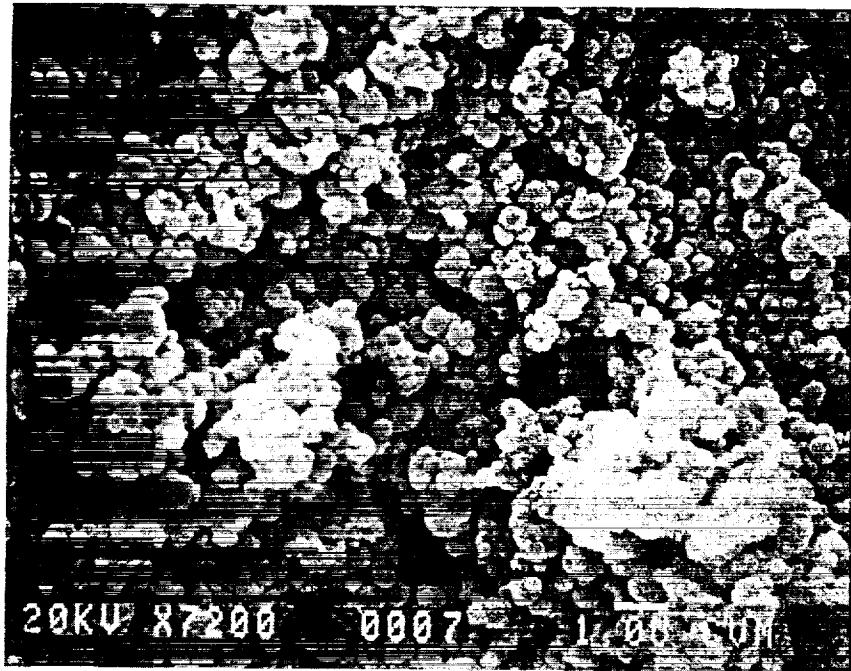


Fig. 2 - IX - Present Filler, Vendor A

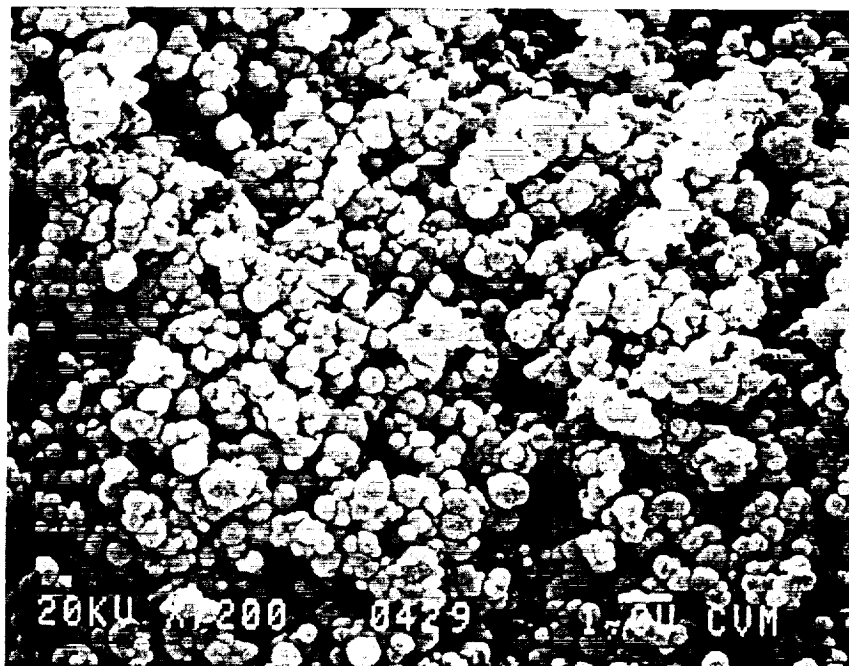


Fig. 3 - IX - Present Filler, Vendor B

TABLE 3

Analytical Analysis of Carbon Blacks F-1069 Compared to Successful Replacement

	C wt%	S wt%	pH	Moisture ppm	Na ppm	K ppm	Ash wt%
F-1069	98.81	0.258	8.2	757	498	27	0.17
Alternate	99.43	0.170	5.6	158	12	2	.005

Unlike the comparisons of Tables 1 and 2, there is a very large difference in the analysis of trace elements (Na + K), pH, moisture, and ash content.

Other Processing Considerations

Even the best filler material will not be effective unless it is processed in an acceptable manner and evenly dispersed throughout the resin matrix with each particle of carbon black in contact with the resin. If the carbon black is not stored properly before use, it may become wet with moisture and agglomerate to the point where it will not disperse in the resin. If proper mixing procedures are not followed, then even a good carbon black material will not be dispersed in the resin and small agglomerates or "chunks" of the carbon black can be found in the cured product.

Uneven carbon black distribution can lead to a dramatic decrease in physical properties of prepregs as well as premature failure of the part. Even carbon black distribution is not always easy to come by. In order to overcome these carbon black dispersion problems in the rubber industry, a technique was developed after World War II which incorporated carbon black into synthetic rubber while the rubber was still in the process of being manufactured. This technique, which is known as carbon black masterbatch, incorporates the carbon black into the rubber while the rubber is in a water emulsion. When the rubber is coagulated into solid particles and dried, the carbon black is finely dispersed around each individual molecule which is very desirable. This degree of

dispersion is impossible to achieve by any mixing method without degrading the physical properties after the rubber has been shipped to the end user.

To prevent the carbon black clumps in the final product, the carbon black is ground to the original manufactured degree of fineness with the use of fluid high energy mills or mechanical grinders. Without the additional grinding, the possibilities of agglomerated carbon black particles being present in the product is very high.

X. REFERENCES FOR PHENOLIC RESINS, CARBON CLOTH AND CARBON BLACKS

1. Hall, W. B.; Standardization of the Carbon-Carbon and Carbon-Phenolic Materials and Processes, Proposal Submitted to Marshall Space Flight Center, NASA, 1985.
2. Munhal, A. K.; Use of Fiber-Reinforced Composites in Rocket Motor Industry, SAMPE Quarterly, Vol.17, No.2, (1986), 1-11.
3. Ismail, I.M.K., Vangsness, M. D., Swords, D. M. and Morlan Jr., P. W.; Critical Technology, October, 1986.
4. Fltzer, E., Gkogkdis, A., and Heine, M.; High Temperatures-High Pressures, Vol. 16, (1984), 363-392.
5. Diefendorf, R. J. and Tokarsky, E.; Polymer Engineering and Science, Vol. 15, No. 3, (1975), 150-159.
6. Williams, W. S., Steffens, D. A., and Bacon, R.; Journal of Applied Physics, Vol.41, No. 12, (1970), 4893-4901.
7. Bacon, R.; Phil. Trans. R. Soc. London, A294, (1979) 437-442.
8. Fabrication of Composite Materials; Composite Materials Handbook, 2.41-2.55.
9. Carbon-Fiber Composites: A Light-Weight Alternative; Mechanical Engineering, September, 1985, 34-40.
10. Konkin, A. A.; Handbook of Composites, North Holland, Amsterdam, 1,(1985) 241-273.
11. Watt, W., Phillips, L. N. and Johnson, W.; The Engineer, 221,(1966), 815-816.
12. Hull, F.; An Introduction to Composite Materials, 1st ed., Cambridge University Press, Cambridge, 1981.
13. Riggs, D. M., Shuford, R. J., and Lewis, R. W.; Raw Materials, 196-271.
14. Moreton, R., Watt, W., and Johnson, W.; Nature, London, 213, (1967), 690-691.
15. Robbins, D.; Progressive Plastics, January, 1970, 24-26.
16. Reynolds, W. N. and Moreton, R.; Phil. Trans. R. Soc. London, A, 294, (1980), 451-461.
17. Edle, D. D., Fox, N. K., Barnett, B. C. and Fain, C. C.; Carbon, Vol. 24, No.2, (1986), 477-482.
18. The American Heritage Dictionary of the English Language, Houghton Mifflin Company, Boston, 1980.

19. Bahl, D. P., Mathur, R. B. and Dhani, T. L.; *Materials Science and Engineering*, 73, (1985), 105-112.
20. Thorne, D. J.; *Handbook of Composites*, North Holland, Amsterdam, 1, (1985), 475-494.
21. Cagliostro, D. E.; *Textile Research Journal*, October, 1980, 632-637.
22. Volk, H. F.; *Fourth London International Carbon and Graphite Conference*, September 23-27, 1974.
23. *Universal Test Stand Model UTSE-2 Instruction Manual*. Force Measurement Division, John Chatillon and Sons, INC., North Carolina, 1-40.
24. Apicella, A., Nicolais, L., Nobile, M. R.; *Composite Science and Technology* (ISSN 0266-3538), Vol. 24, no. 2, (1985), 101-121.
25. Brown, S. C.; *First Interim Report for Process Chemistry Definition for C-Phenolic and C-C Precursor Materials Contract No. NA-58-36296 prepared for NASA*, Huntsville, AL-35812.
26. DeJong, J. L., and DeJong, J.; *Rec. Trav. Chim.*, 72-492, (1953).
27. Era, V. A.; *J of Thermal Annual.*, Vol. 25, (1982), 79-87.
28. Freeman, James J., and Lewis, C. W.; *J. Am. Chem. Society*, 1976, 2080, (1954).
29. Hanus, H., and Fuchs, E.; *J. Pract. Chem.*, (1939), 153, 327.
30. Kirk and Othmer, *Encyclopedia of Chemical Technology*, Vol. 17, (1982).
31. King, P. W., Mitchell, R. H., and Westwood, A. R.; *J. of Apl. Pol. Sc.*, Vol. 18, 1117-1130, (1974).
32. Leckenby, J. N.; *Proceeding of the Third European Symposium on Spacecraft Materials in Space Environment*, Noordwijk, The Netherlands, 1-4 Oct., 1985 (ESA SP-232 Nov. 1985), 215-222.
33. Martin, R. W.; *Alkali-Catalyzed Phenol-Formaldehyde Reaction*, Am. Chem. Society Meeting, Springfield, Mass., Dec. 1948.
34. Martin, R. W.; *The Chemistry of Phenolic Resins*, Wiley, New York, 1956.
35. May, C. A., Whearty, D. K., Fritzen, J. S.; *Society for the Advancement of Material and Process Engineering*, 1976, 803-818.
36. Megson, N. J. L.; *Phenolic Chemistry*, Academic Press, New York, 1958.
37. Moacanin, J., Cizmecioglu, M., Hong, S. D., Gupta, A.; *Chemorheology of Thermosetting Polymers*, Washington, D. C., American Chemical Society (ACS Symposium Series No. 227), 1983, 83-94.
38. Sprengling, G. R., and Freeman, J. H.; *J. Am. Chem. Society*, 72, 1982 (1950).

39. Stenzenberger, H., Herzog, M.; Proceedings of an ESA Symposium on Spacecraft Materials, held at ESTEC, 2-5 Oct. 1979, ESASP-145 (Dec. 1979), 23-34.
40. Taylor, R. E.; Shoemaker, R. L., and Koshigow, L.; TLSP: Annual Report, 15 Feb. 1981, 15 Feb. 1982.
41. Turner, A. B.; Quart Rev., (1964), 18, 347.
42. U. S. Patent 939, 966 (Nov. 15, 1909), L. H. Bakeland; U. S. Patent 942, 852 (Dec. 12, 1909), L. H. Bakeland.
43. John Wiley and Sons, Encyclopedia of Polymer Science and Technology, Vol. 10, 1-122, (1969).
44. Simon, L. E.; An Engineers Manual of Statistical Methods, John Wiley and Sons, New York, (1945).
45. Myers, C. Y. (to Union Carbide Corp.), U. S. Pat. 2,889,374 (June 2, 1959).
46. Stokes, C. A.; ACS Symposium Series 21: Petroleum Derived Carbons, American Chemical Society, New York (1976), 1-17.
47. Mantel, C. L., ACS Symposium Series 21: Petroleum Derived Carbons, American Chemical Society, New York (1976), 18-46.
48. Gould, R. F., editor; ACS Symposium Series 21: Petroleum Derived Carbons, American Chemical Society, New York (1976).
49. Annual Book of ASTM Standards, Vol. 09.01, Rubber, Natural and Synthetic - General Test Methods; Carbon Black, Philadelphia, (1985).

XI. EXPERIMENTAL STUDIES

Various studies were undertaken to investigate specific test methods. The test methods which were looked at first were methods that were utilized to measure specification properties.

A. PERCENT RESIDUAL VOLATILES: The major difficulty with the original residual volatiles test method was the variance in results between the two prepreg suppliers, U. S. Polymeric and Fiberite, and the user of the prepreg, Thiokol. The problem was compounded when one lab obtained results that were high but still within specs, and the other lab obtained results that were too high, i.e., out of specification. During a meeting at MSFC with U. S. Polymeric, Fiberite, Thiokol and MSFC represented, the original test method was rewritten to tighten the test procedure. The reason the test method was tightened was because of concerns that the time required for various steps was different at each lab, as indicated in Figure 1. Although each laboratory was following the same test procedure, there were significant difference in the actual time-temperature-pressure sequence in the preparation of the test specimen. This would give different amounts of staging and resin flow yielding significantly different results. In an attempt to solve this problem, the test procedure was modified to tighten up the test method. The agreed upon new test method is shown graphically in Figure 1 as the compromise, and the written version of each test procedure is at the end of this section. The four labs then agreed to a round robin testing of the same prepreg rolls to evaluate the precision and the ability of each lab to duplicate each others results. The four labs, U. S. Polymeric, Thiokol, Fiberite, and MSFC then tested the same seven rolls of prepreg utilizing the rewritten test method. The results of the tests are given below in Table 1.

Data from MSFC testing is shown in Figure 2, indicating that the precision was excellent, but as shown in the above data, the ability of the labs to reproduce the same results did not improve. It is the opinion of the author that the major reason for this differences in lab agreement is due to differences in personnel and the equipment utilized

RESIDUAL VOLTS PREPARATION TIME PRIOR TO REACHING FINAL CURE PRESSURE

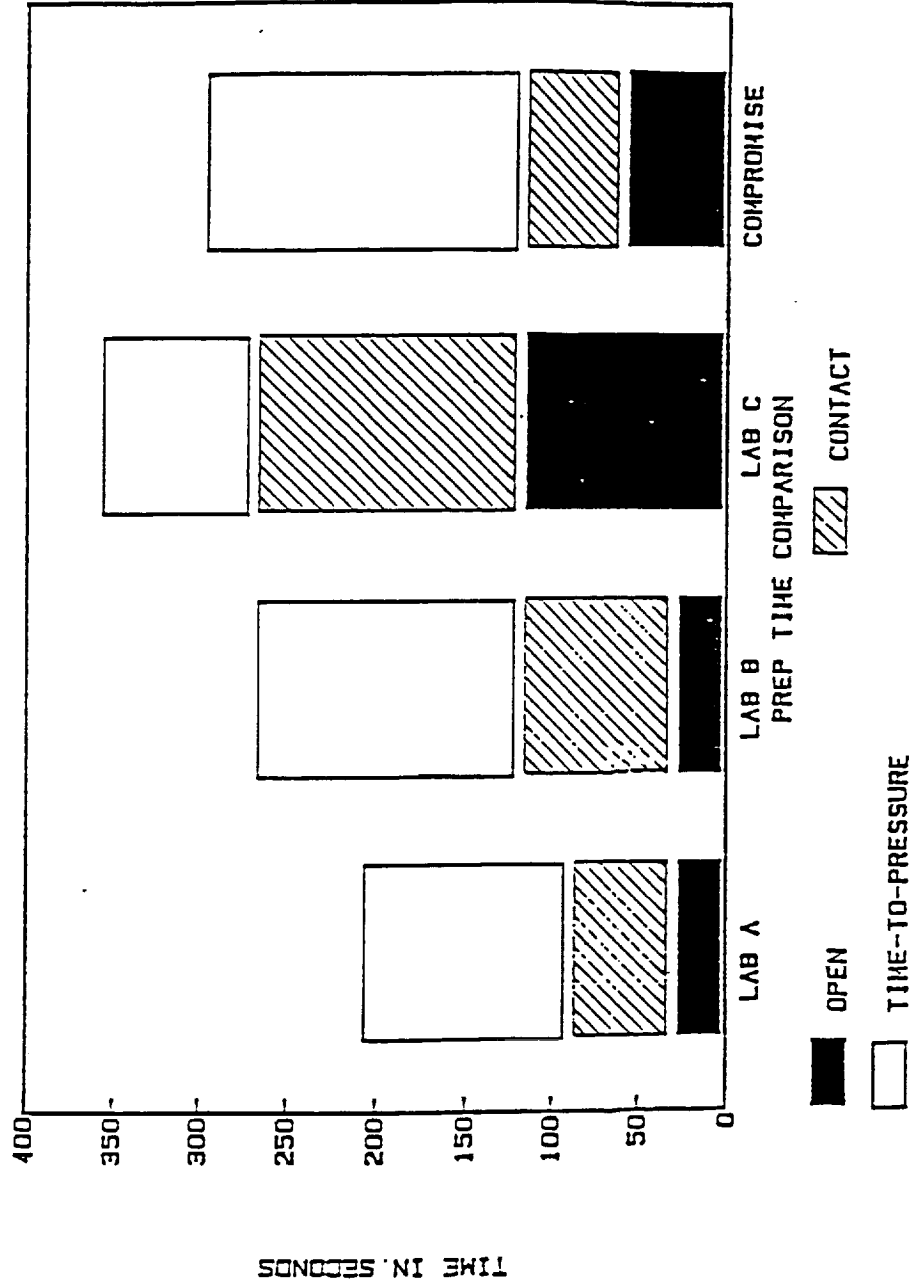


Fig. 1 - XI - Residual Volts Preparation Time

In the testing. Different presses, drying ovens, and bleeder cloth could result in different amounts of resin left in the specimen. In addition, the last time any of the presses and/or ovens were calibrated is also an unknown.

TABLE 1
Round Robin Testing of Residual Volatiles
in Selected Materials

Material A	% Residual Volatiles			
	Roll 40	Roll 46	Roll 56	
Lab A	1.21	1.35	1.52	
Lab B	2.23	1.85	1.89	
Lab C	2.47	2.08	2.21	
Lab D	2.50	2.14	2.63	
Material B	% Residual Volatiles			
	Roll 4A	Roll 19A	Roll 22A	Roll 26A
Lab A	0.99	1.43	1.04	1.44
Lab B	1.31	1.76	1.52	1.51
Lab C	1.79	2.29	1.88	2.21
Lab D	1.44	1.69	1.90	1.94

After the round robin tests were completed, the general consensus was that it appeared that it was not possible under the current laboratory procedures to obtain reproducible results utilizing the residual volatiles test procedure. Therefore, since the first objective of the basic policy was not met, the second overall objective was not addressed. It is the author's opinion that the second basic policy objective was also not met. The minimum additional information needed to meet the second objective would be to identify and quantify the residual volatiles.

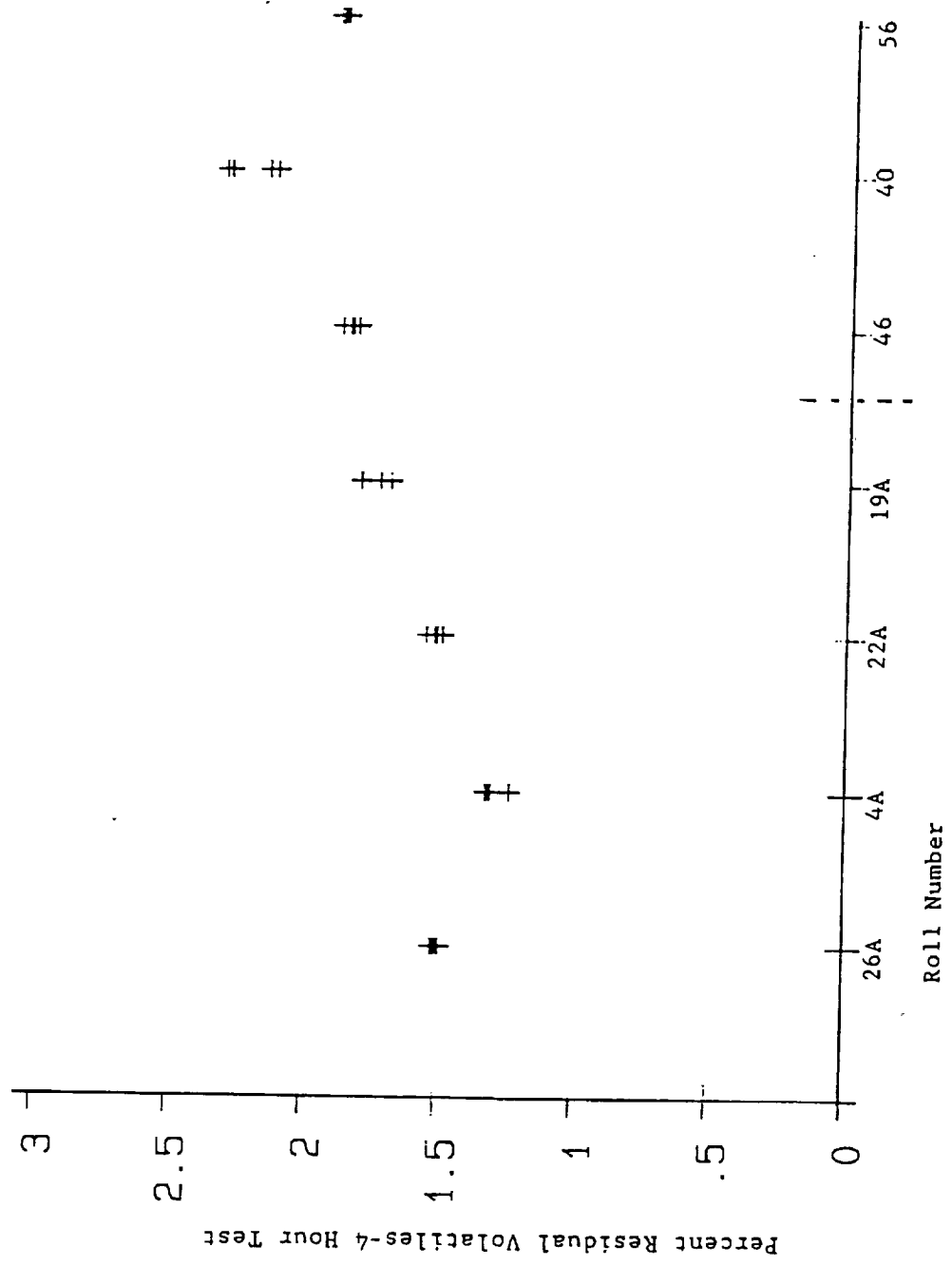


Fig. 2 - XI - MSFC Round Robin Test for Residual Volatiles

B. ORIGINAL RESIDUAL VOLATILES TEST PROCEDURE

Residual Volatile Content: The residual volatile content of the cured material shall be determined in accordance with the following:

- a. Cut sufficient plies to produce a test panel 0.250 ± 0.050 thickness by $4 \times 4 \pm 0.125$ inches. Cure the panel as follows:
 1. Place the stack of plies into a press preset at 325 ± 10 degrees F.
 2. Apply contact pressure for 30 ± 5 seconds and dump pressure for 2 cycles before slowly applying maximum pressure. (The material shall not be prestaged.)
 3. Increase the pressure slowly to 1000 ± 50 psi, allowing the resin to stage to minimize flash at ply edges.
 4. Hold the pressure and temperature for 120 ± 15 minutes.
 5. Decrease the temperature and pressure to ambient.
- b. The outer 1/2 inch of the test panel shall not be used for preparation of specimens.
- c. Cut a specimen 1.000 ± 0.050 inch by 1.000 ± 0.050 inch panel thickness from the center 2 inch by 2 inch section of the test panel. Top and Bottom molded surfaces shall not be machined. Wipe the specimen clean using MEK and allow to air dry 20 minutes minimum before testing.
- d. Place the specimen in a desiccator and desiccate for 18 hours minimum.
- e. Weigh the specimen to the nearest 0.01 gram and record as W_1 .
- f. Place the specimen in an air circulating oven, preheated and stabilized at 325 ± 10 degrees F for approximately 30 minutes; condition the specimen at a temperature of 325 ± 10 degrees F for 24 hours minimum.
- g. Remove the specimen from the oven and cool in the desiccator for approximately 30 minutes or until the specimen reaches room temperature.
- h. Reweigh the specimen to the nearest 0.01 gram. Record as W_2 .

- I. Calculate the percent residual volatiles as follows:

$$\text{Percent volatiles} = \frac{W_1 - W_2}{W_1} \times 100$$

Where: W_1 = original weight of specimen in grams

W_2 = devolatilized weight of specimen in grams

- J. Report residual volatiles to the nearest 0.01 percent.

C. PROPOSED RESIDUAL VOLATILES TEST PROCEDURE

Residual Volatile Content: The residual volatile content of the cured material shall be determined in accordance with the following:

- a. Cut 18 plies to produce a test panel 4 ± 0.125 by 4 ± 0.125 inches. Cure the panel as follows:
 1. Cover top and bottom of lay-up with one layer of non-porous release film.
 2. Place the stack of plies into a press preset at 325 ± 10 degrees F.
 3. Insert into the press and immediately close to contact pressure (closing time ten seconds or less).
 4. Hold for 30 ± 5 seconds (at "contact" pressure).
 5. Open the press to 1-2 inches and allow to "dwell" for 20 ± 5 seconds.
 6. Immediately close to contact pressure and hold for 30 ± 5 seconds.
 7. Open the press to 1-2 inches and allow to dwell for 20 ± 5 seconds.
 8. Immediately close to contact pressure and slowly increase the pressure to 1000-1200 psi over a period of 180 ± 30 seconds.
 9. Total prep time is approximately 300 seconds (assuming 10 seconds close times)
 10. Cure time will be 120-135 minutes at $325^\circ \pm 10F$ and 1000 - 1200 psi.
 11. Decrease the temperature and pressure to ambient.

- b. The outer 1/2 inch of the test panel shall not be used for preparation of specimens.
- c. Cut a specimen 1.000 ± 0.050 inch by 1.000 ± 0.050 inch by panel thickness from the center 2 inch by 2 inch section of the test panel. Top and bottom molded surfaces shall not be machined.
- d. Place the specimen in a desiccator and desiccate for 18 hours minimum.
- e. Weigh the specimen to the nearest 0.01 gram and record as W_1 .
- f. Place the specimen in an air circulating oven, which has been preheated and stabilized at 325 ± 10 degrees F for approximately 30 minutes; condition the specimen at a temperature of 325 ± 10 degrees F for 4 hours minimum.
- g. Remove the specimen from the oven and cool in the desiccator for approximately 30 minutes or until the specimen reaches room temperature.
- h. Reweigh the specimen to the nearest 0.01 gram. Record as W_2 .
- i. Calculate the percent residual volatiles as follows:

$$\text{Percent Residual Volatiles} = \frac{W_1 - W_2}{W_1} \times 100$$

where: W_1 = original wt. specimen in grams

W_2 = devolatilized wt. of specimen in grams

- J. Report residual volatiles to the nearest 0.01 percent.

D. VOLATILE CONTENT

Volatile Content refers to the volatiles that come off during the testing of uncured prepeg and should not be confused with residual volatiles which come off during the testing of cured parts. The same four labs conducted another round robin on volatile content, and to circumvent previous errors, a new volatile content test method was established, and the new test method is at the end of this section. One change in the procedure was to change the phase "place specimen in oven" to "suspend specimen in oven" since laying the specimen

on racks at 325 degrees F causes sticking and excessive resin loss. A round robin evaluation between the same four labs for one roll of prepreg gave the following results shown in Table 2 below.

TABLE 2
Round Robin Testing for Percent Volatiles

Lab	Percent Volatiles (Average of 12 Specimens)	Variance
Lab A	4.3	0.20
Lab D	4.8	0.21
Lab C	4.8	0.41
Lab B	4.9	0.30

The data is also shown graphically in Figure 3. It is noted that Lab A was the lab with the lowest value as it was with all the rolls evaluated in the percent residual volatiles round robin, eight out of eight rolls tested. This would indicate some constant function, such as lower than indicated temperature or other causing the difference in values between Lab A and the other labs. The other three labs were extremely close so it does appear that the percent volatiles test can be duplicated in the various labs. It is still considered necessary, for the second objective or the basic policy for this study to be satisfied, to identify and quantify the volatiles coming from the specimen.

E. PROPOSED VOLATILE CONTENT TEST

The volatile content of 12 specimens taken randomly from the uncured material shall be determined in accordance with the following:

- a. Cut a 16 ± 2 square inch specimen.
- b. Weigh the specimen to the nearest 0.01 gram (W_1).

- c. Suspend the specimen in a recirculating oven, preheated and stabilized to 325 ± 10 degrees F, for 60 ± 1 minutes. Specimen should be suspended to get adequate air circulation.
- d. Remove specimen and place in a desiccator and cool to room temperature.
- e. Remove from the desiccator and weigh the specimen to the nearest 0.01 gram (W_2).
- f. Calculate percent volatiles as follows:

$$\text{Percent Volatiles} = \frac{W_1 - W_2}{W_1} \times 100$$

where: W_1 = uncured weight of specimen, gm.

W_2 = final weight of specimen, gm.

- g. Report volatile content of specimen to the nearest 0.1 percent.

F. HUMIDITY EXPOSURE STUDIES

It is known that carbon-phenolic composites pick up moisture when exposed to humid conditions. Both cured and uncured (prepreg) samples were exposed to 100 percent relative humidity for 30 days. The weight gain versus exposure time curves for both of these materials are shown in Figure 4 (uncured) and Figure 5 (cured). The uncured curve is interesting in that it seems to indicate a weight gain for the first week followed by a weight loss the second week and then another gradual weight gain. The high value specimen on the 21st day is not the same high value specimen on the 29th day. This curve indicates varying reactivities and could be the area of a more complete study. The curve for the cured specimen indicates a gradual increase in weight for the entire exposure time of 30 days. The values remain approximately the same for the 36 day exposure time, so it would appear that a constant weight was achieved at 29-30 days of exposure time to 100 percent relative humidity conditions. The normal testing for residual volatiles that had picked up extra moisture was to desiccate for a minimum of 24 hours or a minimum of 72 hours on retest.

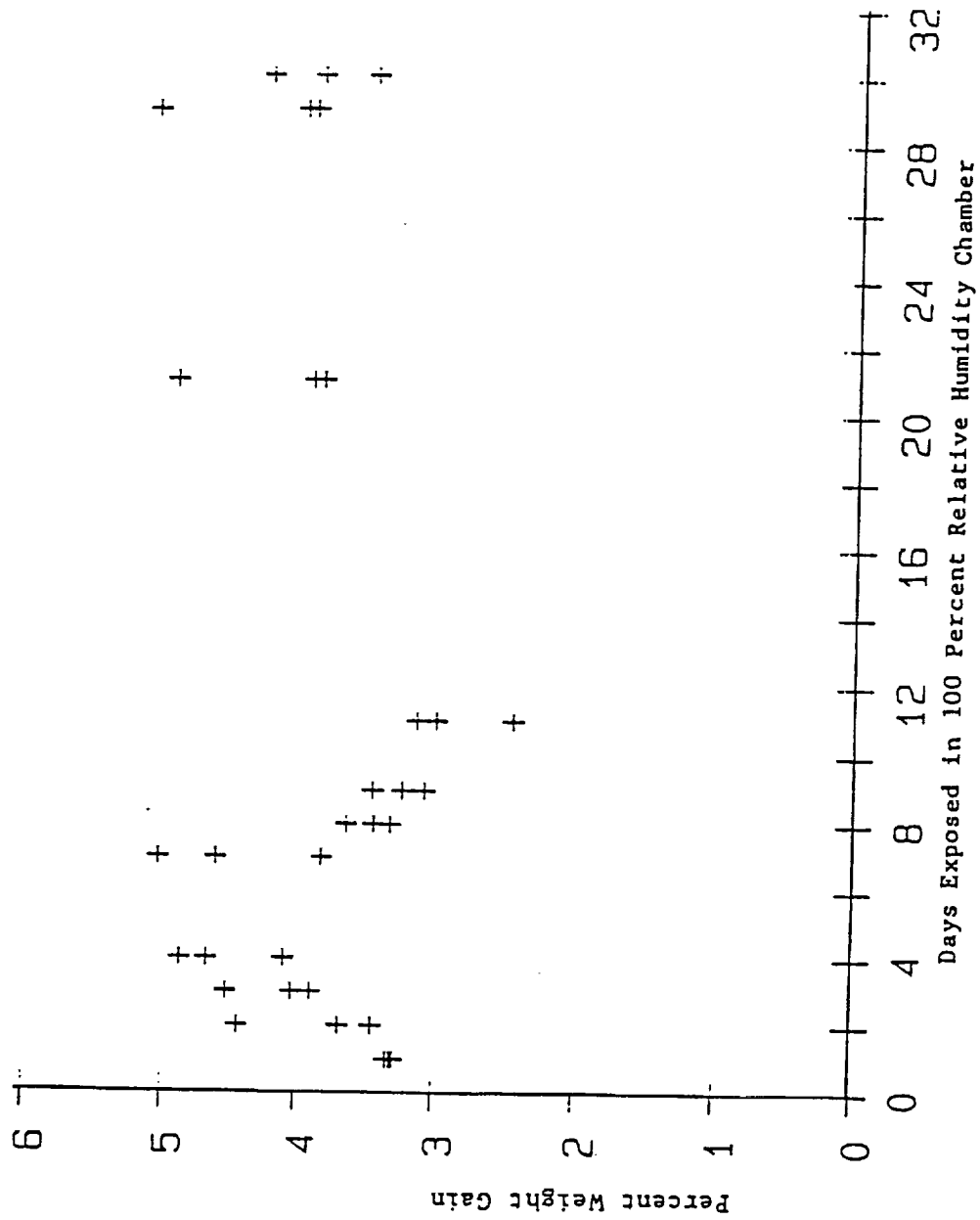


Fig. 4 - XI - Effect of Humidity on Uncured Prepreg

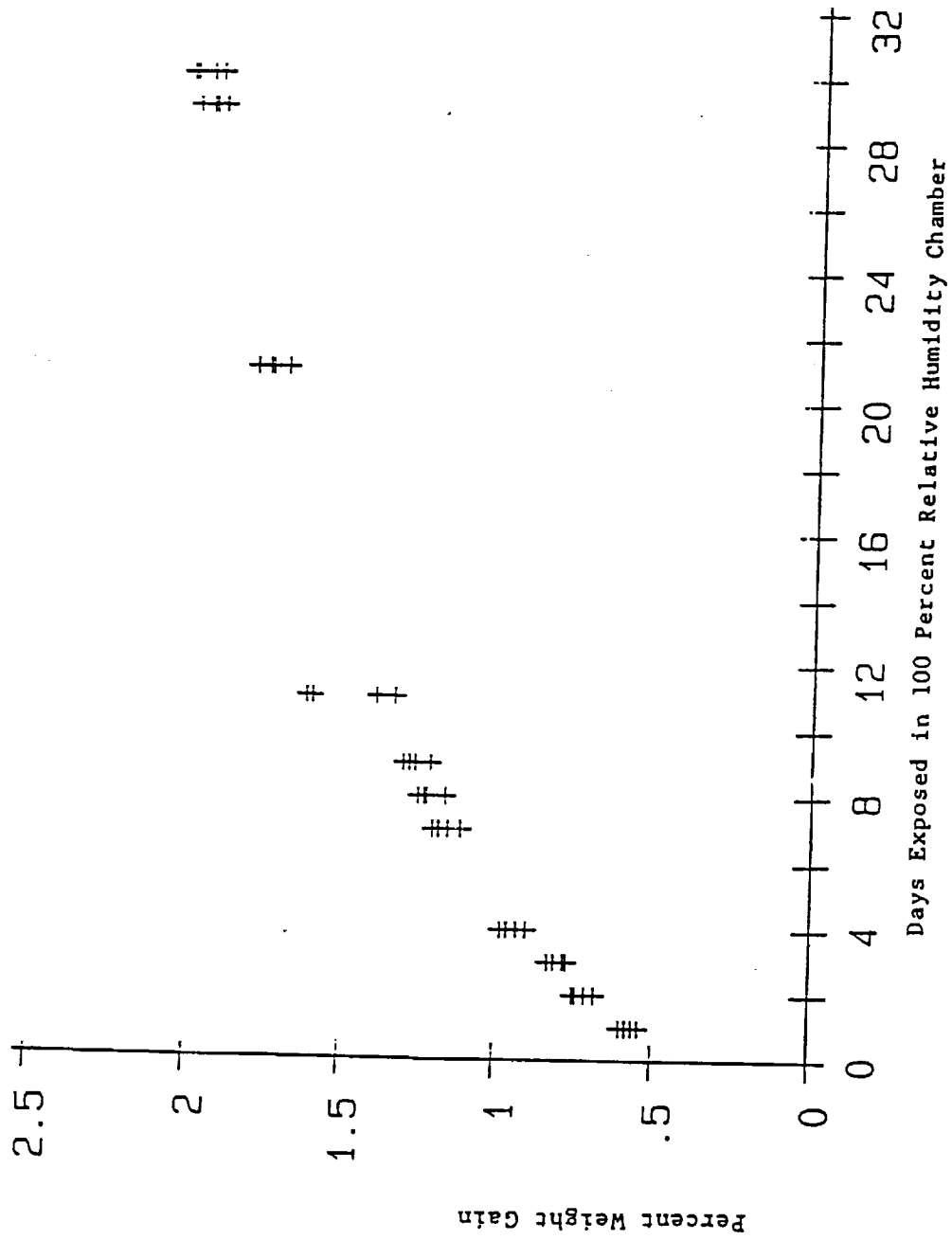


Fig. 5 - XI - Days of Exposure to 100% Relative Humidity

The weight loss versus time in desiccator is shown in Figure 6 and indicates an increase in weight loss continuing up to the 72 hours. Therefore, time in the desiccator should be specified in a plus or minus frame instead of a minimum value. The weight loss when placed in a desiccator versus exposure time in humidity chamber is shown in Figure 7 indicating fairly constant loss of weight in the desiccator regardless of the time in the humidity chamber.

After the 72 hours in the desiccator, percent residual volatiles were determined for the exposed specimens. The results of this study is shown in Figure 8, indicating a slight increase in percent residual volatiles with an increase in exposure time in the humidity chamber. This was expected since Figure 5 indicates increase in weight versus exposure time while Figure 7 indicates essentially constant weight loss in the desiccator.

G. EFFECT OF PERMEABILITY ON RESIDUAL VOLATILES

The removing of volatile material from the interior of a solid requires two different processes. First the volatiles must be transported to the surface, and then removed from the surface. The driving force for the movement of the volatiles is the difference in concentration of the volatiles in the interior and that on the surface. The volatiles on the surface must then be removed to maintain the effective driving force (movement). The removal is normally accomplished by flowing air unsaturated with the expected volatiles. A vacuum would normally accelerate the removal thereby requiring less time to completely remove the volatiles. The rate of transporting the material to the surface is a function of temperature, concentration difference, and permeability. Temperature furnishes the energy for heat of vaporization, diffusion and surface activity. Permeability is a measure of the lengths of the paths to the surface for the volatiles. Figure 9 shows the percent residual volatiles for an oven curing time up to 48 hours while Figure 10 extends the curing time up to 360 hours. These times are for the standard 1" x 1" x 0.25" (thick) specimen. These tests were on 4 replications and notice the precision results. Pinoli of Lockheed Research

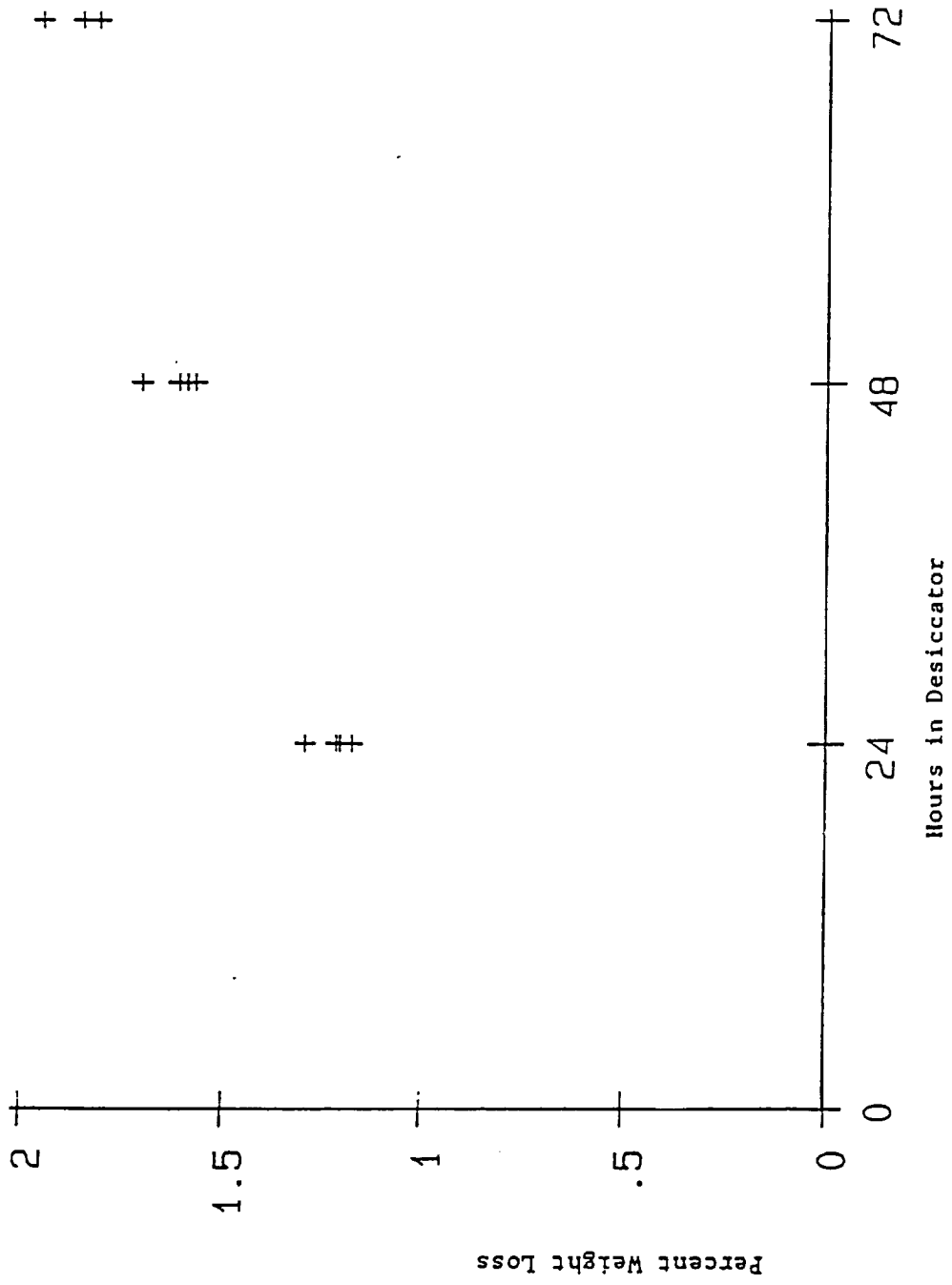


Fig. 6 - XI - Weight Loss After Exposure to Desiccation.

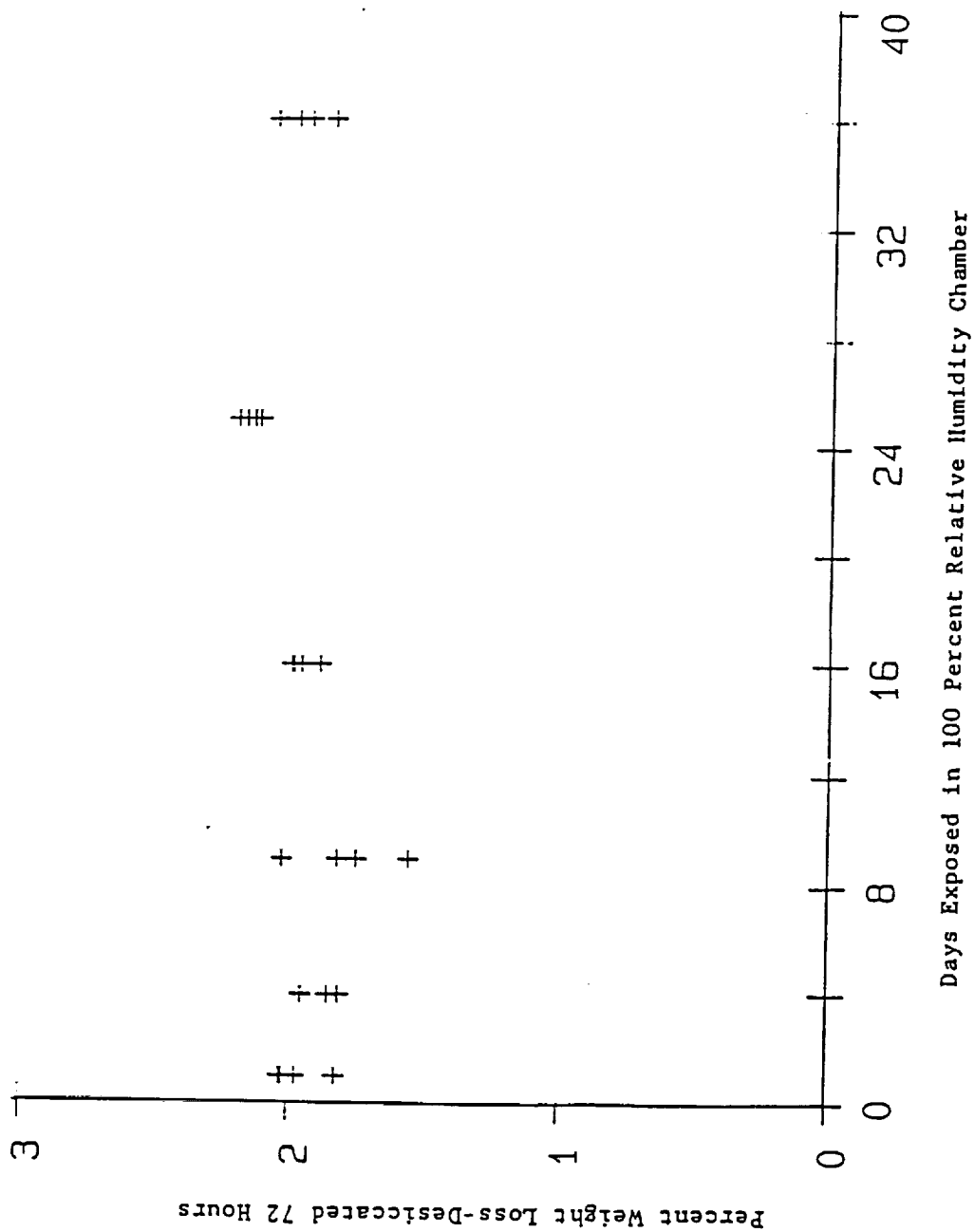


Fig. 7 - XI - Days of Exposure in 100% Humidity

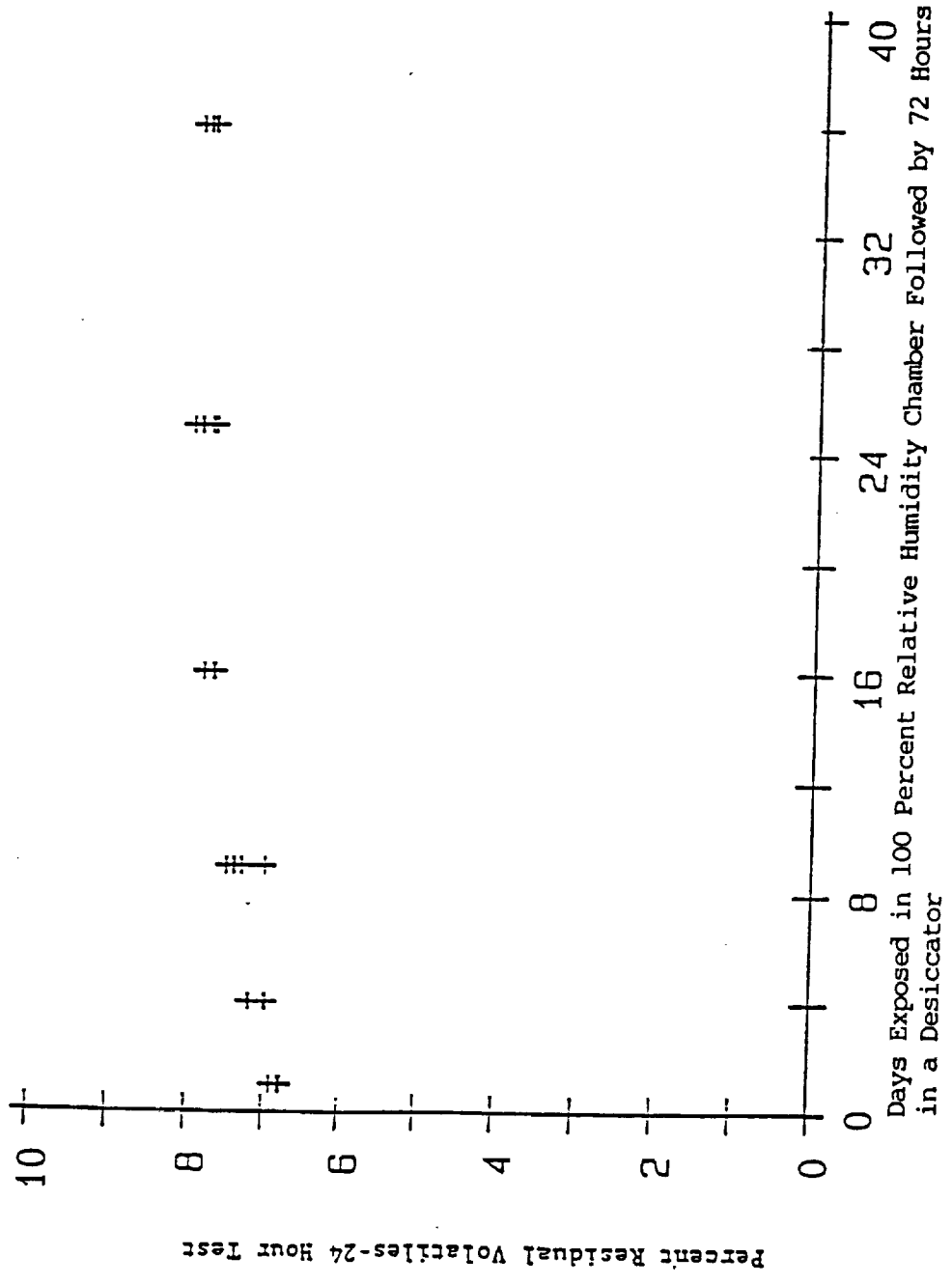


Fig. 8 - XI - Days Exposed in 100% Relative Humidity Chamber Followed by 72 Hours in a Desiccator

Facilities in Palo Alto, CA did some permeability studies on Carbon-Phenolic specimens varying the temperature and vapor removal system. Figure 11 shows the percent volatiles loss versus time on the different size cubes. It can be seen that the time to reach equilibrium (i.e., not further weight loss) increases with cube size. Since temperature and original concentration gradient can be assumed to be constant then permeability is the remaining variable, and the experimental results follow the predicted results. Figure 12 has the same size cubes, but the temperature is lower and the volatiles removal system was changed from circulating air to a vacuum. Again the experimental results follow the predicted results. However, because of the lower temperature, the rate of diffusion was so low that after over 50 hours, equilibrium had not been achieved in any of the cubes. The results of residual volatiles testing is dependent on several variables besides composition, therefore, it is very difficult for results from lab to lab to be comparable.

PERCENT RESIN FLOW: The test procedure for percent resin flow is given at the end of this section. This test is important because it assures that the prepreg can be tape wrapped and properly cured. The percent resin flow not only is a measure of staging of the resin, but of total resin content. The content is a function of the cloth itself in that the amount retained is a function of several characteristics of the cloth and the filler/resin mixture. However, there is a wide variance in the percent resin flow data, especially when tested in different laboratories. The initial explanation for this variance was the delay in closing the press, as the test method just specifies immediately. Closing time versus percent resin flow was determined for three different rolls of prepreg with the following results as shown in Table 3.

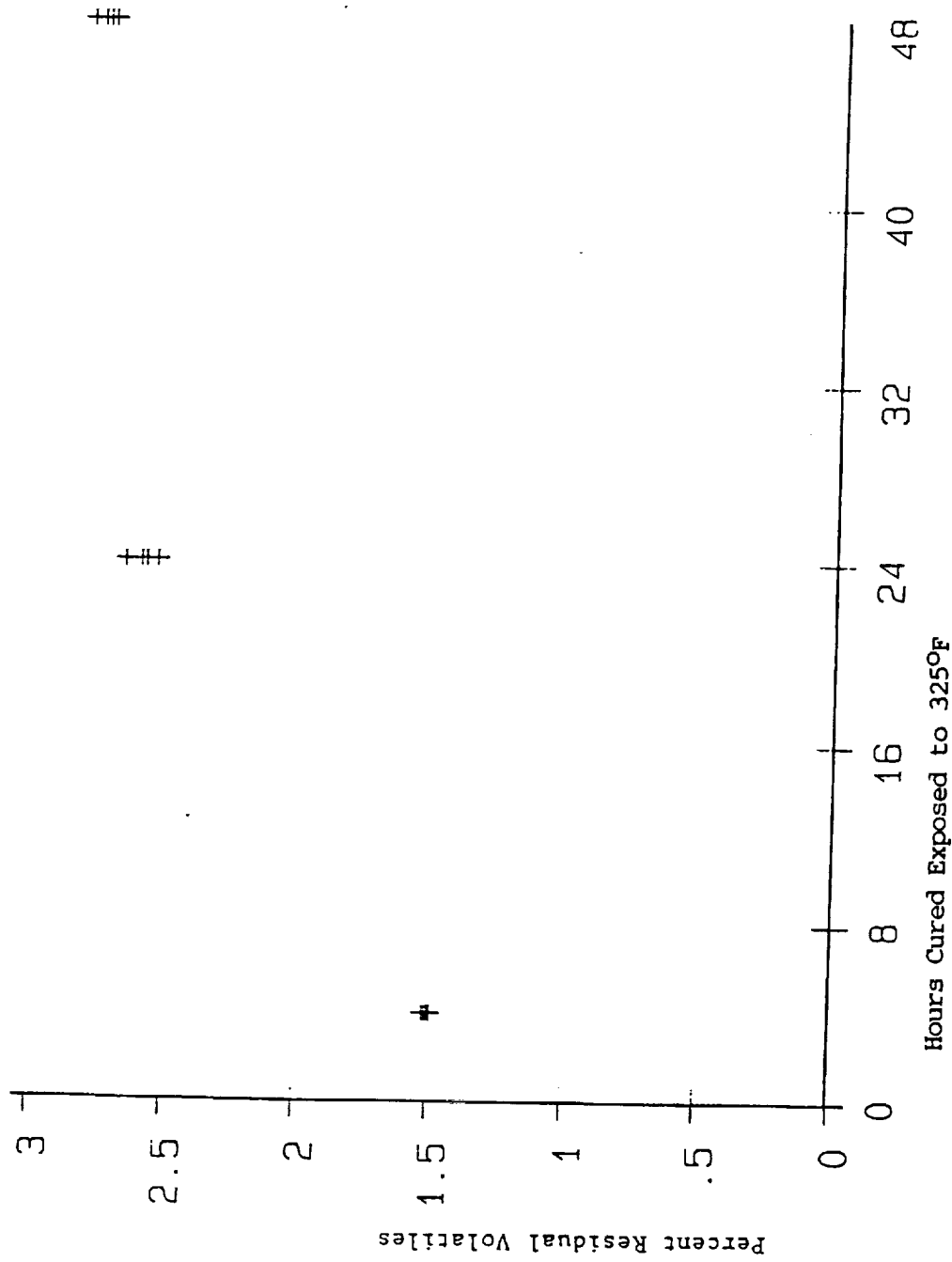


Fig. 9 - XI - Hours Cured Exposed to 325°F

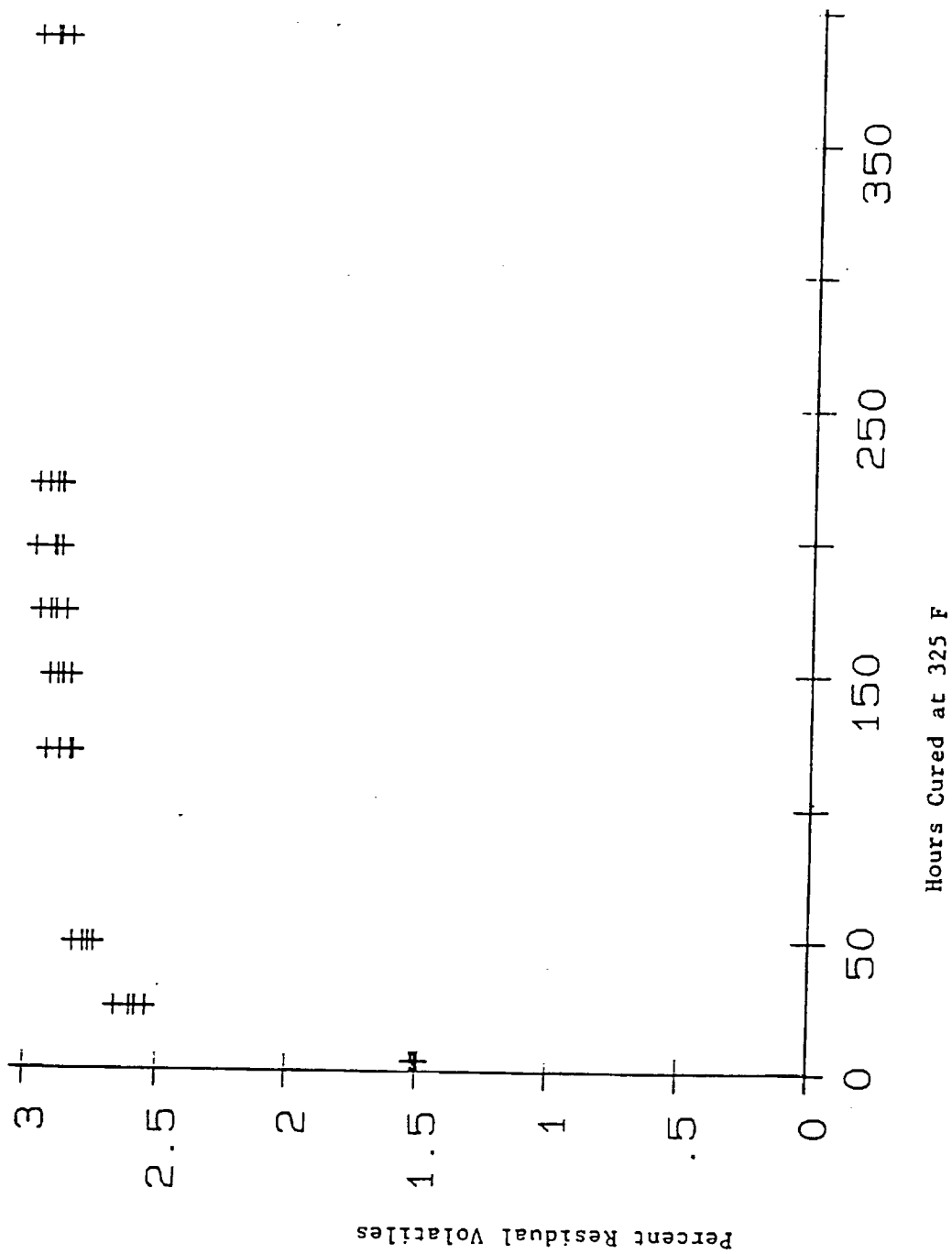


Fig. 10 - XI - Percent Residual Volatiles vs Hours Cured at 3250

DESORPTION TIME DEPENDENCY STUDY
 PANEL 8 CUBES DEVOL IN AIR CIRCULATING OVEN 325 F

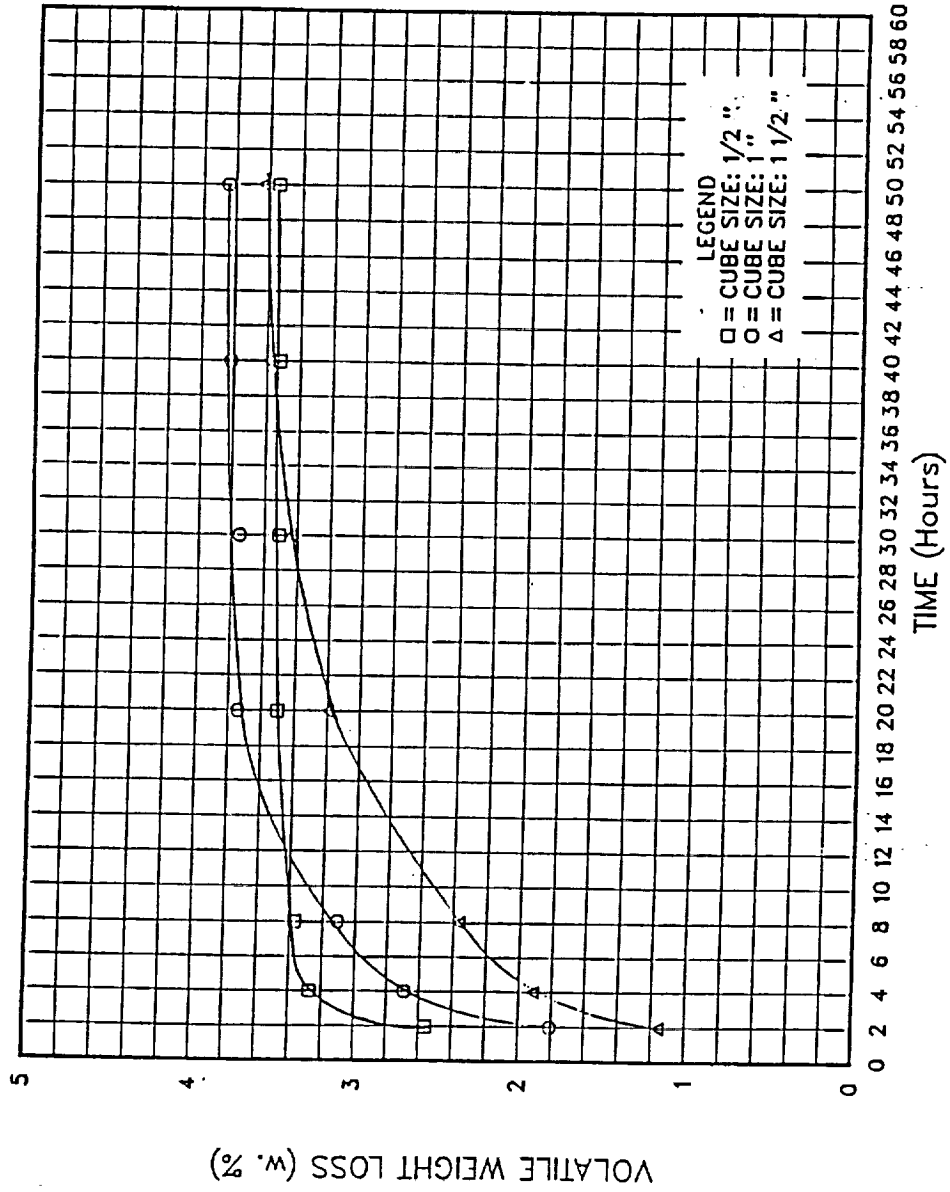


Fig. 11 - XI - Desorption Time Dependency Study In Air Circulating Oven at 325°F

ORIGINAL PAGE IS
OF POOR QUALITY

DESORPTION TIME DEPENDENCY STUDY
PANEL 8 CUBES VACUUM DEVOL 220 F

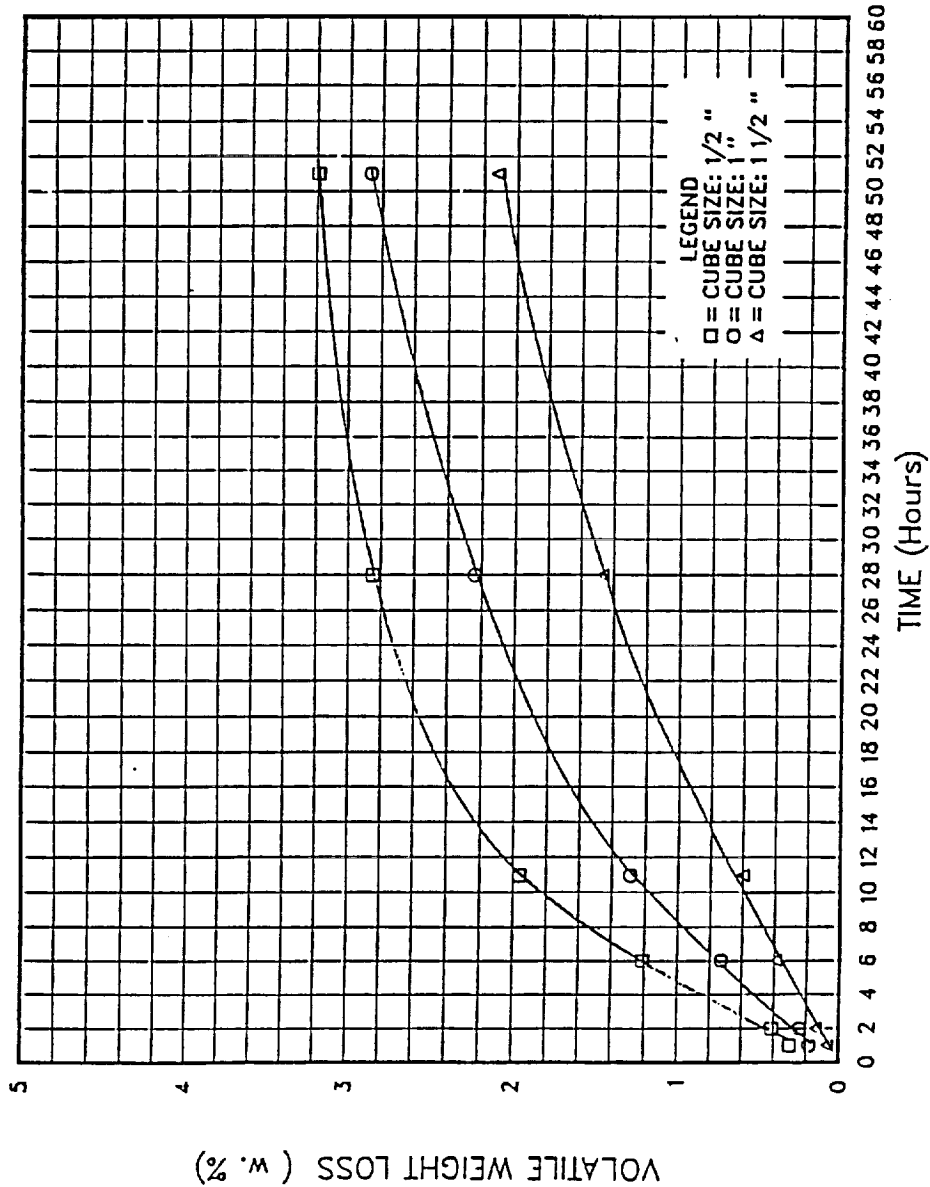


Fig. 12 -- XI -- Desorption Time Dependency Study in Vacuum at 220°F

TABLE 3

Percent Resin Flow

Delay in Closure	Roll		
	1	2	3
0 sec.	29.6	18.7	31.5
20 sec.	31.1	19.1	30.0
40 sec.	30.0	20.1	
60 sec.	29.3	22.1	30.7
120 sec.	29.9	1.4	24.8

The closure time with 0 seconds delay was 15 seconds, so the total closure time was delay time plus 15 seconds. It can be seen that total closure time of 75 seconds and less had a negligible effect on the percent resin flow.

It should be noted that this test really measures weight loss, a combination of resin flow and volatile content. It should be rewritten to subtract volatile content with the remainder shown as resin flow. This would require some adjustment in the specifications.

H. PERCENT RESIN FLOW TEST PROCEDURE

Resin Flow: Resin flow of each sample of the uncured material shall be determined in accordance with the following:

- a. Cut a 4-inch by 4-inch \pm 1/8-inch squares across the width of the fabric. All squares shall be bias cut to eliminate fiber loss in testing. Stack the squares uniformly on each other to make a specimen. Where the width of the tape is less than 4-inches wide, cut the tape in 4-inch lengths and place side by side to fabricate a 4-inch by 4-inch specimen ply. Stack four plies alternately placed 90 degrees to the previous ply roll direction. Place each ply uniformly on each other to make up a specimen.
- b. Weigh the specimen of 4 plies to the nearest 0.01 gram and record as W_1 .

- c. Place the specimen between release film. Preheat the press to 325 ± 10 degrees F, position the specimen in the middle of the press plate and apply the press load of 150 ± 10 psig immediately. Press load the specimen for a minimum of 10 minutes at 325 ± 10 degrees F.
- d. Remove the specimen from the press and cool to ambient temperature.
- e. Using a knife, scrape off the resin flash to the original size of the specimen. Do not remove any reinforcement from the original dimensions.

NOTE: Any fibers which may be displaced and scraped off during the process shall be included in the weighed back specimen weight (W_2).

- f. Reweigh the specimen to the nearest 0.01 gram and record as W_2 .
- g. Calculate the percent resin flow as follows:

$$\text{Percent Flow} = \frac{W_1 - W_2}{W_1} \times 100$$

where: W_1 = uncured weight of specimen, gm.

W_2 = final weight of specimen, gm.

- h. Report resin flow to the nearest 0.1 percent.

I. PREPREG STORAGE CONDITIONS/LIFE

The effect of storage of prepreg on percent volatiles and percent resin flow was investigated. The prepreg was stored within the guidelines established. These being: prepreg sealed in a plastic bag which must contain one-unit of desiccant (minimum) and temperature not to exceed 50°F. The results of the initial study were:

Prepreg:	%Volatiles	%Resin Flow
As received	5.2	18.4
After 17 weeks in storage	6.9	20.0
After 27 weeks in storage	7.3	23.7

Fikes at Marshall Space Flight Center continued the study by evaluating the effect on percent volatiles and percent resin flow due to the following bagging conditions at room temperature.

9 samples unbagged for 0 days (Note: Tested on the day they were cut). U0

9 samples unbagged for 15 days, U15

9 samples unbagged for 30 days, U30

9 samples bagged in polyethylene bags for 15 days, 215

9 samples bagged in polyethylene bags for 30 days, 230

9 samples bagged in aluminized polyethylene bags for 15 days, AL 15

9 samples bagged in aluminized polyethylene bags for 30 days, AL 30

The results of the resin flow test are given below in Table 4.

TABLE 4

Results of Resin Flow Tests

Carbon Cloth Phenolic Prepreg Out-Time Study

Percent Volatiles

Sample No.	U0	U15	U30	Z15	Z30	AL15	AL30
1	20.8	25.6	24.3	21.2	21.8	21.5	15.5
2	18.5	24.7	23.1	17.7	20.4	20.1	16.7
3	17.2	23.5	23.2	20.2	19.9	19.1	16.8
4	21.3	22.8	24.5	21.7	15.0	21.2	19.9
5	18.1	22.9	23.7	20.1	20.0	18.8	22.7
6	18.5	22.3	19.7	20.0	19.5	17.3	17.3
7	21.3	23.6	24.3	21.2	20.7	20.2	19.6
8	19.1	23.4	23.9	19.5	20.0	18.3	18.9
9	18.5	22.6	23.2	19.4	19.9	18.1	19.3
Avg.	19.3	23.5	23.3	20.1	19.7	19.6	18.5
Stan.Dev.	1.50	1.59	1.46	1.21	1.88	1.20	2.18

These results are what would be expected when considering that resin flow results are a weight loss test. The unbagged material picked up more than enough moisture to over ride the slight decrease in resin flow due to staging. The polyethylene and aluminized-polyethylene bags, however, had essentially no moisture pickup, therefore, staging just about balanced out this slight moisture pick up for no overall change.

These tests again point out that the resin flow test should be modified. The results of the volatile content test are shown below in Table 5.

TABLE 5
Results of Volatile Content Tests
Carbon Cloth Phenolic Prepreg Out-Time Study

Sample No.	Percent Volatiles						
	U0	U15	U30	Z15	Z30	AL15	AL30
1	5.77	9.05	8.60	5.37	6.50	5.60	6.10
2	5.50	8.87	8.52	5.30	6.40	5.50	6.00
3	5.76	8.50	8.25	5.13	6.20	5.40	5.80
4	5.64	8.97	8.60	5.21	6.50	5.60	6.70
5	5.47	8.79	8.63	5.16	6.30	5.40	6.00
6	5.33	8.69	8.42	4.97	6.30	5.30	5.90
7	5.48	8.78	8.54	5.19	6.60	5.50	3.50
8		8.64	8.56	5.10	6.80	5.60	8.40
9	5.20	8.52	8.27	5.27	6.80	5.50	6.00
Avg.	5.52	8.76	8.49	5.19	6.49	5.49	6.04
Stan.Dev.	0.19	0.19	0.14	0.12	0.21	0.10	1.25

u - unbagged, z - polyethylene bag, AL - aluminized polyethylene bag

The percent volatiles increased with time in each of the bagging conditions with the most significant increase in the unbagged condition. It would appear from this data the equilibrium conditions are achieved at or before fifteen days for the unbagged prepreg. Since 30 days

of out of storage time is permitted, without specified bagging conditions, it would appear that bagging and storage would have little effect on final volatile content of the prepreg at the time of tape wrapping.

XII. TRAVEL

Since extensive travel was considered to be an important part of this project a report on project travel will be included in each report. For the period October 1985 through August 1988, the following travel was performed:

TRIPS	COMPANY
101	NASA, MSFC; Huntsville, AL
5	U. S. Polymeric; Santa Ana, CA
2	Aerojet Strategic Corp.; Sacramento, CA
1	Fiberite; Winona, MN
2	Morton Thiokol; Brigham City, UT
1	Hitco; Gardena, CA
1	AF Wright Aero Lab; Wright Patterson AFB, OH
2	ASTM Composite Testing; Charleston, SC
3	JANNAF Nozzle Tech Washington, D.C. Patrick AFB Florida Marshall Space Flight Center
1	Lockheed Missiles and Space Company, Inc.; Palo Alto, CA
1	Southern Research Institute; Birmingham, AL
1	Avtex Fibers Inc.; Front Royal, VA
1	Highlands Industries; Cheraw, SC
2	Polycarbon Inc.; Valencia, CA
1	Fiberite; Laguna Hills, CA
1	Borden Inc.; Louisville, KY

XIII. CONCLUSIONS

1. The nozzle of the solid rocket motor utilized in the space shuttle system has performed adequately for the 25 flights (50 nozzles) of the shuttle system.
2. Pocketing (uneven ablation/erosion) has occurred in most nozzles but potentially catastrophic pocketing only in Flight STS-8, with frequency and severity decreasing since Flight 51-F.
3. The manufacturers/suppliers of the materials and fabricated nozzle are open and helpful, and are desirous of putting out the best nozzle possible under the free enterprise system.
4. In general, the test methods and specifications utilized in the SRM nozzle program were designed to assure repeatability of a proven system, not to accurately measure some physical/chemical property of the nozzle system.
5. Engineering test and data are not available on the effects of varying materials and processes in the manufacture of the SRM, so changing specifications and/or test methods is most difficult.
6. Most of the test methods used to obtain data on materials and processes utilized in the SRM system are quite satisfactory, yielding acceptable values within specifications with good precision.
7. Carbon cloth, especially when underfired, is very reactive and has a high affinity for moisture which is a source of variability for some material properties of carbon-phenolic prepreg and cured composites.
8. No specifications exist for the filler material used in the manufacture of the carbon-phenolic prepreg which is the starting material for nozzle fabrication.
9. Variability of materials/suppliers and test methods causes wide fluctuations in a few measured properties of the nozzle system which in some instances exceeds three sigmas. The effects of these variations on the nozzle performance is an unknown, per conclusions 1 and 5.

10. Results of some measured properties of materials and parts of the nozzle system are equipment, personnel, and laboratory dependent, yielding nonreproducible data.
11. The test method for percent resin flow measures weight loss, not resin flow, as written.
12. The test method for residual volatiles measures permeability, not residual volatiles, as written.
13. The three test methods utilized to measure percent resin, cloth, and filler in prepregs yield different results when testing the same prepreg at the same laboratory.
14. The problems outlined above should not negate the 50 successful firings of the shuttle nozzles, but is an indication that a more homogeneous, less variable, nozzle system might be manufactured.

XIV. RECOMMENDATIONS

1. Rewrite resin flow test method to eliminate the effect of volatiles coming off at the same time, collect data base, and then change specifications appropriately.
2. Rewrite residual volatile content test method to eliminate permeability effects, collect data base, and then change specifications appropriately.
3. Select one of the three currently used resin, filler, cloth content test methods, collect data base, and then change specifications appropriately.
4. Complete writing specifications and test methods for the filler utilized in the carbon-phenolic prepreg.
5. NASA should maintain quality control authority at all supplier sites that produce materials/parts of the solid rocket motor of the shuttle system.
6. Increase the required carbon content of the carbon cloth to a minimum of 98 per cent.
7. Establish a procedure for changing the test methods utilized in the carbon-phenolic composite system and accompanying specification limits.